MUSCLE PLASTICITY AND REPEATABILITY TO ALTERATIONS IN MECHANICAL LOADING CONDITIONS

A Dissertation

by

KEVIN LEE SHIMKUS

Submitted to the Office of Graduate and Professional Studies of
Texas A&M University
in partial fulfillment of the requirements for the degree of

DOCTOR OF PHILOSOPHY

Chair of Committee,	James D. Fluckey
Committee Members,	Susan A. Bloomfield
	Harry A. Hogan
	Michael P. Massett
	Joseph P. Kerwin
Head of Department,	Richard B. Kreider

December 2016

Major Subject: Kinesiology

ABSTRACT

The breadth and depth of muscle biology research has consistently demonstrated the ability for skeletal muscle to adapt quickly and specifically to stimuli placed upon it, often regarded as plasticity. Changes in muscle mass are often tied to losses, recoveries, and gains in muscle function during mechanical unloading, reloading, or overloading (respectively). While a cadre of research has studied the impacts of disuse or exercise training on muscle, few efforts have detailed the capacity for muscle to fully recover after chronic disuse, which we define as an example of biological resilience. Furthermore, there are no known works that have characterized the effects of multiple bouts of long-duration unloading and recovery, which we propose as biological repeatability. To determine if resilience and repeatability should be considered facets of muscle plasticity, a cross-sectional study design was created to assess muscle protein turnover throughout several changes in mechanoloading. Male Sprague-Dawley rats (*n* = 108) were placed in one of the following groups: 28 d unloading (HU), 28 d unloading with 56 d recovery with either passive ambulation reloading (HU+REC) or chronic resistance training (HU+EX), groups exposed to 28 d unloading, one of the recovery strategies, and then a second 28 d unweighting period (HU+REC+HU & HU+EX+HU), animals undergoing two unloading and two passive recovery cycles (HU+REC+HU+REC), or control (CON). At the end of the study, muscle mass, rates of synthesis, and markers of anabolism/catabolism were assessed in the lower limbs. Results included muscle mass being highly coupled to anabolic signaling and subsequent

protein synthesis. Muscle mass was significantly and consistently lower during unloading, but fully recovered with each reloading period. Our moderate-intensity, moderate-volume resistance exercise was insufficient to further improve recovery. And finally, the anabolic regulator DEPTOR was proven to correlate inversely with muscle mass. This study provides the first known evidence that repeatability is a component of muscle plasticity. The value in this work adds immediate benefits to manned space travel, clinical populations affected by serial unloading, as well as expands our general understanding of muscle biology.

DEDICATION

To my parents-

Who provided all of the love, resources, and opportunities that I could ever ask for. I am nothing without my family.

ACKNOWLEDGEMENTS

My professional career to date has been a long, blessed omnibus of poorly-made decisions, mistakes, failures, and uncanny luck that has allowed me to chase the future I wish to make for myself and fellow man. It is largely due to the help and guidance of so many individuals that I complete this dissertation and advance to the next stage in my academic life.

I would like to thank Dr. Jonen, who brought knowledge, inspiration, and guidance to a deflated pre-med undergraduate. His serendipitous arrival to RIT came at a time when I needed direction, and through his classes, I gained an appreciation for physiology. When home and family called Dr. Jonen away from Rochester, he ensured that I would have professional and research mentors to continue nurturing my budding interests. Thank you to Dr. Doolittle, who had far too much on his plate to be my undergraduate mentor, for his willingness to meet with me far too often, and whom I still believe created an undergraduate major simply to get me out of RIT. To Dr. Welle, I want to thank you for opening up your laboratory to me and showing me the amazing possibilities that exist in basic muscle research, it was immeasurably valuable to me.

To Dr. Jim Fluckey- I owe thanks that I cannot adequately express. You helped shape the way I think, the way I write, and the way I wish to conduct myself as I someday transition into overseeing a lab of my own. I don't think the student-mentor relationship was supposed to be this carefree and without conflict (I truly cannot recall any issues between you and I), but I appreciate that I always felt that you were in my

corner, supporting me even when I had gone out of my way to make your life more difficult. I hope I've left your lab in better shape than it was in when I arrived…barring the occasional flood or misplaced paper clip. Thank you for letting me overstay my welcome in your lab.

I wish to extend my gratitude to the rest of my committee. Thank you to Dr. Bloomfield, for allowing me to participate in the fascinating 3M project. To Dr. Massett, for his insight on the postdoctoral job search. To Dr. Hogan, for all of the study tissues, the research funding, and (perhaps most importantly) all the laughs. And to Dr. Kerwin, for advancing science and manned spaceflight through his lifetime efforts prior to, during, and following Skylab 2.

I am humbly thankful for Dr. Turner and the entire Space Life Sciences program of the National Space Biomedical Research Institute and the Human Research Program of NASA. The Fellowship was an amazing opportunity to enhance my career in a unique, integrative way, and the memories and opportunities afforded to me through the program are immense. Likewise, I would like to thank the Physical Education Activity Program, the Huffines Institute for Sports Medicine, the American College of Sports Medicine, the Department of Health & Kinesiology, the College of Education & Human Development, and Texas A&M University, for providing funding and support. And to the library at Texas A&M University, for letting me check out a textbook for nearly seven years.

To all of the students I've watched graduate from our department, and to the few that I somehow beat out of here, I thank you. Mats, Nic, and especially Michael, you

will always be the MBL in my mind. I am honored to have learned from each of you, and I wish you all success as your careers continue to grow. Mikey, you gave me all of the tools to not screw up. Thank you for that. I look forward to competing against you for each and every faculty opening at Texas A&M, as we both attempt to come home. To Sean, Johnny, Brandon, Steve, Brad, Andrew, Dan, Teak, Jackie, Chad, Clayton, Jorge, Heather, Corinne, Kayleigh, Evelyn, and all of the other students I've been blessed to interact with along the way, I am grateful. Keep working hard, but always find time to step out of lab and blow off some steam. I also must thank Josh Swift, for basically grabbing me by the collar and walking me down the hall to discover my dissertation topic. And lastly, to those who will undoubtedly carry on the reputation of the MBL, I wish you all the best. To Yang, Chelsea, Colleen, and Jessica, I will always be here to help in any way I can. Keep asking questions and searching for answers. Will, I know you'll do great things for Dr. Fluckey. Work hard and take care of the lab, and it will advance your career in more ways than you can imagine.

In this day and age, science is rarely completed solely by an individual researcher, and this project is certainly no different. Without the hard work of Dr. Hogan and his students, I wouldn't have a dissertation to write. I am also grateful for Dr. Bloomfield allowing us to use her lab facilities for the tissue harvest, as well as her pQCT. Additionally, the hard work by Dan Schiferl of Bone Diagnostic Inc. in providing protocols for the muscle and fat analyses for the pQCT has been very helpful. Drs. Chad Carroll and Delbert Gatlin, as well as the assistance by their technician, Kathryn and post doc, Camilo, respectively; I'm truly appreciative for your

involvement, as it broadens the scope of the study by allowing us to cast a wider net on our search for changes in plasticity. Dr. Carroll's processing of the collagen analyses and Dr. Gatlin's work on the amino acid quantification was a great boost to this work. I want to thank Shaik, for his execution of the bulk of the cytosolic amino acid preparation. This study could not have succeeded without the hard work of Liz Greene, who handled the chaos of science with a grace I haven't seen prior to or since her tenure at A&M. I am thankful for the hard work of Ray, who was the perfect training partner for those early mornings in the vivarium, as well as all of the graduate students (Scott M, Josh D, and Josh K) and undergraduates who were imperative to the success of the Hogan study. Your consistent dedication and high standards allowed this study to be the achievement it was. The brunt of the animal care was handled by this group, and with a study of this magnitude, it was certainly a Herculean task. My gratitude extends to all of the vivarium staff, who assisted throughout the project in maintaining the highest quality of animal care. I have to thank Yasaman, who was the heart and soul of the study. I owe my dissertation to you, Yasi. You taught me how to run a project, and you managed it in a way that set the bar high (possibly too high). Overseeing every detail of dozens of workers and hundreds of rats, I cannot find the superlatives to truly express my gratitude. Finally, this work could not have been done without NASA, and grant number NNX08AQ35G allowed us to complete so much quality research.

To Emily, who ran her way right into my heart and never stopped. Thank you for all you give, every day. The puppy and I don't deserve you.

NOMENCLATURE

HU	Hindlimb Unloading
REC	Recovery
EX	Resistance Exercise
CON	Control
pQCT	Peripheral Quantitative Computed Tomography
HPLC	High-Performance Liquid Chromatography
UPLC	Ultra-Performance Liquid Chromatography
SDS-PAGE	Sodium Dodecyl Sulfate Polyacrylamide Gel Electrophoresis
MHC	Myosin Heavy Chain
EDTA	Ethylenediaminetetraacetic acid
FSR	Fractional Synthesis Rates
FBR	Fractional Breakdown Rates
GCMS	Gas Chromatography-Mass Spectrometry
ULLS	Unilateral Leg Suspension
m-TBS	Tris-Buffered Saline in milk
SDS-PAGE	Sodium Dodecyl Sulfate Polyacrylamide Gel Electrophoresis
IDV	Integrated Density Value
EDL	Extensor Digitorum Longus

TABLE OF CONTENTS

Page

SECTION

LIST OF FIGURES

Page

Page

LIST OF TABLES

Page

I. INTRODUCTION

The term ‘plasticity’ was first described in 1959 to denote muscle’s inherent ability to substantially, swiftly, and specifically alter its form and function in response to a change in stimuli (55). It has long been appreciated that increases in skeletal muscle mass (hypertrophy) regularly occur during adolescent growth (133), sex hormone (38, 177) or anabolic steroid presence (225), and strength training (41), whereas chronic reductions of muscle mass (atrophy) are distinct in conditions of starvation (29), cachexia (57), sarcopenia (108), and disuse (54). Therefore, it would be plausible to hypothesize that the musculoskeletal system- as well as the majority of the human body, would undergo rapid and ample changes during spaceflight due to the microgravity environment contributing to sustained unloading. A cursory search of the literature pertaining to skeletal muscle during disuse atrophy in humans and murinae generates over 8,500 unique research articles, demonstrating the breadth and depth of our current understanding of muscle’s plastic adaptation to unloading and responses to countermeasures against disuse or inactivity. Less is known about the rates, magnitudes, and devices of recovery following the conclusion of spaceflight, bed rest, injury, or other conditions that result in mechanical unloading. If muscle is truly plastic, one might surmise a complete recovery in muscle size, function, and structure. And in cases of career astronauts- individuals who fly repeated long-duration missions in space, we should expect to see skeletal muscle change fully and appropriately to each condition, each time. The same would be expected of a number of subjects with chronic illness that require long periods of bed rest. The following review seeks to assess muscle’s

plasticity (ability to change) and biological resilience (capacity to change) during modifications in mechanical load; namely unloading, reloading, and overload. It also strives to demarcate biological repeatability, which we propose herein as muscle's ability to react in a predictable and complete manner to multiple recurring alterations in loading conditions. As the scope of all conditions of disuse and inactivity is beyond this review, we will focus on spaceflight-derived muscle alterations, or similar models, whenever possible, but much of the information presented has relevance in a number of atrophic stimuli (29, 54, 57, 108).

Unloading

Muscle Atrophy During Unloading

There are no shortage of studies to demonstrate that inactivity and disuse result in reductions in muscle mass or volume (1, 14, 21, 23, 30, 32, 43-45, 52, 56, 63, 64, 70, 82, 84, 92, 103, 108, 110, 115, 129, 153, 175, 176, 211, 215, 216). Complete unloading, such as that experienced during spaceflight, has been shown to be particularly atrophic. Spaceflight data from 6 m NASA and MIR missions report losses of 13-20% calf volume (218, 234)- despite their respective countermeasure programs, and 60-90 d bed rest studies demonstrate significant (25-29%) reductions in calf cross-sectional area (CSA) (176) and volume (220). Rodent models have shown losses of over 50% muscle mass, particularly in the vulnerable postural soleus muscle of the lower leg (127, 196, 216). Figure 1.1 shows the relationship between days of unloading and the losses in soleus muscle mass. Notably, the work by Thomason et al. demonstrates that the rates

of soleus atrophy slow down after 28 d, which is noted in the similar muscle masses displayed in 56 d unloaded soleus muscle (216), which suggests that muscle losses due to unloading may reach an eventual minimum, at least in rodents. Understanding if this steady-state disuse exists in humans is paramount to knowing the extreme limits or risks of unloading-induced atrophy.

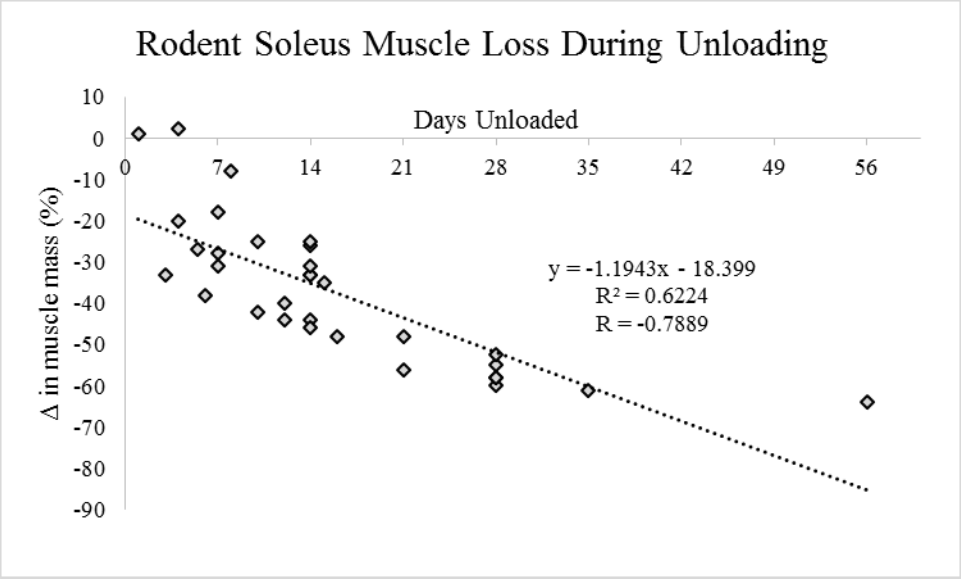

Figure 1.1. Muscle Atrophy During Unloading. A compilation of research demonstrating the relative loss of soleus muscle mass during hindlimb unloading studies (9, 12, 53, 64, 69, 93, 104, 113, 127, 140, 143, 180, 201, 216, 227, 229, 231).

Changes in muscle mass are the long-term result of muscle protein turnover, which is the final effect when muscle protein synthesis (anabolism) is assessed in conjunction to muscle protein breakdown (catabolism). Both processes operate continuously in muscle at some magnitude, and can often work independently of the

other system. When rates of protein synthesis exceed those of breakdown, there is a net gain in muscle protein and muscle mass/volume increases. When the protein is being synthesized at the same rate as older fibers are being broken down and recycled, there is no overall change in muscle mass. But when synthesis rates are exceeded by breakdown rates, a net loss of protein results and muscle atrophy occurs. A schematic of this interaction is provided in Figure 1.2.

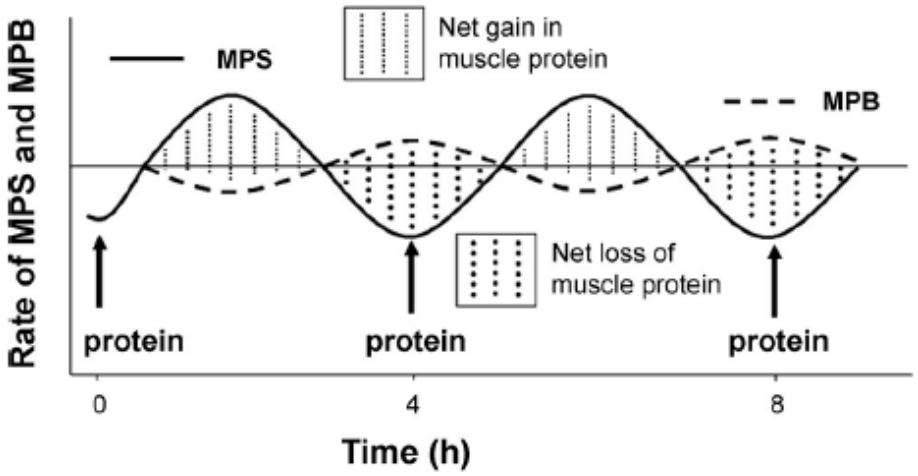

Figure 1.2. Muscle Protein Turnover. Rates of muscle protein synthesis (MPS; solid line) and muscle protein breakdown (MPB; dashed line) both fluctuate throughout the day and are individually affected by several stimuli, including protein-rich meals (pictured). Reprinted with permission from (161).

The net difference between protein accretion and resorption is muscle protein turnover, which in this illustration is showing a net balance. Net gains (hypertrophy) or losses (atrophy) can occur with altered synthesis, degradation, or both. The onset of disuse

has been reported to result in immediate and substantial reductions in protein synthesis that remain declined for long-duration disuse (22, 58, 191, 214) and increases in proteolysis (39, 40, 59, 213), but the rates of breakdown have been shown to slow or reverse in steady-state disuse (1, 214). In fact, this was first modeled by Thomason et al. in 1989, which is presented in Figures 1.3A-B.

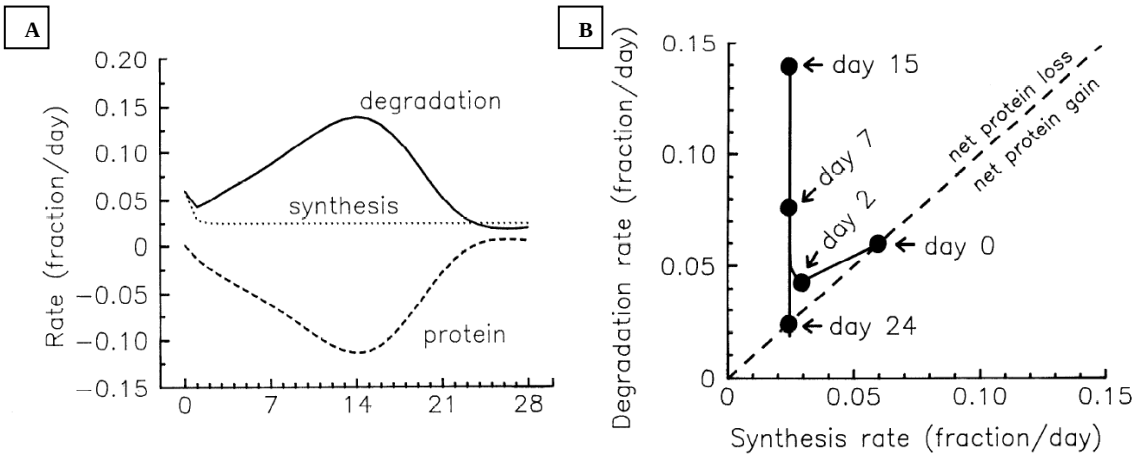

Figure 1.3. Muscle Protein Turnover Steady-State Timeline. Soleus protein turnover is demonstrated to (A) be heavy affected by protein degradation (solid line) in the early phase (Day 0-15), then returns to basal values, while protein synthesis remains similarly reduced for the entirety of the disuse period. Figure (B) demonstrates a second representation of the magnitude of breakdown, which appears to be highest at Day 15, as well as the chronic suppression of synthesis rates relative to Day 0. Reprinted with permission from (214).

Both figures suggest that muscle disuse atrophy, at least in rodents, reaches a steady-state that results in a new set-point for mass, synthesis, and breakdown, and that catabolic markers for steady-state disuse may not be altered from control values.

As degradation markers may not be ideal measures for assessing the later timepoints of steady-state muscle protein turnover during disuse, it appears that anabolism may be the primary driver of muscle mass during long-duration unloading. While the signaling pathways involved in muscle anabolism are vast, this review will give a brief description.

Other Models/Conditions of Disuse

Hindlimb unloading is a ground-based model that simulates the effects of microgravity on skeletal muscle with muscle mass losses that have been comparable to both space flown rats and astronauts (For Review; (60, 149). Its strength for skeletal muscle studies is in part due to a cardiovascular fluid shift similar to that observed during spaceflight (94) and a substantial reduction in lower limb muscle activity (173). Its value for modeling general disuse or inactivity has been stated, but other models of disuse do exist. Here we highlight some examples of muscle atrophy models, and when necessary, contrast the findings between the different stimuli on muscle mass regulation.

Spinal dissection and denervation, while highly effective at generating anterograde muscle loss (17, 51, 99, 204), are fairly permanent and therefore beyond the scope of this review.

Casting studies have been used, often in short-duration studies but some longer duration studies exist (23). Casting has demonstrated rapid and substantial muscle atrophy compared to the contralateral control leg (115, 119), even eliciting muscle losses in the extensor digitorum longus (EDL) (68), a muscle typically not impacted by

unloading in healthy rats (44, 99). A key difference between the casting and hindlimb unloading models is that muscle atrophy during casting appears to be independent of declines in muscle protein synthesis and is contingent upon increases in degradation (119). A 10 d casting study by Childs et al. found no changes in ERK1/2 activity- a participant in MAPK-mediated regulation of muscle translation initiation, during cast immobilization or recovery (36), a stark difference from the hindlimb unloading work by Dupont et al. that illustrates ERK1/2 phosphorylation (and subsequent activation) is diminished in the soleus at Day 7, 14, and 28 of (hindlimb) suspension (53). Dupont et al. continue to demonstrate that casting did alter key regulatory signals in the PI3K/Akt/mTOR pathway, with 10 d of casting resulting in decreased anabolic activity in these proteins that was quickly reversed and even elevated upon removal of the cast (36).

One final model of skeletal muscle atrophy poses a unique challenge to clinicians. The diaphragm muscle is known to be a high-endurance skeletal muscle that is rapidly atrophied upon the onset of mechanical ventilation (103, 132, 192), which carries immediate health risks to a number of patients who begin assisted breathing for any reason. In fact, McClung et al. highlight a unique problem when comparing mechanical ventilation-induced atrophy of the diaphragm versus the atrophy observed in hindlimb muscles during traditional disuse. They note that the increased proteolysis (42) and decreased protein synthesis (191) that occur in their model are much more substantial that the reductions in rates of synthesis observed in hindlimb unloading studies (141).

Reloading

Most human work shows full recovery of muscle area/volume with adequate time (175, 181, 218), and this ability to recover appears to be supported by animal models (23, 168, 226), likely due to recovered anabolic signaling (17) and altered protein breakdown (17, 210), although some work suggests complete recovery of mass may be only in some muscles (196). Prior work by our collaborators has also demonstrated muscle's ability for a full recovery of mass, given appropriate time (6, 226). However, it does appear that some risks and ill-effects are present with recovery from steady-state disuse.

The study by Krippendorf and Riley demonstrated that long-duration unloading created myofibrillar damage upon reloading conditions (121), and their group has expanded by detailing how disuse atrophy contributes to alterations in actin-myosin concentrations and cytoskeletal proteins (169-171, 173) and human rehabilitation research has confirmed that atrophied muscle is highly susceptible to load-induced damage (163). Fortunately, the fiber type shift observed during spaceflight (56, 218) and other forms of mechanical unloading (88, 219), appears to be reversed with as little as 14 d normal ambulatory recovery (100, 114).

Overload

While exercise during disuse is certainly relevant in trying to mitigate muscle atrophy, there have been mixed results on its effectiveness, with bed rest human data showing promise (13, 59, 219) and human spaceflight data showing less effectiveness

(218). NASA has recognized that major knowledge gaps in their understanding of muscle physiology in space include optimizing an exercise prescription to minimize or fully mitigate the risks of long-duration unloading, as well as to understand the time-course for loss of muscle mass, strength, and function during missions of differing durations (162). That being said, assessing exercise *during* steady-state disuse is beyond the scope of this Dissertation, and overload will be discussed in regards to muscle plasticity following and preceding periods of disuse.

The 30 yr follow-up to the famous Saltin et al. "Dallas Bed Rest and Training Study" concludes that 21 d of bed rest in healthy 20 yr old men had a more profound impact on their functional capacity than 30 years of aging did (145). If steady-state disuse has that substantial of an effect on overall health and function, efforts must be made to better understand the impact of recovery after unweighting. As mentioned above, there are substantial risks with increased tissue damage from unloading (163, 168), as well as decreased strength and altered functional capacity (82, 218), so therapies must pay heed to these added risks.

Endurance exercise post-disuse can provide improvements to normalize the myosin heavy chain isoform transition that occurs during unweighting, as endurance exercise for 14 d after a 14 d unloading period improved the percentage of type I fibers, the fiber cross-sectional area, and oxidative enzyme activity, but cannot improve mass above that observed with 14 d passive recovery after disuse (106). When focusing on resistance training paradigms following mechanical unloading, a great deal of the information came from rehabilitative research in elderly patients, particularly hip surgery

recipients. While some have found increases in strength after surgery via resistance exercise training (95, 148, 185, 193), none of these studies quantified muscle mass or volume. The study by Suetta et al. found that 12 wk resistance training after long-term disuse resulted in improved quadriceps area and strength over standard rehabilitation practices, as well as provided benefits to muscle morphology and architecture, maximal isometric strength, rapid muscle force, and muscle activation (205, 206). Aging rodent studies have demonstrated that young animals lose more relative muscle mass during 28 d casting (vs. older rats), but that the younger animals recovered more fully than the older animals, demonstrating an aging effect on resilience with disuse and recovery (235). Therefore, if aging individuals can make marked improvements in muscle volume and strength following disuse by employing overload training principles, and young muscle has demonstrated a greater ability to grow, it is fully plausible that the correct exercise prescription during recovery can have a hypertrophic effect in young, healthy muscle. Studies such as those above highlight muscle's biological resilience, demonstrating that elderly individuals still have the capacity for hypertrophy, but aging research suggests that this may be impaired, at least in passive recovery.

Repeatability

While many researchers tout skeletal muscle as a 'plastic' tissue, we know surprisingly little about muscle's capability to respond to repeat cycles of disuse. To date, the field that best offers insight on repeatability is with exercise training/detraining studies (90, 91, 101, 102, 202).

In one study women were trained for 20 wk with resistance exercise, then detrained for 30-32 wk, and then had a second 6 wk retraining period. The initial training period resulted in increases in maximum dynamic strength, increased fiber diameter (of each myosin isoform), and a decrease in type IIx fibers. Detraining did not affect CSA of any fibers but did alter the distribution of myosin- the percentage of type IIx fibers increased. Retraining increased CSA and readjusted the percentage of type IIx fibers to the original proportions, but no markers of overall mass or volume were assessed (202).

Hakkinen et al. carried out a study in middle-aged and elderly individuals that used 24 wk of resistance training (2x/wk) followed by either a 3 wk detraining period followed by 21 wk retrain or a 24 wk detraining period. The main finding they discussed was that the 3 wk short-term detraining only led to minor changes (-6% change in maximum isometric force in middle-aged), whereas 24 wk prolonged detraining resulted in muscle atrophy with decreases in CSA, one repetition maximum, and isometric force measurements. Retraining did not clearly lead to any improvements above detraining values (90). In another study with elderly subjects, men and women trained for 24 wk (strength increased +49% vs. pre-training control), detrained for 24 wk (-18% strength vs. trained), and then had a 12 wk retraining period (+20% strength vs. detrained). Strength changes during detraining were accompanied by increases in fat infiltration (assessed by density), with decreases after retraining. Interesting, muscle volume did not change throughout the study (209), suggesting that the gains in strength were due to neural adaptations (For Review; (72)).

In perhaps the best known study design to date that could discuss biological repeatability in muscle mass adaptations, Ogasawara et al. compared continuous resistance training (3x/wk) to a time-matched periodic resistance training (6 wk train, 3 wk detrain, 6 wk retrain, 3 wk detrain, 6 wk retrain). After the initial training period, CSA of the triceps brachii and pectoralis major muscles as well as the maximum isometric voluntary contraction and one repetition maximum of the elbow extensors were similar, noting that overall improvements to the same initial training were similar. The results for CSA of the triceps brachii, pectoralis major, one repetition maximum (elbow extension), and maximum voluntary contraction (elbow extension) is presented in Figures 1.4A-D, respectively. Whereas persistent gains are observed in Figures 1.4A-D for continual training, net losses (albeit isometric strength was unchanged) of each measurement are observed for each detraining period. The impact of detraining/retraining cycles did not impact the overall outcomes when compared to 24 wk continuous training (157).

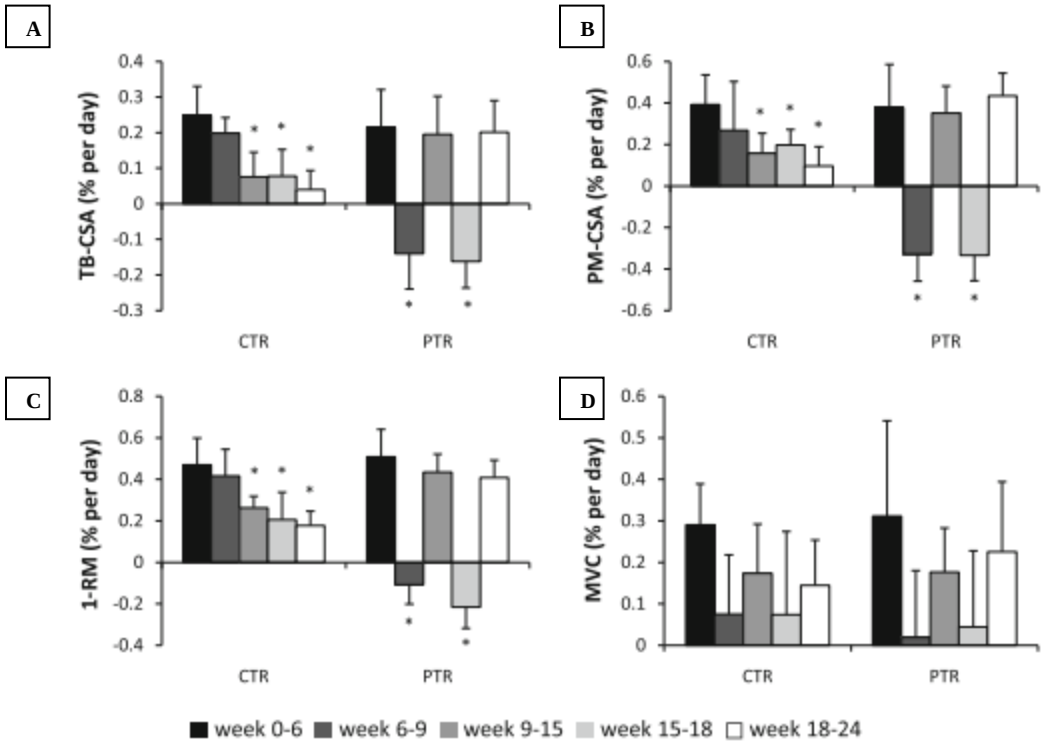

Figure 1.4. Evidence of Repeatability in Muscle in Response to Training/Detraining/Retraining. Using 24 wk continuous resistance training (CTR) or 24 wk of periodic resistance training (PTR), training effects measured include (A) % change in CSA of the triceps brachii, (B) % change in CSA of the pectoralis major, (C) % change in one repetition maximum (elbow extension), and (D) % percent change in maximum voluntary isometric contraction (elbow extension). For PTR subjects, week 0-6 was initial training, week 6-9 and 15-18 were detraining, and week 9-15 and 18-24 were retaining. Reprinted with permission from (157).

Implications for physical training notwithstanding, this work offers clear evidence that muscle plasticity is a highly repeatable function and is closely driven by mechanotransduction. Yet there is a paucity of supporting studies to further examine this phenomenon. In fact, there is no known research that chronicles and rationalizes

skeletal muscle's capacity to adapt to mechanical stimuli observed during multiple long-duration bouts of unloading and recovery. Thus, there is a *critical need* in the fields of not only manned spaceflight and other catabolic conditions resulting from muscular unloading, but also muscle biology- to demarcate the plasticity and repeatability of skeletal muscle to respond to unloading, reloading, and overloading. It is with this goal that the following Sections are presented.

II. IMPACT OF MULTIPLE BOUTS OF LONG-DURATION UNLOADING AND RECOVERY ON SKELETAL MUSCLE

Synopsis

Mechanical unloading, particularly that experienced during spaceflight, has long been understood to contribute to rapid and substantial adaptations within skeletal muscle. Previous works have often demonstrated that many of the alterations resulting from mechanical disuse are reversed with a reintroduction of load, and have supported the concept of muscle plasticity and biological resilience. This study sought to challenge the range of muscle plasticity through exposure to repeat bouts of mechanical loading changes, similar to what an astronaut might experience over the course of several missions throughout a career. Male Sprague-Dawley rats were assigned to one of the following groups: 28 d of disuse through hindlimb unloading (HU), 28 d of HU followed by 56 d of normal 1 g recovery (HU+REC), two unique bouts of HU with recovery between (HU+REC+HU), animals undergoing two full cycles of unloading and recovery (HU+REC+HU+REC), and an age-matched control group (CON). Following the completion of their final time point, muscles of the lower limb (gastrocnemius, soleus, and plantaris) were collected for study. Muscle weights and cross-sectional areas were reduced following 28 d of mechanical loading, with no notable differences between HU and HU+REC+HU. With few exceptions, all three muscles fully recovered their masses to CON values following 56 d of normal ambulation. Mixed muscle protein synthesis rates directly coincided with mass and loading condition, with no apparent changes due to repeated alterations. Myofibrillar protein synthesis was unchanged by load in the

soleus muscle, but both the gastrocnemius and plantaris muscles demonstrated consistent reductions following 28-d unloading bouts. Challenging muscle plasticity, muscle collagen concentrations were found to be higher following the second unweighing period and remained elevated following 56 d of recovery. Notably, amino acid availability was assessed in the gastrocnemius and did not contribute to muscle atrophy associated with mechanical unloading. We conclude that muscle's anabolic responses to alterations in mechanical loading are preserved throughout multiple perturbations, but repeated periods of unloading may cause additive strain to muscle structure (collagen). This study provides the first known evidence that repeatability is a component of muscle plasticity.

Introduction

Rapid and substantial musculoskeletal atrophy remains one of the greatest physiological limitations of manned space exploration. Mechanical unloading during long-duration (≥ 14 d) microgravity exposure results in reductions in muscle volume (128, 234) and strength (8, 211), and previous interventions have been unable to fully mitigate these losses (218). Muscle adaptations to spaceflight at the cellular level include reduced muscle fiber size and contractile properties (228), a myosin heavy chain shift towards a faster isoform (218), and a predisposition to sarcolemma damage upon reloading (122, 163). Many researchers agree that muscle atrophy and strength reductions are the result of a negative protein turnover due to decreased muscle protein synthesis, confirmed with astronaut data (203) and supported by human ground-based

analogs of spaceflight (58, 80) as well as in-flight (4, 183) or ground-based rodent work (64).

While there is a paucity of information on the physical and physiological alterations to skeletal muscle of astronauts returning from long-duration spaceflight, various models have helped shape our understanding of muscle's recovery from microgravity. Most human work shows full recovery of muscle area/volume with adequate time (175), and appears to be supported by animal models (23, 168, 226). Fiber size (26) and contractile properties (189, 226) return with adequate time, and the fiber type distribution recovers to pre-unloading values (43). And finally, muscle protein synthesis rates are elevated soon upon the onset of reloading and is maintained throughout the recovery process (210). Overall, it appears that skeletal muscle recovers to pre-flight characteristics with adequate reloading, although these findings may not persist in aging tissue (207).

Much of the previous works studying astronaut physiology during and following spaceflight agree with the concept of muscle plasticity. First described in 1959, muscle plasticity denotes muscle's inherent ability to substantially, swiftly, and specifically alter its form and function in response to a change in stimuli (55). Observations during initial exercise studies have largely shaped our understanding of muscle plasticity and responses to training (41, 81, 98, 182), whereas research detailing the time-course and effects of disuse atrophy in various clinical situations (29, 54, 57, 108) exhibit the opposing end of the plasticity spectrum. The breadth and complexity of muscle plasticity are detailed in Table 1 of the thorough review by Flück and Hoppeler (62), but

little is known about the skeletal muscle effects of repeated (and opposing) alterations to stimuli. Questioning muscle's biological resilience (capacity for change) or repeatability (ability to replicate previous changes) has been briefly explored through training/detraining/retraining studies (102, 202), but little disuse work has been attempted. To date, only two studies have studied muscle's response to multiple unloadings and recoveries (86, 196), but neither work expanded their findings beyond simple muscle wet mass measures.

The intent of the current study was to characterize the sequential responses of repeated long-duration mechanical unloading and passive recovery on muscle mass, morphometry, and anabolism. We opted to utilize the well-accepted rodent model of hindlimb unloading to elicit rapid and severe muscle atrophy, for a duration deemed sufficient for complete atrophy (194, 216), and gave the animals adequate time to fully recover muscle mass to pre-unloading mass (196). Based on previous works (6), we believe that muscle will generally respond predictably and consistently with each unloading and reloading period, at least within tissue types, in which unloading (first and second disuse bout) will result in atrophy, and reloading (via passive ambulation) will result in a full recovery of mass and composition. This work seeks to first reaffirm the field's previous findings on plasticity in response to mechanical unloading, then discern the capacity of biological resilience as well as determine if muscle outcomes observed during unloading and recovery are repeated with subsequent changes in load.

Materials and Methods

Animals

All procedures described herein were approved by and conducted in accordance with the Institutional Animal Care and Use Committee of Texas A&M University. Male Sprague-Dawley rats (Harlan Laboratories Inc, Houston, Texas) were selected for this study and obtained at 5.5 months of age. Animals were group-housed for 2 wk in a standard environment (23ºC ± 2ºC, 12:12 h dark/light cycle) and given water and standard rodent chow *ad libitum*. The Teklad 8604 chow (Harlan Laboratories Inc, Indianapolis, Indiana) supplied 3.0 kcal/g, was comprised of 54% carbohydrates, 32% protein, and 14% fat, and provided sufficient micronutrients to support normal growth. Following transport recovery and acclimation, all animals were singly-housed, normalized by body weight, and assigned to one of the following groups: 1) 28 d of constant hindlimb unloading (HU, n = 16), 2) 28 d HU session immediately followed by a 56 d recovery bout of normal ambulation (HU+REC, n = 16), 3) two HU cycles of 28 d with a 56 d recovery bout between unloadings (HU+REC+HU, n = 16), 4) two alternating cycles of 28 d HU and 56 d recovery (HU+REC+HU+REC, n = 14), and 5) an age- and housing-matched control group (CON, n = 14). Figure 2.1 illustrates the experimental design. Body weights were recorded weekly, and twice-daily health checks were carried out to ensure each animal was healthy and loaded appropriately.

In order to prevent any effects due to food consumption (proven to affect body and

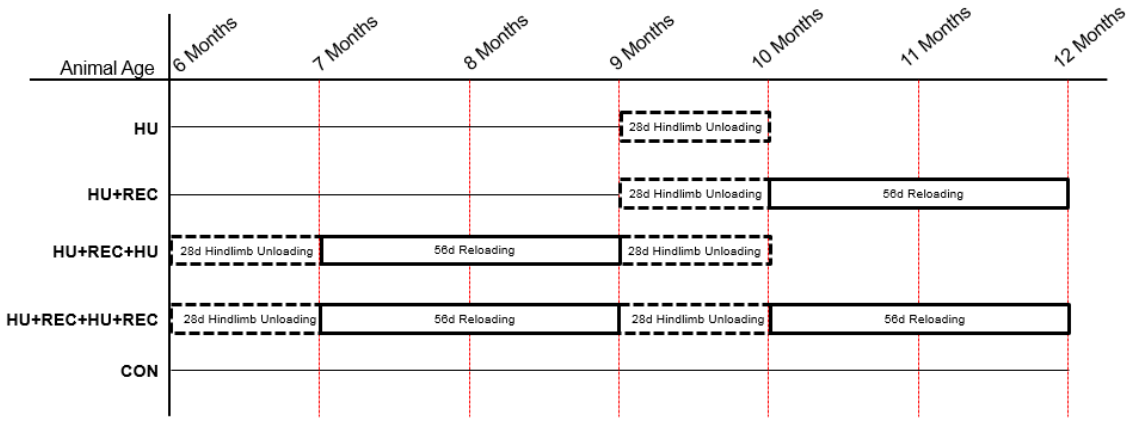

Fig. 2.1. Study I Experimental Study Design. Hindlimb Unloading (HU) was achieved via a tail suspension harness and carried out continuously for 28 d, and Reloading (REC) was carried out by passive recovery through normal cage ambulation.

muscle masses), all animals were pair-fed during the first week of each unloading period.

At the conclusion of the study, each animal was anesthetized with ketamine/xylazine (100 $mg \cdot kg^{-1}$ & 10 $mg \cdot kg^{-1}$, respectively) prior to tissue harvest. All animals that were non-weight-bearing at their final time point (HU, HU+REC+HU) were anesthetized prior to removal from their tail suspension, in order to prevent any undesired consequences that could come with weight-bearing. Cardiac puncture was used to draw approximately 2 - 4 ml of whole blood under anesthesia, using a Serum Separator Tube (Becton, Dickinson and Company, Franklin Lakes, New Jersey). Blood samples were gently inverted five times to activate clotting, allowed to rest at room temperature for 30 min, centrifuged at 1,200 g for 30 min in order to collect blood serum, which was then stored at -80 °C. Cardiac puncture was immediately followed by euthanasia via decapitation, and removal of the tibia as well as the gastrocnemius,

soleus, and plantaris muscle of each hindlimb. Tibiae were cleaned of soft tissue and stored in 70% ethanol at 4 °C, and the gastrocnemius, soleus, and plantaris muscles were excised, cleaned of extraneous blood, fat, and connective tissue, weighed and recorded, and finally snap-frozen in liquid nitrogen before -80 °C storage.

Hindlimb Unloading

Simulated microgravity was accomplished through the use of hindlimb unloading (HU), a well-published ground-based analog to spaceflight (For Review; (149)) commonly utilized by our group to study muscle atrophy (50, 63, 64, 118). Tail harnesses were attached 24 h prior to each suspension period and removed for each recovery bout. Animals were briefly anesthetized with 2% isofluorane (US Pharmacopia, Rockville, Maryland) in order to attach the custom tail harness. A thin layer of non-irritant adhesive (Amazing Goop, Eclectic Products, Los Angeles, California) was generously applied around the base of the tail, and was firmly attached to porous athletic tape (Kendall, Mansfield, Massachusetts) and allowed to dry. The athletic tape attached to the base of the tail (~2.54 cm of contact) on each lateral side and extended ~15.24 cm distally, where each end of the tape connected and joined a paper clip. The animal was allowed to recover from anesthesia and wore the harness while ambulating normally. On Day 0 of each unloading period the paper clip of the harness was then attached to a swivel apparatus overhead that was connected to a steel bar bisecting the top of the custom-built 45.72 cm x 45.72 cm x 45.72 cm cage. When attached, the animal's hindquarters would be elevated high enough that they could not

come in contact with the floor of the cage, resulting in a 30° head-down tilt and complete disuse of the hindlimbs. The steel bar allowed for nearly complete movement about the cage with the forelimbs, but prevented the animal from resting its rear quarters on the walls. This system did not inhibit the rats' ability to feed, drink, or groom.

On Day 28 of HU, animals reaching their final time point were anesthetized, removed from HU, and subjected immediately to tissue harvest. Animals that would continue on to a reloading bout were anesthetized, had their harnesses removed, and allowed full ambulation throughout their 56 d recovery session before being harvested (HU+REC & HU+REC+HU+REC) or subjected to a second unloading (HU+REC+HU). Any animal found out of its harness during a health check was immediately removed from the study, as were animals facing any sort of health concern. Overall, the study maintained a 95% success rate in animals completing each 28 d HU bout.

Peripheral Quantitative Computed Tomography

Peripheral Quantitative Computed Tomography (pQCT) scans were carried out immediately prior to tissue harvest, and allowed for both *in vivo* measures and *ex vivo* supporting data. Under the aforementioned ketamine/xylazine anesthesia, animals were firmly secured and had their left lower limbs scanned on a Stratec XCT Research-M device (Norland Corp., Fort Atkinson, Wisconsin) calibrated with a hydroxyapatite standard cone phantom. A custom 3D-printed brace (ABS polymer) was used to prevent movement of the lower limb during the scanning procedure. Total tibia length was first recorded by the machine, and then the left lower hindlimb was scanned *in vivo* at a rate

of 2.5 $mm \cdot s^{-1}$ with a voxel resolution of 100 μm^2 and a scanning beam thickness of 500 µm. Two slices were scanned at 50% tibia length (middiaphysis), 1 mm apart, and were later assessed for total limb cross-sectional area (CSA_{TOT}), muscle tissue CSA (CSA_{MM}), and fat (both subcutaneous and intramuscular) CSA and percentage. Excised tibiae were scanned *ex vivo* when necessary to determine tibia length for normalized mass analyses (see Results).

Scan images were analyzed using Stratec software (ver. 6.00, Norland Corp., Fort Atkinson, Wisconsin). The software, originally designed for bone research and clinical assessments, was adjusted to allow for skeletal muscle measurements using methods revised from other works (174). Standardized analysis schemes were utilized for all muscle acquisitions. A region of interest was established around the entire limb circumference, and specific values were discerned through image filters and density thresholds available with the XCT550 software. Limb cross-sectional area (CSA_{TOT}) of the midshaft was determined with a Calcbd analysis (outer threshold of -101 $mg \cdot cm^{-3}$, contour mode 1, peel mode 2, inner threshold of 40 $mg \cdot cm^{-3}$, and visualized with filter F03F05F05), which the software determined as the total area assessed, and additional analyses allowed for the determination of the muscle cross-sectional area (CSA_{MM}) and fat cross-sectional area (CSA_{FAT}). The software also computes a "trabecular area" (all tissues with densities < 40 $mg \cdot cm^{-3}$) in this case representing fat and bone marrow area ($CSA_{FAT\&MARROW}$) and "cort-subcort area" (all tissues with densities > 40 $mg \cdot cm^{-3}$) indicative of bone, muscle, and skin area. Additional analyses were used to remove the bone, marrow, and skin values. Bone and marrow ($CSA_{BONE\&MARROW}$) was calculated

(outer threshold of 710 $mg \cdot cm^{-3}$, inner threshold of 710 $mg \cdot cm^{-3}$), with "trabecular" values representing marrow total area (CSA_{MARROW}) and "cort-subcort" determined bone tissue area of the tibia and fibula of each slice (CSA_{BONE}). Finally, skin area (CSA_{SKIN}) was isolated from CSA_{TOT} with a Cortbd analysis (outer threshold of -101 $mg \cdot cm^{-3}$, separation mode 4, inner threshold of 2000 $mg \cdot cm^{-3}$). Collectively, these analyses provided the following data:

CSA_{TOT}, CSA of the entire limb at the midshaft of the tibia

$CSA_{MM} = CSA_{TOT} – (CSA_{FAT\&MARROW} + CSA_{BONE} + CSA_{SKIN})$

$CSA_{FAT} = CSA_{FAT\&MARROW} - CSA_{MARROW}$

$\%_{FAT} = CSA_{FAT} / CSA_{TOT}$

Each slice was analyzed individually and then averaged for each animal.

Collagen

Collagen concentration was measured by quantification of the collagen-specific amino acid hydroxyproline via High Performance Liquid Chromatography (HPLC) using previously published methods (33, 166). Approximately 10 mg of pulverized gastrocnemius muscle was carefully cleaned of extraneous collagen fibers, weighed, freeze-dried for 36 h and then reweighed to provide a dry weight and water concentration measure. Samples were derivatized and injected onto an HPLC (LC-20AB and SIL-20, Shimadzu Scientific Instruments, Columbia, Maryland) and separated on an XTerra RP 18 column (Waters, Milford, Massachusetts). Hydroxyproline samples were normalized to an internal standard and compared with a standard curve (33).

Unless otherwise noted, all chemicals were obtained from Sigma Aldrich (St. Louis, Missouri).

Intramuscular Amino Acid Concentration

Individual concentrations of 29 amino acids commonly found in the skeletal muscle cytosolic pool were assessed with ultra-performance liquid chromatography (UPLC) using techniques previously described (27). In short, 500 mg of pulverized gastrocnemius tissues were homogenized using a Polytron (Brinkmann Lab Equipment, Westbury, New York) in 3 ml 1.5 M perchloric acid, vortexed, and centrifuged until pelleted. The supernatants (containing the cytosolic pool) were neutralized with 2 M potassium carbonate (1:1 v/v) and lipid extracted with diethyl ether (1:3 v/v), vortexed, and the ether layer removed. The lipid-free samples were filtered through 0.2 µm polycarbonate syringe filters and derivatized with o-phtaldialdehyde before analyzed on a UPLC (Waters Corporation, Milford, Massachusetts). Identification and quantification of amino acids was accomplished using external standards. Samples were analyzed in triplicate.

Measurement of Protein Synthesis

Twenty-four hour fractional synthesis rates (FSR) for the mixed (total) and myofibrillar (contractile) fractions were assessed in the gastrocnemius, soleus, and plantaris muscles using deuterium oxide (^2H_2O) incorporation techniques well-described by our lab (76, 156). Animals were given a bolus dose of 99.9% deuterium oxide

(Cambridge Isotopes, Andover, Massachussetts) in a saline solution (0.9% NaCl) via intraperitoneal injection (20µl·g^{-1} body weight) 24 h prior to tissue harvest. The priming bolus was supplemented with 4% $^{2}H_2O$ drinking water provided *ad libitum* to maintain enrichment during the final 24 h of the study. FSR was determined by measuring the levels of ^{2}H incorporation into the muscle protein and the precursor pool, described in detail below. To isolate the myofibrillar subfraction for FSR, differential centrifugation was employed using methods detailed elsewhere (156). Pulverized skeletal muscle (~60 mg) was homogenized with a Polytron in a 0.4 ml Norris buffer (25 mM Hepes, 25 mM benzamidine, 10 mM magnesium chloride ($MgCl_2$), 5 mM β-glycerophosphate, 4 mM EDTA, 2 mM phenylmethanesulfonylfluoride (PMSF), 0.2 mM ATP, 0.5% protease inhibitor cocktail P8340 (v/v), 0.1% Triton-X 100 (v/v), 10 mM activated sodium orthovanidate (Na_3VO_4), and 100 mM sodium fluoride (NaF); pH 7.4). Each sample rested on ice for 1 h before centrifugation at 30,000 g for 30 min at 4 °C. The pellet, containing the myofibrillar subfraction, was then prepared identically to the mixed fraction samples.

Sample preparation for total protein FSR was determined in the mixed subfraction as previously described by our lab (76). Both pulverized mixed muscle tissues (~30 mg) and myofibrillar pellets were homogenized with a Polytron in 0.3 ml of 10% (w/v) trichloroacetic (TCA) acid. Samples were centrifuged at 5,000 g for 15 min at 4 °C, the supernatant (containing free, unbound amino acids) was decanted and removed, 0.3 ml TCA added to the pellet and vortexed until broken down, and the wash-spin step repeated two additional times. After the third and final wash step the protein-

bound pellet was dissolved in 0.4 ml of 6 N hydrochloric acid for 24 h at 100 °C. 100 µl of the hydrolysate was dried down and derivatized with 100 µl of a 3:2:1 (v/v/v) solution of methyl-8 (N,N-Dimethylformamide dimethyl acetal, Thermo Fisher Scientific, Waltham, Massachusetts), methanol, and acetonitrile for 1 h at 70ºC. Derivatized samples were injected into a GCMS (Agilent 7890 GC & 5975 VL MSD, Agilent Technologies, Santa Clara, California) using previously described parameters (74, 75). All muscle samples were analyzed in triplicate and calculated from a linear regression formula generated by known ^{2}H-alanine standards (0-2.0% ^{2}H-alanine:alanine) prepared identically to the sample procedure.

Deuterium (^{2}H) enrichment of the available precursor pool was determined by quantifying $^{2}H_2O$-enriched serum based on a linear regression formula generated by deuterium standards identically prepared. A 20 µl serum sample was allowed to react with 2 µl of 10 N sodium hydroxide and 4 µl of a 5% (v/v) acetone in acetonitrile solution at room temperature for 24 h. Then, ~0.5 g sodium sulfate decahydrate was added as a drying agent, and 0.6 ml chloroform was introduced to the sample to stop the isotopic exchange between $^{2}H_2O$-enriched serum samples and acetone. A small aliquot (1 µl) was injected into the GCMS, volatilized, separated, and detected using methods detailed in earlier publications by our lab (74, 75, 156). All serum samples were prepared and measured in duplicate, and the average value used in FSR calculations.

FSR was calculated using the following equation:

$$FSR = E_A \cdot [E_{BW} \times t(d) \times 3.7)^{-1} \times 100,$$

where E_A represents the amount of protein-bound ^2H-alanine (mole percent excess), E_{BW} is the quantity of ^2H_2O in the precursor pool (mole percent excess), *t*(d) designates the total time of incorporation (in days), and 3.7 represents the exchange coefficient of ^2H between body water and alanine (e.g. 3.7 of 4 carbon-bound hydrogens of alanine exchange with water (49)).

Statistical Analysis

All analyses were carried out using SigmaStat v3.5 (Systat Software Inc., San Jose, California). A one-way analysis of variance (ANOVA) was used to compare groups, and when significant F-ratios were present a Student-Newman-Keuls (SNK) post hoc procedure was used to test differences among group means. Significance levels were predetermined at $p < 0.05$. For all results described in this study, groups sharing a similar letter are not significantly different ($p \geq 0.05$) and exact *p* values may be included for results that warrant highlighting and discussion, even if deemed not statistically significant.

Results

Skeletal Muscle Mass, Body Weight, and Body Composition

As expected, 28 d of hindlimb unloading (HU) resulted in significant ($p < 0.05$) reductions in mass in the gastrocnemius (72% of control mass), soleus (46%), and plantaris (80%) muscles, as shown in Figures 2.2A-D.

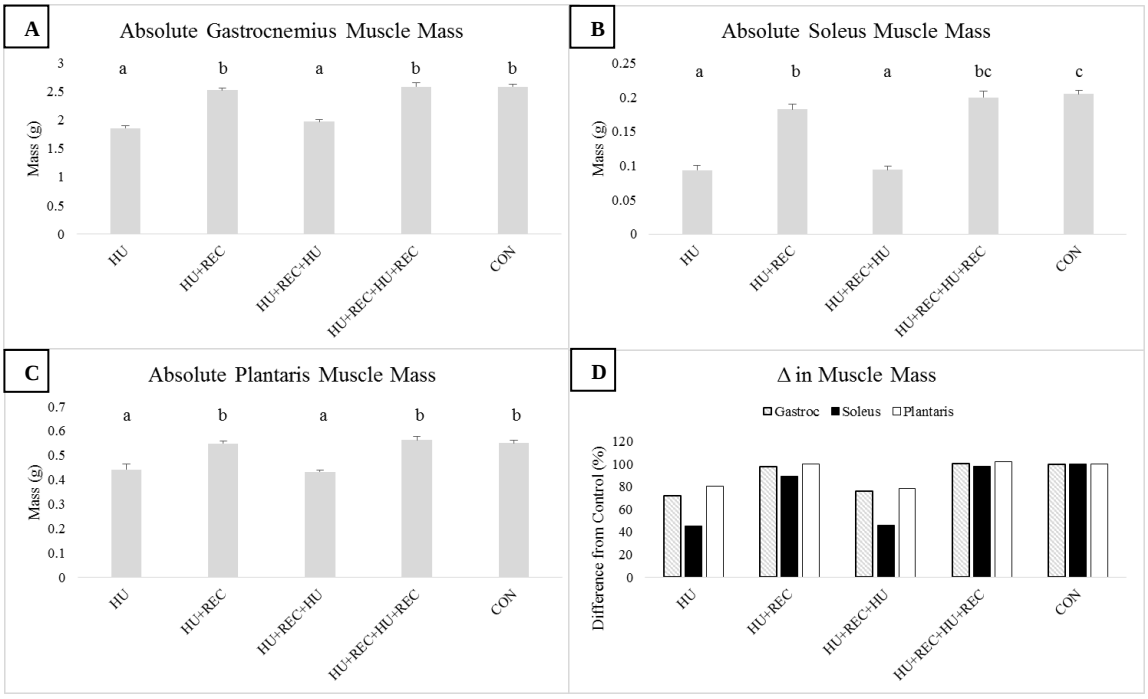

Fig. 2.2. Study I Muscle Mass (Absolute). Muscle wet mass for the (A) gastrocnemius, (B) soleus, and (C) plantaris tissues, as well as (D) percent change from control for each tissue type. Values are means ± SE. Bars displaying similar letters in each graph are not significantly different from one another.

And as previous works (23, 232) have suggested, 56 d of passive recovery through normal cage ambulation following long-duration disuse was sufficient loading to return muscle mass to control values ($p \leq 0.05$) for the gastrocnemius (98% of control) and plantaris (99%), although the HU+REC soleus did fail to recover to control values (89%). Animals exposed to a second bout of unloading (HU+REC+HU) had lower muscle mass in all three sural tissues, and to the same extent as the animals exposed to a single unloading period (HU). Finally, all muscles were at control values after the second reloading period (HU+REC+HU+REC).

To determine if the muscle atrophy observed was a result of body mass alterations, final time point body weights were recorded and presented in Figure 2.3D, and gastrocnemius, soleus, and plantaris muscle masses were normalized by body weight (Figures 2.3A-C, respectively). Body masses were reduced in HU and HU+REC+HU to a similar extent, and 56 d of reambulation allowed for a complete recovery of body weight.

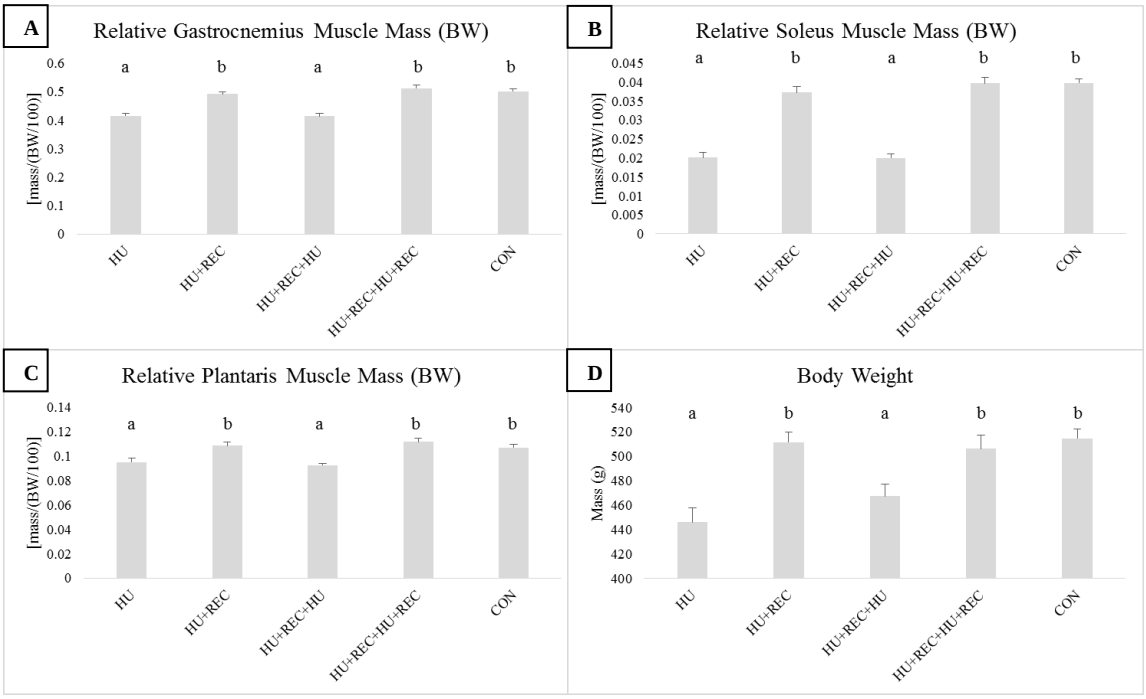

Fig. 2.3. Study I Muscle Mass (Relative to Body Weight). Endpoint data for muscle mass normalized by body weight (g muscle · g body weight^{-1}) for the (A) gastrocnemius, (B) soleus, and (C) plantaris tissues, when assessed by (D) body weight (g). Values are means ± SE. Bars displaying similar letters in each graph are not significantly different from one another.

As body weights were expected to differ between groups, final tibia length was selected as a marker indicative of body size (but not altered by changes in mechanical loading conditions in adult rodents) and muscle masses were normalized by tibia length (g muscle mass · mm tibia length^{-1}). Some differences in mean tibia length were observed among groups, as presented in Figure 2.4D. HU animals revealed significantly shorter tibiae, though only a mean difference of 2.3% vs. CON. Animals in the HU+REC+HU+REC treatment had the longest mean tibia length, that while not different from CON or HU+REC groups, were significantly different than HU (3.1% difference) and HU+REC+HU (2.2%).

Muscle mass, when observed relative to tibia length, produced similar results to the values of body weight-normalized mass and identical findings presented for absolute values (Figures 2.4A-C). HU observed reduced muscle weights (gastrocnemius, soleus, and plantaris) that were comparable to those that occurred during HU+REC+HU, and while the gastrocnemius and plantaris returned to CON values in both recovery groups (Figures 2.4A & 2.4C), the soleus muscle (Figure 2.4B) failed to fully recover during the first reloading cycle.

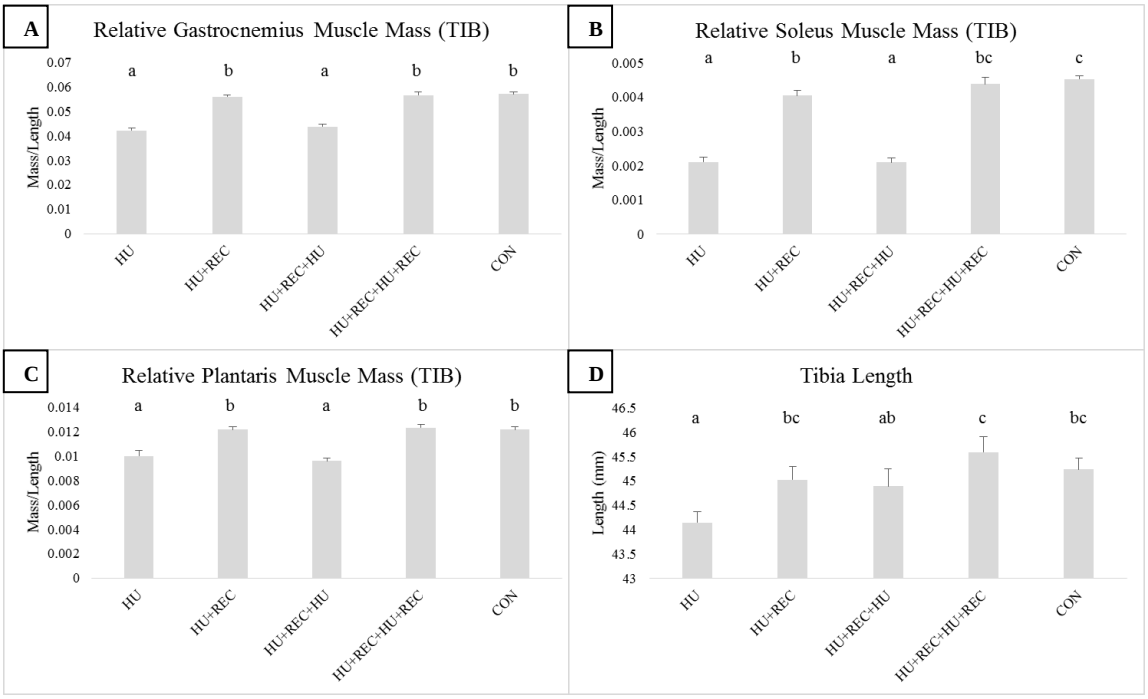

Fig. 2.4. Study I Muscle Mass (Relative to Tibia Length). Endpoint data for muscle mass normalized by bone length (g muscle· mm tibia length^{-1}) for the (A) gastrocnemius, (B) soleus, and (C) plantaris tissues, as well as (D) *in vivo* tibia lengths. Values are means ± SE. Bars displaying similar letters in each graph are not significantly different from one another.

In vivo pQCT scans of the lower limb were analyzed at the midshaft of the tibia (representative image in Figure 2.5D) to discern the effects of changes in mechanical loading on limb CSA (Figure 2.5A), muscle CSA (Figure 2.5B), and fat percentage (Figure 2.5C). The plastic brace to prevent movement during pQCT measurements is shown in the representative image for the HU+REC+HU animal (bottom left scan; Figure 2.5D). Limb CSA and muscle CSA results are consistent with all of the mass

data above. Fat percentage (determined as $CSA_{FAT} \cdot CSA_{LIMB}^{-1}$) was highest among control animals and lowest among HU+REC+HU rats.

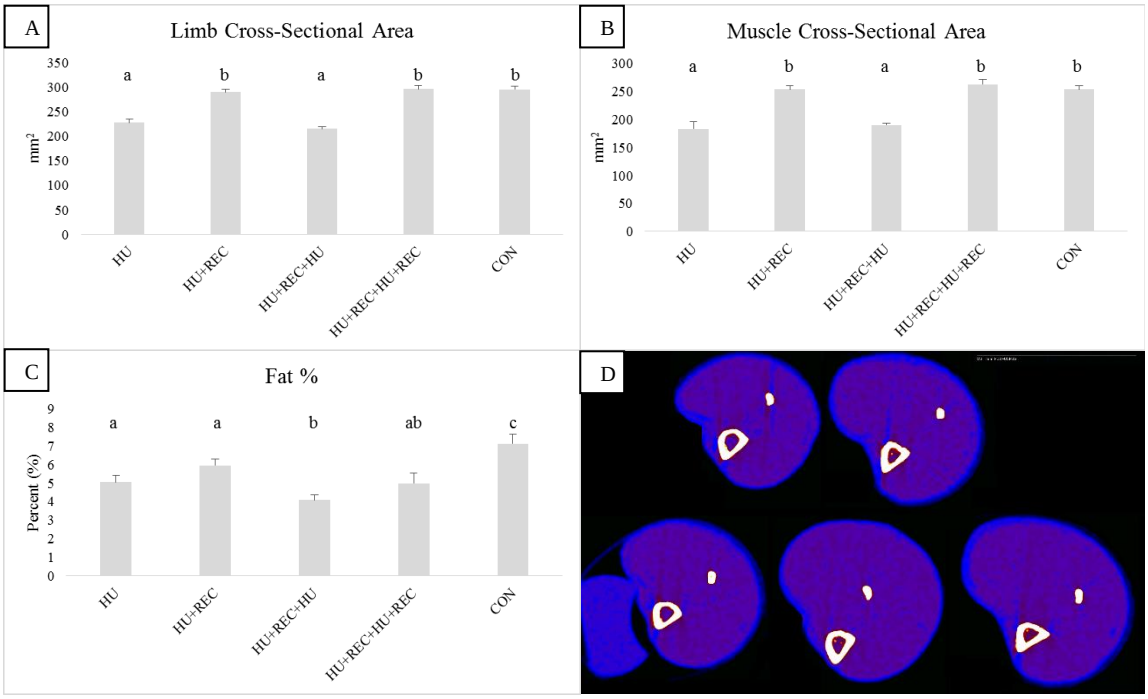

Fig. 2.5. Study I Peripheral Quantitative Computed Tomography (pQCT) Morphometry. *In vivo* assessments of the lower limb (at 50% tibia length) were taken just prior to sacrifice and evaluated for (A) limb CSA, (B) Muscle CSA, and (C) Fat Percent, Figure (D) poses representative scans of experimental groups (top line: HU, HU+REC; bottom line: HU+REC+HU [with brace], HU+REC+HU+REC, and CON). Values are means ± SE. Bars displaying similar letters in each graph are not significantly different from one another.

Gastrocnemius Water and Collagen Content

A small aliquot of gastrocnemius wet muscle was weighed, desiccated, and reweighed to determine muscle water concentration, and is displayed in Figure 2.6. Water percent was lower in HU and HU+REC+HU compared to HU+REC+HU+REC and CON, and HU+REC was not different than any other group.

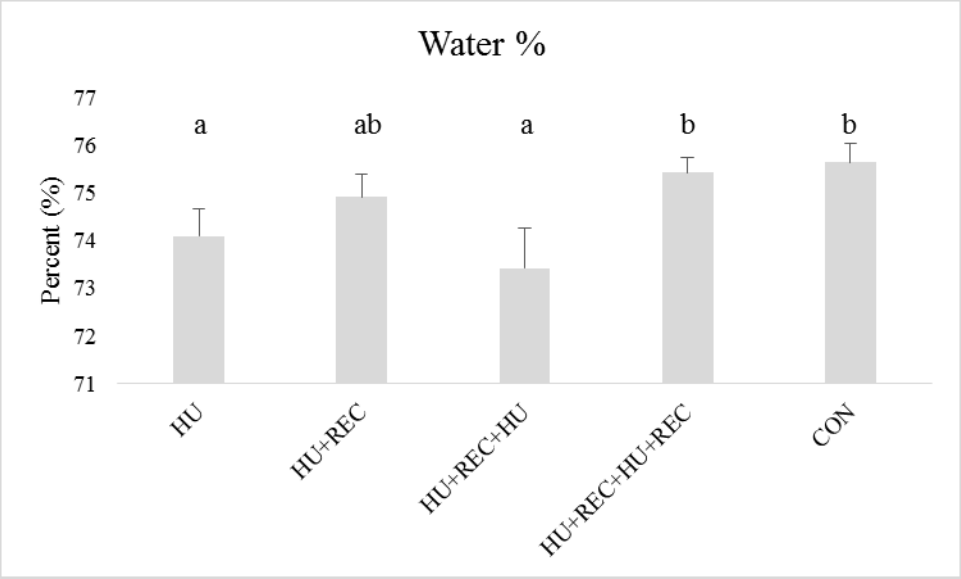

Fig 2.6. Study I Muscle Water Content. Muscle weights were taken before and after desiccation to determine water concentration. Values are means ± SE. Bars displaying similar letters in each graph are not significantly different from one another.

Collagen concentration was quantified in the gastrocnemius muscle using hydroxyproline concentrations determined using HPLC techniques. Muscle collagen was not elevated due to a singular event of long-duration unloading, but was increased (83% increase vs. CON) following the repeat bout of unweighting. Muscle collagen

concentrations returned to non-significant values in the HU+RE+HU+REC group (vs. CON), although there was a 43% difference among these groups.

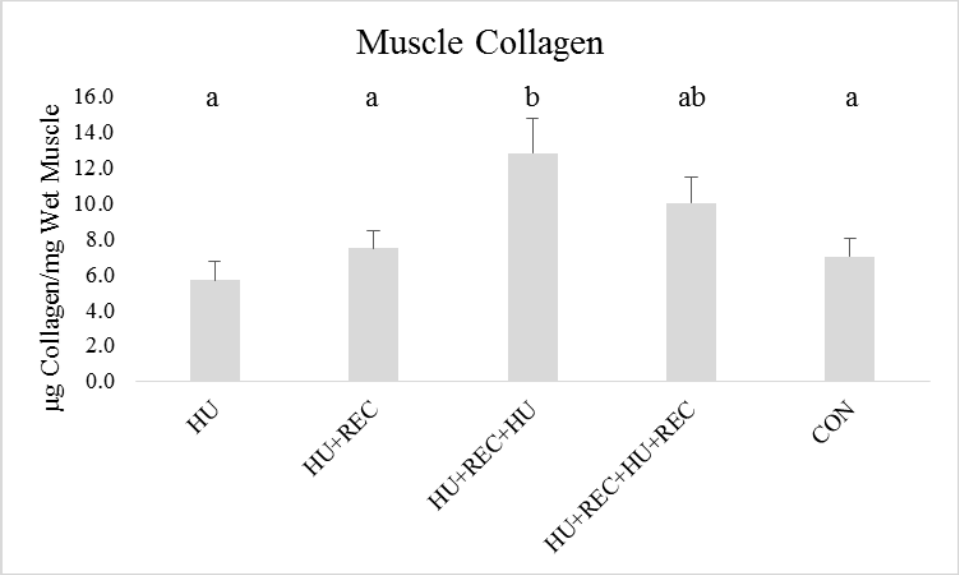

Fig. 2.7. Study I Gastrocnemius Collagen Concentration. Collagen concentration assessed in the gastrocnemius by quantifying hydroxyproline content per mg wet tissue. Values are means ± SE. Bars displaying similar letters in each graph are not significantly different from one another.

Gastrocnemius Cytosolic Amino Acid Profile

Individual concentrations of 29 amino acids were measured in the free pool of the gastrocnemius as an indication of amino acid availability and to investigate which (if any) essential amino acids appeared to rate-limit muscle anabolism during mechanical unloading. Presented in Table 2.1, no essential amino acids are reduced by long-duration unloading, and

	HU	HU+REC	HU+REC+HU	HU+REC+HU+REC	CON
BCAA					
Isoleucine	0.1657 ± 0.0246[a]	0.0934 ± 0.0045[b]	0.1544 ± 0.0082[a]	0.0819 ± 0.0085[b]	0.0850 ± 0.0041[b]
Leucine	0.2929 ± 0.0439[a]	0.1520 ± 0.0066[b]	0.2729 ± 0.0161[a]	0.1348 ± 0.0104[b]	0.1420 ± 0.0066[b]
Valine	0.3204 ± 0.0392[a]	0.1993 ± 0.0071[b]	0.3016 ± 0.0180[a]	0.1885 ± 0.0120[b]	0.1871 ± 0.0076[b]
EAA					
Histidine	0.1535 ± 0.0138	0.1717 ± 0.0076	0.1614 ± 0.0079	0.1532 ± 0.0103	0.1594 ± 0.0100
Lysine	0.2528 ± 0.0445	0.2910 ± 0.0194	0.2553 ± 0.0313	0.2975 ± 0.0328	0.2647 ± 0.0266
Methionine	0.0439 ± 0.0082	0.0296 ± 0.0034	0.0380 ± 0.0024	0.0281 ± 0.0045	0.0248 ± 0.0031
Phenylalanine	0.1022 ± 0.0166[a]	0.0719 ± 0.0038[b]	0.0982 ± 0.0063[a]	0.0593 ± 0.0062[b]	0.0690 ± 0.0041[b]
Threonine	0.3514 ± 0.0801	0.3776 ± 0.0175	0.3593 ± 0.0223	0.3932 ± 0.0336	0.3784 ± 0.0256
Tryptophan	N/A	N/A	N/A	N/A	N/A
Other Common					
Alanine	2.1768 ± 0.1937	2.2515 ± 0.0923	2.0905 ± 0.1146	2.1624 ± 0.1591	2.3031 ± 0.1205
Arginine	0.1130 ± 0.0273	0.1073 ± 0.0057	0.1137 ± 0.0146	0.1099 ± 0.0145	0.0944 ± 0.0098
Asparagine	0.2977 ± 0.0327	0.4832 ± 0.1594	0.5618 ± 0.2710	0.4206 ± 0.0933	0.4548 ± 0.1467
Aspartate	0.0726 ± 0.0047[a]	0.0725 ± 0.0043[a]	0.0495 ± 0.0068[b]	0.0791 ± 0.0073[a]	0.0786 ± 0.0041[a]
Cysteine	N/A	N/A	N/A	N/A	N/A
Glutamate	0.4634 ± 0.0148[a]	0.5649 ± 0.0300[b]	0.6040 ± 0.0533[ab]	0.5158 ± 0.0483[ab]	0.4366 ± 0.0240[a]
Glutamine	4.3383 ± 0.2829	4.7407 ± 0.2745	4.7276 ± 0.4532	4.9578 ± 0.3956	4.8488 ± 0.4000
Glycine	2.8103 ± 0.2395	2.4545 ± 0.1025	2.8013 ± 0.1810	2.4735 ± 0.1844	2.4305 ± 0.1862
Proline	0.2355 ± 0.0246[a]	0.2928 ± 0.0099[b]	0.2309 ± 0.0142[a]	0.2733 ± 0.0194[ab]	0.2703 ± 0.0135[ab]
Serine	0.4917 ± 0.0360	0.5577 ± 0.0217	0.5413 ± 0.0311	0.5614 ± 0.0408	0.5581 ± 0.0422
Tyrosine	0.1014 ± 0.0125	0.0954 ± 0.0044	0.1046 ± 0.0066	0.0885 ± 0.0075	0.0867 ± 0.0048
All Other					
3-Methylhistidine	0.0632 ± 0.0096	0.0643 ± 0.0049	0.0560 ± 0.0089	0.0685 ± 0.0098	0.0650 ± 0.0057
α-Aminobutyric Acid	0.5510 ± 0.0388	0.4763 ± 0.0241	0.5513 ± 0.0515	0.5155 ± 0.0507	0.4904 ± 0.0292
Anserine	10.6103 ± 0.8998[a]	7.4142 ± 0.3011[b]	10.1498 ± 0.6731[a]	7.0908 ± 0.4397[b]	7.7005 ± 0.3310[b]
β-Alanine	0.1384 ± 0.0089[ab]	0.1298 ± 0.0039[a]	0.1511 ± 0.0069[b]	0.1235 ± 0.0031[a]	0.1284 ± 0.0052[a]
Carnosine	2.1357 ± 0.1699	2.3507 ± 0.1015	2.3833 ± 0.1192	2.3497 ± 0.156	1.9775 ± 0.0758
Citrulline	0.2080 ± 0.0226	0.2368 ± 0.0108	0.2182 ± 0.0172	0.2455 ± 0.0202	0.2335 ± 0.0145
Ethanolamine	0.0707 ± 0.0070[a]	0.0556 ± 0.0025[ab]	0.0667 ± 0.0037[a]	0.0508 ± 0.0035[a]	0.0530 ± 0.0035[b]
Hydroxyproline	0.1171 ± 0.0182[ab]	0.1122 ± 0.0074[ab]	0.1056 ± 0.0092[ab]	0.0634 ± 0.0086[b]	0.0703 ± 0.0090[ab]
Ornithine	0.0168 ± 0.0029[a]	0.0249 ± 0.0013[b]	0.0170 ± 0.0016[ab]	0.0227 ± 0.0023[ab]	0.0228 ± 0.0020[ab]
Phosphoethanolamine	0.0698 ± 0.0107[a]	0.0444 ± 0.0038[b]	0.0651 ± 0.0080[a]	0.0378 ± 0.0035[b]	0.0446 ± 0.0042[b]
Taurine	17.9230 ± 1.5208	15.5782 ± 0.6011	16.8416 ± 0.8655	14.3525 ± 1.0718	14.6455 ± 0.7223

Table 2.1. Study I Gastrocnemius Cytosolic Amino Acid Profile. Cytosolic amino acid composition determined by UPLC. Values are means ± SE. Data displaying different letters within each amino acid are significantly different.

only 2 of the 29 amino acids were below control values (aspartate and ornithine) in HU or HU+REC+HU, but neither was consistently reduced in both disuse groups. Notably, the concentrations of the branched-chain amino acids (isoleucine, leucine, and valine) were elevated (72-117%) in the unloaded animals, compared to all loaded groups.

Muscle Protein Synthesis

Muscle anabolism was evaluated by following the incorporation of a stable labeled isotope (deuterium oxide) into muscle tissue over the final 24 h of each animal's final loading condition. The method allows for quantification of the mixed (Figure 2.8) and myofibrillar (Figure 2.9) fractions in each of the study tissues.

The mixed (total) FSR presented in Figures 2.8A-C display the 24 h synthesis rates in the (A) gastrocnemius, (B) soleus, and (C) plantaris muscles. All three muscles exhibit significant reductions of FSR over the final 24 h period of unloaded animals (HU and HU+REC+HU), and demonstrate that mixed FSR after 56 d of ambulatory recovery was similar to mixed FSR in controls.

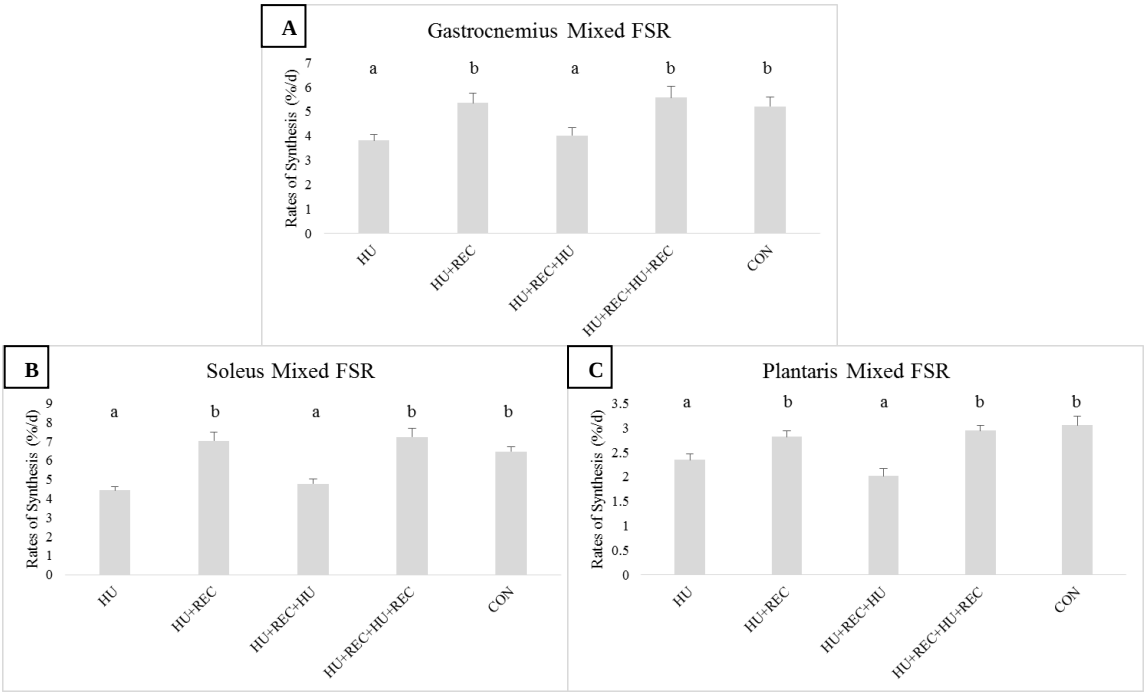

Fig. 2.8. Study I 24 h Mixed Fractional Synthesis Rates. Deuterium oxide tracer methods were used to quantify 24 h cumulative mixed FSR in the (A) gastrocnemius, (B) soleus, and (C) plantaris muscles. Values are means ± SE. Bars displaying similar letters in each graph are not significantly different from one another.

Figures 2.9A-C provide the myofibrillar (contractile) fractional synthesis rates observed during this study. Myofibrillar FSR was not different (vs. CON) by any loading condition in the soleus muscle (Figure 2.9B), but 28 d of hindlimb unloading demonstrated lower myofibrillar FSR in both the gastrocnemius (Figure 2.9A) and plantaris (Figure 2.9C) muscles. There were no differences between HU and HU+REC+HU rates for either muscle, and HU+REC was identical to control levels, but plantaris myofibrillar FSR was higher than control in HU+REC+HU+REC.

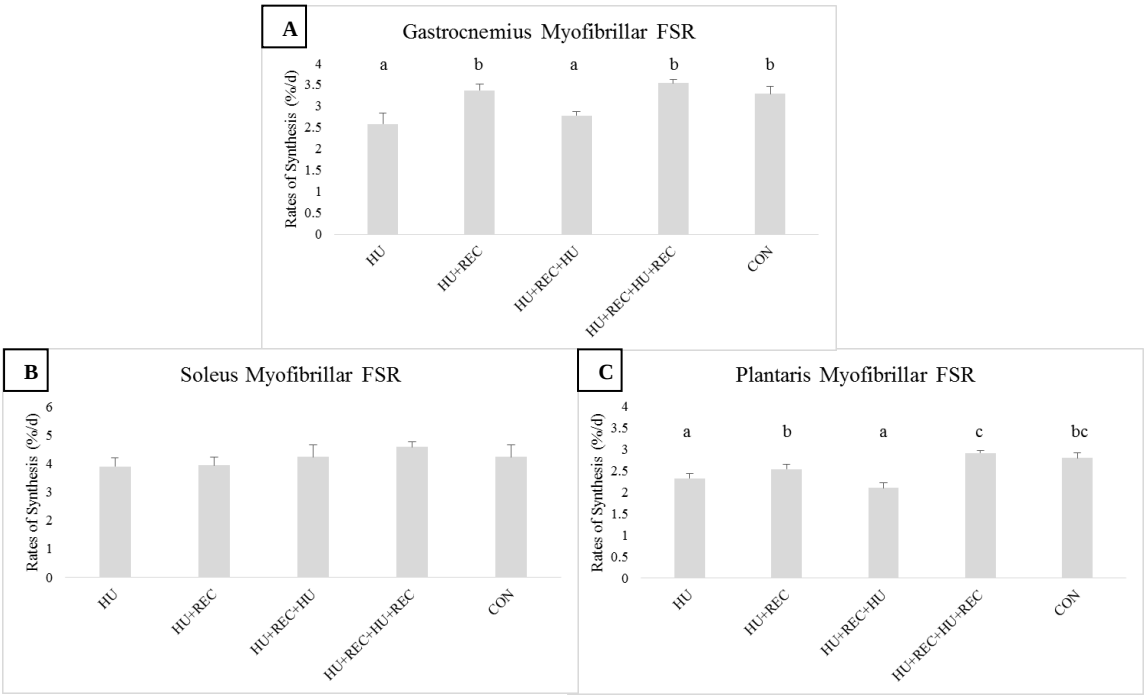

Fig. 2.9. Study I 24 h Myofibrillar Fractional Synthesis Rates. Deuterium oxide tracer methods were used to quantify 24 h cumulative myofibrillar FSR in the (A) gastrocnemius, (B) soleus, and (C) plantaris muscles. Values are means ± SE. Bars displaying similar letters in each graph are not significantly different from one another.

Discussion

While numerous works have outlined the impact of mechanical unloading on skeletal muscle mass, composition, and anabolism (For Review; (1, 61, 161)), fewer works have delved into the same details with regards to the reversal of these effects during recovery after unloading, and there are no known studies to follow these findings throughout multiple perturbations in mechanical loading status beyond that of wet mass measure (86, 196). In the current study, we sought to challenge the notion of muscle plasticity by invoking a study design to produce a known atrophic response, allow ample

time to make a full recovery, and then repeat these conditions of mechanical unloading and reloading. The aim of this study was to establish biological resilience (capacity to change) and repeatability (similar responses to repeated stimuli) as functions of muscle plasticity to mechanical loading. For the first time, we provide evidence that changes in muscle mass due to mechanical loading are replicable throughout serial bouts of disuse and recovery in response to repeated anabolic reactions to load conditions, but morphological changes (collagen, in the present study) may challenge muscle plasticity.

Muscle Mass and Cross-Sectional Area is Plastic and Repeatable

Spaceflight data in rats has demonstrated that there are fiber type- and biomechanical-associated factors in regards to degree of atrophy, with the entire plantarflexor complex more predisposed to disuse atrophy than similar muscles positioned on the anterior compartment of the lower limb, and the predominantly slow-twitch soleus having greater losses compared to the mixed- and fast-twitch compositions of the gastrocnemius and plantaris, respectively (111, 159, 217). The soleus and gastrocnemius have relatively normal EMG activity during HU, whereas the tibialis anterior (TA) muscle has 2- to 4-fold increases in activity over that same timeframe (3), which may help explain why the TA may be better preserved compared to the plantarflexors. Previous work by our colleagues has demonstrated a full recovery of mass from 28 d of hindlimb unloading was achieved with 14 d of ambulatory recovery in the plantarflexor group (6). This information is strongly supported by the muscle mass data presented in Figures 2.2A-D. Twenty-eight days of hindlimb unloading (HU)

resulted in substantial losses of muscle mass in the gastrocnemius (Figure 2.2A), soleus (B), and plantaris (C), but these weights returned to control values at the completion of a 56 d recovery period of ambulatory reloading (HU+REC), with one exception. Additionally, when a second bout of mechanical disuse was added to the experiment, the losses in muscle mass observed during HU+REC+HU were similar to those during the single unloading bout (HU), and was again fully returned to control muscle masses with a 56 d reloading period (HU+REC+HU+REC). When expressed as its respective change from control (Figure 2.2D), the soleus muscle observed the greatest losses during HU and HU+REC+HU (45.6% and 45.9% of CON, respectively). As the rat soleus muscle is comprised of ~87% slow-twitch, type I myosin heavy chain (10), there is rationale for it to sustain greater losses during mechanical unloading compared to the mixed-fiber gastrocnemius (71.8% and 76.3% of CON) and fast-twitch plantaris (80.4% and 78.5%) muscles. Interestingly, the present data indicate that soleus absolute mass did not recover to CON values in HU+REC, but did reach control values in the HU+REC+HU+REC group. This might suggest that there is incomplete recovery with 56 d of ambulatory recovery following the first HU, but there are no other data presented in the study to corroborate this proposition.

To determine if changes in body mass impacted muscle masses, we then opted to evaluate tissue weight based on body weight. Body weight (Figure 2.3D) was significantly reduced in each unloading bout and returned to control values with each recovery period. Relative muscle masses [muscle wet weight $\cdot$ (body weight/100)$^{-1}$] for each tissue type was identical to the findings presented for absolute muscle masses, and

alleviated the anomaly observed in HU+REC for the absolute soleus mass. While not directly assessed in this study, food intake during unloading and recovery was taken into consideration. Unloaded animals were pair-fed with ambulatory rats during the first week of each suspension period, and previous works by Allen et. al have reported that food intake was unchanged during the early portion of unloading and then was actually elevated during Weeks 2-4 of unloading (vs. CON) (5). Another paper reported that food intake did decrease, albeit not significantly, during the early phases of unloading in mice (31). We therefore conclude that changes in body masses are due to physiological alterations rather than nutritional deficits, and similarly, that muscle atrophy during unloading is not due to caloric constraints.

Because body weights were known to fluctuate during prolonged mechanical unloading, we also decided to normalize muscle mass by tibia length, a variable not known to change during unloading or recovery parameters. Muscle mass (relative to tibia lengths) are presented in Figures 2.4A-C, and tibia lengths are presented in Figure 2.4D. Relative muscle weights match the absolute mass values identically, demonstrating the same reductions in mass with unloading in each tissue (gastrocnemius, soleus, and plantaris) are recovered with ambulatory reloading. Remarkably, mean tibia length was lowest in the two unloading groups, with only the HU animals having a significantly lower tibia length than control. This was likely due to poor randomization during the group assignments, as male rates are considered skeletally mature around 5-6 m of age, with minimal long bone growth (6, 112), and

there are no known studies to suggest that mechanical disuse contributes to a change in tibia length or growth.

One major contribution of this study was to use peripheral Quantitative Computed Tomography (pQCT) to assess muscle parameters *in vivo* in the rat. Commonly utilized to study outcomes in bone (5, 6, 15), pQCT has been used to study limb CSA, muscle CSA, and muscle density in humans (174), but to our knowledge, has not been used in this capacity in rodents. Limb CSA and muscle CSA (Figures 2.5A and B, respectively) are qualitatively identical to the previously discussed muscle weight data, and suggest that alterations in muscle mass may be determined *in vivo* in rats by assessing cross-sectional areas from scan slices of the middiaphysis. The implications for this would allow for serial measures of muscle alterations without terminating the animal, and could greatly decrease the number of animals necessary for certain research studies assessing alterations in muscle mass. Further works should confirm these findings and seek to model a correlative measure of pQCT morphometry to specific muscle masses with high confidence. Additionally, the pQCT determined the percentage of fat present in the slices measured, and is presented in Figure 2.5C. All groups demonstrated a reduction in their fat percentages when compared to CON, suggesting that a single unloading bout may result in marked losses of limb (and potentially whole-body) adipose tissue that does not fully recover with 56 d of ambulation. In fact, a second unloading period further compounds this loss of fat tissue relative to the limb area. Considering the points made above in regards to body weight during unloading, our work collectively suggests that the reductions in body weight observed during

hindlimb unloading are not due to caloric restriction, but do result in preferential losses in fat tissue. LeBlanc et al. report that while fat loss in humans was observed on shorter, 17 d missions in space, they did not observe changes on the long-duration 16-28 wk shuttle and Mir missions (128). Collectively, all of the aforementioned findings on muscle mass and CSA reaffirm muscle plasticity and support the proposal of biological repeatability in muscle.

Muscle Collagen is Elevated and Persistent Following a Second Disuse Period

The changes observed in gastrocnemius muscle water concentration (Figure 2.6) may contribute to the changes in muscle mass previously described, and several groups have similarly reported either increased protein concentration or decreased water concentration in atrophied muscle following mechanical unloading (109, 110, 152).

Muscle collagen concentration was quantified by hydroxyproline detection via HPLC, and is provided in Figure 2.7. The increase in collagen concentration observed in HU+REC+HU persists, albeit not significantly (vs. CON) in the HU+REC+HU+REC group. Previous works have shown increases in intramuscular collagen concentrations in rats during mechanical unloading or spaceflight (139, 147) which has been shown to compromise muscle function (83). While these findings occurred with a single bout and we found no such increase in our HU group, this may be due to specific muscle and spaceflight nuances, as Haus et al. observed their increased collagen concentration in their bed rest study but not in their unilateral leg suspension work (96). This finding also disagrees with the concept of muscle plasticity and suggests disconnects in biological

repeatability. Clinically, this work may highlight functional risks for career astronauts or other populations plagued with serial periods of long-duration disuse.

Changes in Muscle Mass Coincide with Plastic and Repeatable Anabolism

Changes in muscle mass are due to the chronic muscle protein turnover, which is the culmination of muscle protein synthesis rates (FSR) and muscle protein degradation, or fractional breakdown rates (FBR). True quantification of FBR is difficult to accomplish with current methodologies due to the nuances of assessing bygone molecules, and qualitative markers of FBR were not utilized in the current study. While catabolic markers and protein degradation are rapidly elevated at the onset of mechanical unweighting (215, 221), several studies indicate that FBR returns to control or even depressed levels during long-duration unloading (1, 78, 214). Focusing on anabolism's role on regulating muscle mass during repeated disuse and recovery, we opted to utilize a 24 h measure of muscle protein synthesis via deuterium oxide, which can effectively detect anabolic responses during a longer assessment window (74, 76, 124, 156), and more readily presents muscle anabolism in a free-living state, which is valuable as FSR is known to be severely impacted by a number of stimuli, including feeding (73), stress (144), and sleep (164). The mixed (total) FSR for gastrocnemius, soleus, and plantaris muscles is presented in Figures 2.8A-C, respectively. Each muscle demonstrates considerable reductions in FSR in the HU group, with the greatest reduction present in the soleus muscle (68.5% of CON FSR). FSR recovers fully to CON values in the HU+REC group, strongly supporting the notions of muscle plasticity and biological

resilience, and demonstrates that muscle mass is tightly coupled to muscle anabolism measures in a free-living state. The study further embraces muscle plasticity in the subsequent unloading and recovery groups, with HU+REC+HU values for mixed FSR being depressed vs. CON to rates similar to those observed during HU. Likewise, mixed FSR in HU+REC+HU+REC is not different than HU+REC or CON values. To our knowledge, no published works to date have demonstrated muscle's repeated anabolic responses to serial changes in chronic loading conditions.

The late-stage values for muscle mass following chronic disuse or recovery may possibly be accomplished almost completely by alterations in muscle anabolism, which may indicate that catabolism's role in shaping muscle mass during loading stimuli may be at the initial onset of said condition, if at all. Further works should determine the status of catabolic markers on the end-point Day 28 of unloading and Day 56 of reloading.

The contractile component of skeletal muscle- the myofibrillar fraction, is presented in Figure 2.9A-C for the study tissues. The gastrocnemius and plantaris myofibrillar responses are similar to those presented in the mixed fraction, and are shown in Figures 2.9A and 2.9C, respectively. A ULLS study carried out over 10 and 20 d of single leg disuse demonstrated reduced quadriceps myofibrillar FSR at Day 10 that was similarly depressed at Day 20, suggesting a rapid decline that plateaus after Day 10 (39). The soleus (Figure 2.9B) showed no change in myofibrillar synthesis rates throughout the study. While the explanation for this is not inherently clear, the perseverance of myofibrillar FSR in highly oxidative tissue may lie in its mitochondrial

responses to unloading. In work by Taillandier et al., 21 d of hindlimb suspension in rats contributed to increased mitochondrial density (13.2% vs. 9.6% CON; $p < 0.05$), particularly interfibrillar mitochondria (11.1% vs 7.2% CON; $p < 0.05$). More recent work found that 7 d of unloading in mice resulted in decreased mitochondrial yields, but only in the subsarcolemmal fraction (223). Similar work in the gastrocnemius found reduced mitochondria following 28 d of mechanical unloading (134), which may suggest a protective mechanism in the soleus that maintains high or even elevated mitochondrial densities to support locomotion and/or maintenance of contractile elements, arguably a robust preventative measure to maintain some semblance of tone in a high-activity postural muscle. So while mass is lost and closely tied to total protein synthesis rates in the soleus, compensatory mechanisms on the anabolic side of protein turnover may prevent myofibrillar atrophy.

Reductions in Anabolism and Muscle Mass are not due to Reduced Amino Acid Availability

The final highlight of this study is that this work appears to be the first known findings of free amino acid concentrations in the cytosol of unloaded skeletal muscle. We hypothesized that at least one essential amino acid would be significantly reduced during HU and HU+REC+HU in the gastrocnemius cytosol, suggesting a rate-limiting juncture of skeletal muscle protein synthesis. Contrary to our prediction, we observed the highest concentrations of the branched-chain amino acids (isoleucine, leucine, and valine) in the unloaded groups. This observation led us to the work by J. Bohé et al., in

which they determine that human muscle protein synthesis correlates with the essential amino acid concentrations found in blood, not intramuscularly. They conclude by suggestion that oversaturation of intracellular essential amino acid concentrations may slow protein synthesis via reduced membrane sensing of extracellular amino acid availability, which may inhibit protein synthesis signaling generated by extracellular amino acids (18). As meals rich in leucine (and the other branched-chain amino acids) are known to stimulate protein synthesis (117), and the work by McDonald et al. establishes that steady-state muscle blood flow is not inhibited during hindlimb unloading (142), this may collectively suggest that exercise during disuse is required to not only stimulate normal anabolic machinery, but to help reduce intracellular essential amino acid concentrations in order to become more receptive to amino acid- and insulin-dependent increases in mRNA translation. Alternatively, the presence of cytosolic amino acids in the face of reduced FSR in unloaded tissue may also suggest that diminished FSR is due to factors beyond amino acid availability, and will be discussed later in this Dissertation. Regardless, intracellular amino acid concentrations appear to respond in a plastic and repeatable manner to mechanical unloading and reloading.

Conclusion

This is the first known work to investigate if disuse atrophy and recovery affects muscle plasticity in a repeatable manner. These findings may be significant because its information not only yields immediate value to NASA via operational strategies, post-flight rehabilitations, and even astronaut crew selection, but may also advance our

overall understanding of muscle biology. The concept of muscle plasticity, while well-established, may now need to consider the repeatability of muscle's responses to various chronic stimuli, which was carried out in this study via a novel animal that allowed for the first known work to assess muscle anabolism with repeat bouts of unloading and reloading. So far, we were able to confirm our hypothesis that muscle can fully recover from each catabolic insult without any considerable or permanent alterations in muscle form or function, with only a few exceptions (e.g., muscle collagen content).

III. CELLULAR SIGNALING OF MUSCLE PROTEIN TURNOVER FOLLOWING MULTIPLE BOUTS OF UNLOADING AND RECOVERY

Synopsis

Muscle protein turnover is a delicate balance between anabolism and catabolism, with both being dictated by a cadre of signaling cascades. This study elucidated the expression of key regulatory proteins of muscle protein synthesis, degradation, and apoptosis, using a unique experimental design generated to test if muscle's responses chronic changes in mechanotransduction is replicated through serial alterations in mechanical unloading and reloading. Male Sprague-Dawley rats (n = 76) were assigned to the following groups: animals undergoing 28 d of hindlimb unloading (HU), animals performing 28 d of HU followed by 56 d of passive recovery from unloading via normal ambulation (HU+REC), animals experiencing 28 d HU, 56 d REC, and then a second 28 d unloading (HU+REC+HU), animals performing two full unloading bouts with full recovery from each (HU+REC+HU+REC), and age-matched controls (CON). At the end of the study, the gastrocnemius muscles from each animal were removed and tested for signaling patterns of key regulatory proteins via immunoblotting. Key findings include: end-point translation signaling closely resembles the muscle protein synthesis data from Section II- mostly via the PI3K/Akt/mTOR pathway and the final regulating protein of elongation, and protein catabolism and apoptosis at late unloading (steady-state disuse) does not agree with previous studies' reportings on expression. Collectively, this work is the first to suggest that muscle mass homeostasis at the later stages of long-duration unloading is highly coupled to 24 h assessments of muscle

protein synthesis, and that this relationship is highly conserved through serial chronic undulations between mechanical unloading and reloading.

Introduction

Muscle plasticity has been studied extensively. Discussed in Section II, we explored muscle plasticity (ability to rapidly and precisely change to adapt to specific stimuli) in response to sustained changes in mechanical load; long-duration disuse atrophy and recovery from unload-related insults, focusing on muscle mass, structure, and anabolism. We expanded current muscle biology principles by defining biological resilience (capacity for change) and biological repeatability (aptitude to replicate previous changes) with a novel experimental design to produce serial periods of atrophic disuse and hypertrophic recovery from said disuse, and found that muscle plasticity is repeatable in muscle mass and anabolism, but may have shortcomings in muscle structure.

Skeletal muscle is determined by the culmination of muscle protein synthesis and muscle protein breakdown. During mechanical unloading, as observed during spaceflight, denervation, or casting injury, rapid changes in mechanosignaling contribute to decreases in muscle protein synthesis (151) and increases in muscle proteolysis (213), and result in substantial losses in muscle mass (6). Some of the ramifications of severe muscle atrophy include decreased strength (77, 220), altered functional properties (30, 56, 238), and an increased risk of muscle-related injury (122, 163), among countless others that result in a diminished functional capacity and quality of life. Most human

work shows full muscle mass/volume recovers with adequate time following the cessation of unloading (175), and appears to be supported by animal models (23, 168, 226), although some work suggests complete recovery may be tissue-dependent (196). Recovery after unloading appears to include elevated anabolism (208), and decreased catabolism and apoptosis (210), though some argue that catabolism is elevated to facilitate tissue remodeling (7, 222). Our work is the first to investigate muscle anabolism or catabolism in serial bouts of chronic and opposing loading states.

The control mechanisms for these pathways are complex and often shared at various regulatory sites. Muscle anabolism is governed, in part, by the PI3K-Akt-mTOR and MAPK pathways (For Review; (48) and (188), respectively), and three different pathways account for protein catabolism in muscle (107). We have previously demonstrated the sensitivity of these pathways to alterations in mechanical impact (50, 124, 155), but not with steady-state unloading that also included successive recovery. Using the well-accepted rodent model of disuse atrophy (150), we designed a thorough cross-sectional study to assess the functional status of these regulatory proteins to discern if the losses of muscle mass are tightly coupled to protein signaling for synthesis, degradation, and apoptosis. The ramifications of this work on clinical situations are immense- as therapies or interventions derived from the present study could immediately improve quality of life and alleviate morbidities for at-risk populations of muscle-wasting conditions (29, 54, 57, 108).

In this study we wanted to elucidate the regulation of the anabolism and muscle mass discussed in Section II. To do so we employed immunoblot techniques to assess

the expression of key proteins of muscle anabolism, catabolism, and apoptosis under the conditions detailed in the first study. We hypothesized that alterations of muscle anabolism would be consistent with changes of key signaling cascades in response to altered mechanical load status, and that catabolism and apoptosis signaling would also reflect changes of muscle mass during unloading and reloading.

Materials and Methods

Animals

All animal procedures described in this study were approved by the Institutional Animal Care and Use Committee of Texas A&M University. Male Sprague-Dawley rats (Harlan Laboratories Inc, Houston, Texas) were purchased at 5.5 months of age and allowed to acclimate to the vivarium for 2 wk in group-housing in a standard environment (23ºC ± 2ºC, 12:12 h dark/light cycle) and given water and standard rodent chow *ad libitum*. At the completion of the acclimation period, all animals were normalized by body weight and singly-housed after being assigned to one of the following groups: 1) animals undergoing 28 d of chronic hindlimb unloading (HU, n = 16), 2) 28 d of HU immediately followed by removal of the HU harness and allowed 56 d of ambulatory recovery (HU+REC; n = 16), 3) 28 d HU period, 56 d REC period, and then a second 28 d unloading period (HU+REC+HU; n = 16), 4) two complete cycles of unweighting and recovery (HU+REC+HU+REC; n = 14), and age- and housing-matched controls (CON; n = 14). The study design is represented in Figure 3.1.

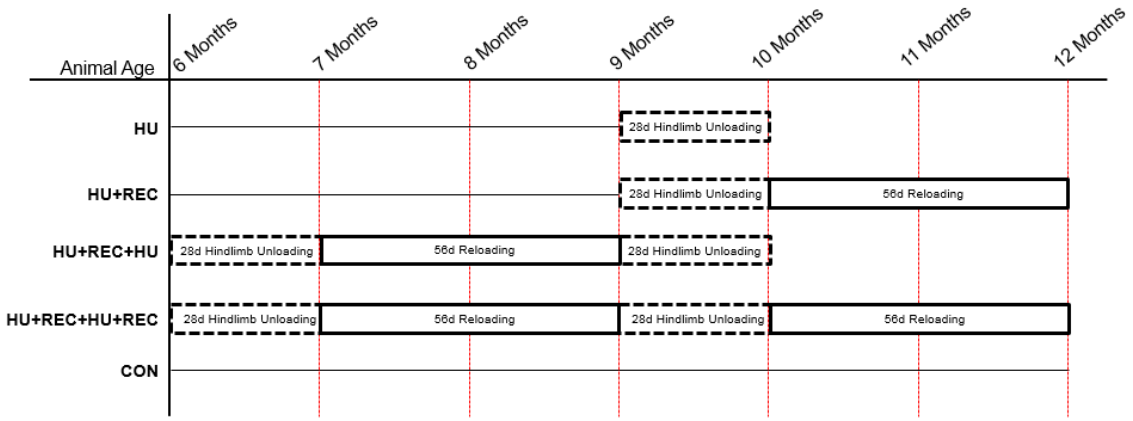

Fig. 3.1. Study II Experimental Study Design. Hindlimb Unloading (HU) was achieved via a tail suspension harness and carried out continuously for 28 d, and Reloading (REC) was carried out by passive recovery through normal cage ambulation.

Animal weights were recorded each week, and health checks were performed twice per day to confirm each animal's health as well as loading condition. Animals were pair-fed (unloading vs control) during the first week of each unweighting bout.

Each animal was harvested on the final day of their last load condition. Following anesthesia (100 $mg \cdot kg^{-1}$ ketamine/10 $mg \cdot kg^{-1}$xylazine), animals were sacrificed via decapitation and prepared for tissue harvest. Animals whose end-point was a non-weight-bearing condition (HU & HU+REC+HU) were anesthetized prior to removal from the unloading apparatus to ensure no unwarranted weight-bearing would take place. The left gastrocnemius muscle of each rat was excised, cleaned of extraneous matter, weighed, and snap-frozen in liquid nitrogen prior to -80 °C storage.

Hindlimb Unloading

Mechanical disuse was accomplished via hindlimb unloading (HU), a well-accepted model of disuse and ground-based analog to spaceflight (For Review; (149). A more detailed description of the methods is described above in Section II. Briefly, animals were anesthetized (2% isoflurane [US Pharmacopia, Rockville, Maryland]) to attach the custom harness with non-irritating adhesive and porous athletic tape to the base of the tail. The harness extended 15.24 cm distally along the lateral sides of the tail, culminating in a paper clip that would allow attachment to the overhead apparatus to allow unloading. Tail harnesses were attached 24 h prior to each suspension period and removed for each recovery bout. The animal would awaken from anesthesia and wear the harness while ambulating normally. On Day 0 of each disuse period the paper clip would be attached to the overhead swivel attached to a steel bar bisecting the top of each animal's custom HU cage. When attached, the animal's hindquarters would be elevated high enough that they could not come in contact with the floor of the cage, resulting in a 30° head-down tilt and complete disuse of the hindlimbs. The steel bar allowed for nearly complete movement about the cage with the forelimbs, but prevented the animal from resting its rear quarters on the walls. This system did not inhibit the rats' ability to feed, drink, or groom, but contributes to similar physiological effects of microgravity due to a cardiovascular fluid shift (94) and a substantial reduction in lower limb muscle activity (173).

On Day 28 of HU, rats reaching their final time point (HU & HU+REC+HU) were anesthetized, removed from HU, and subjected immediately to tissue harvest

described above. Animals that would continue on to a reloading bout were anesthetized, had their harnesses removed, and allowed full ambulation throughout their 56 d recovery session before being harvested (HU+REC & HU+REC+HU+REC) or subjected to a second unloading (HU+REC+HU). Any animal found out of its harness during a health check was immediately removed from the study, as were animals facing any sort of health concern. Overall, the study maintained a 95% success rate in completing each 28 d HU bout.

Immunoblotting

Immunoblotting was carried out on the cytosolic-rich fraction of the gastrocnemius muscle. To isolate this fraction we employed methods detailed elsewhere (155). Briefly, differential centrifugation was carried out in 60 mg of pulverized gastrocnemius muscle tissue. The sample was homogenized with a Polytron (Brinkmann Lab Equipment, Westbury, New York) in 0.4 ml ice-cold Norris buffer (25 mM Hepes, 25 mM benzamidine, 10 mM $MgCl_2$, 5 mM β-glycerophosphate, 4 mM EDTA, 2 mM PMSF, 0.2 mM ATP, 0.5% protease inhibitor cocktail P8340 (v/v), 0.1% Triton-x 100, 10 mM activated Na_3VO_4, and 100 mM NaF; pH 7.4). Samples were allowed to rest for 1 h on ice before centrifugation at 30,000 g for 30 min at 4ºC. The supernatant (the cytosolic-rich fraction) was decanted and saved for determining protein expression.

A small (10 µl) aliquot was used to determine protein concentration quantification via bicinchoninic acid (BCA) assay (199), and 60 µg of protein was

selected for each sample to ensure even loading and qualitative analyses. Samples were randomly selected and blocked by gel to ensure a minimum $n = 2$ for each group was represented on each gel, and location within each gel was randomized to minimize any potential bias. Samples were added to 4x Laemmli buffer (123) and denatured at 100 °C before being loaded onto 4-15% gradient polyacrylamide gels (Lonza, Switzerland) for protein separation via 1 h SDS-PAGE (40 mA in standard electrode buffer [25 mM Tris, 19.2 mM glycine, 0.1% SDS (w/v)]) and a 45 min semi-dry transfer (350 mA) onto a nitrocellulose membrane, 5% (w/v) non-fat dry milk in tris-buffered saline (m-TBS) was used to block the membrane before primary antibody incubation. MuRF1 and MAFbx were acquired from ECM Biosciences (Versailles, Kentucky), and all remaining antibodies described herein were purchased from Cell Signaling Technology (Beverly, Massachusetts). The following proteins were assessed for total content, and when applicable, for phosphorylation content of key sites: Akt (phosphorylated at Ser473), mTOR, rpS6 (Ser235/236), 4E-BP1 (Thr 37/46), eIF4E (Ser209), ERK1/2 (Thr202/Tyr204), eEF2k (Ser366), eEF2 (Thr56), Ubiquitin, FoxO3a, MuRF1, MAFbx, Bcl-2, and Bax. Membranes were incubated in the appropriate antibody dilution (typically 1:1000) in m-TBS overnight with gentle agitation at 4 °C. Membranes were washed three times in 1x TBS for 5 min each, then incubated in the appropriate (anti-rabbit or anti-mouse) secondary antibody (1:2000) in m-TBS for 1 h with gentle agitation at room temperature. Blots were washed a second time, followed by a 5 min incubation with enhanced chemiluminescence (Thermo Fisher Scientific), and were detected using an Alpha Innotech (San Leandro, California) imaging system. Bands

were developed with a CCD camera and optical densities were determined using Alpha Innotech's AlphaEase FC software, which was automatically set to remove non-specific binding from densitometry values. All bands were normalized by the average density of the CON animals' band (minimum $n = 2$ per blot) to allow qualitative comparisons between membranes, and when necessary Ponceau S staining was used as a loading control (178), arguably a stronger correction method (2). Ubiquitin was assessed as the entire band to capture total ubiquitination levels. All values are displayed as Integrated Density Values (IDV) to provide qualitative comparisons.

Statistical Analysis

All analyses were carried out using SigmaStat v3.5 (Systat Software Inc., San Jose, California). A one-way analysis of variance (ANOVA) was used to compare groups, and a Student-Newman-Keuls (SNK) post hoc procedure was used to test differences among group means when significant F-ratios were present. Significance levels were predetermined at $p < 0.05$. For all results described in this study, groups sharing a similar letter are not significantly different ($p \geq 0.05$) and exact p values may be included for results that warrant highlighting and discussion, even if deemed not statistically significant.

Results

Expression of Anabolic Markers Involving Peptide Chain Initiation

Akt was assessed by the phosphorylation status of Ser473 (Figure 3.2), and was found to be higher ($p < 0.05$) in the HU and HU+REC animals compared to CON, but were not different ($p \geq 0.05$) from the repeat unloading or recovery groups (HU+REC+HU & HU+REC+HU+REC).

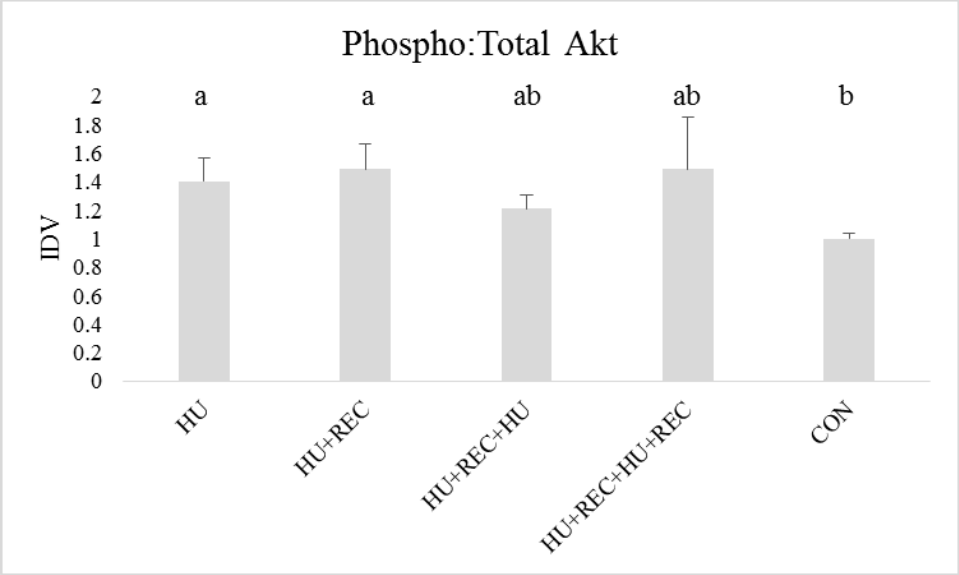

Fig. 3.2. Study II Expression of Akt (Ser473). Immunoblot of the anabolic protein Akt in the gastrocnemius. Assessed as phosphorylated protein to total. Values are means ± SE. Bars displaying similar letters in each graph are not significantly different from one another.

Total mTOR expression was determined and is presented in Figure 3.3. Total content of the anabolic regulator was lower ($p < 0.05$) in each disuse group, but not

similarly, as HU < HU+REC+HU < CON. Only the first recovery period (HU+REC) returned to control levels, and total mTOR content in HU+REC+HU+REC muscle was higher than CON ($p < 0.05$).

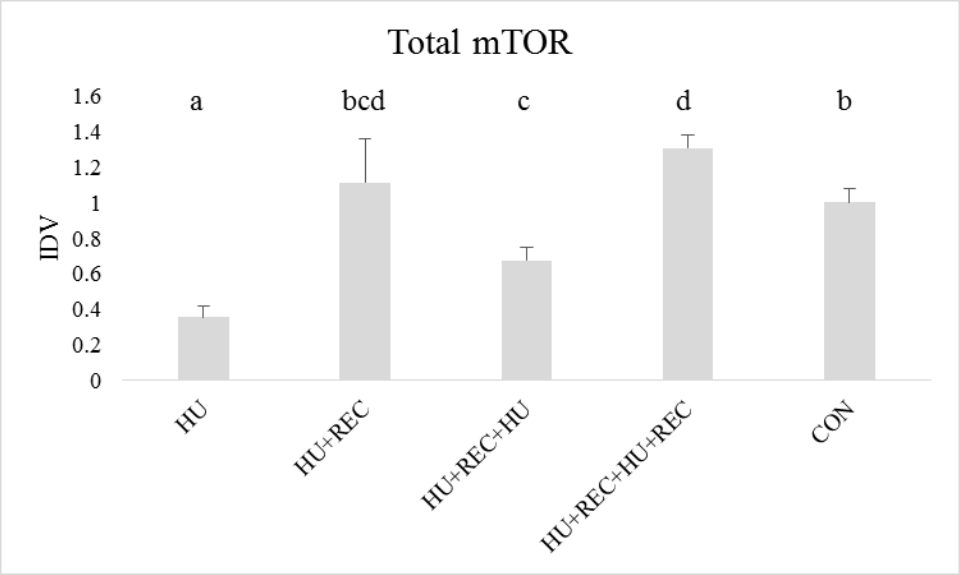

Fig. 3.3. Study II Expression of Total mTOR. Immunoblot of the anabolic protein mTOR in the gastrocnemius. Assessed as total protein. Values are means ± SE. Bars displaying similar letters in each graph are not significantly different from one another.

The negative regulator of mRNA translation initiation that is a direct substrate of mTOR, 4E-BP1 (Figure 3.4)- was not different among groups. Notably, 4E-BP1 activity was 23.8% lower in HU (vs. CON; $p = 0.27$) and HU+REC+HU was reduced by 26.9% vs. control ($p = 0.22$).

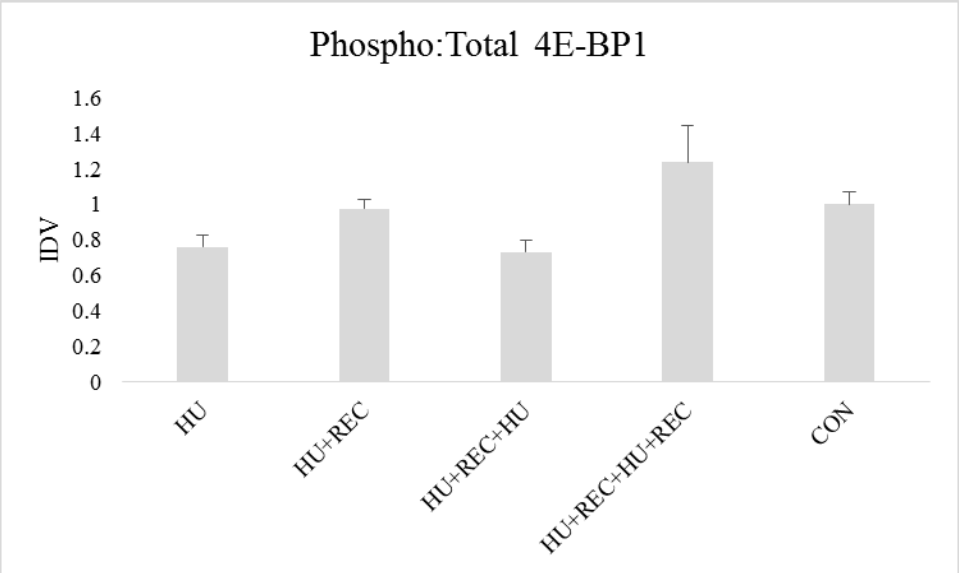

Fig. 3.4. Study II Expression of 4E-BP1 (Thr37/46). Immunoblot of the anabolic protein 4E-BP1 in the gastrocnemius. Assessed as phosphorylated protein to total. Values are means ± SE. Bars displaying similar letters in each graph are not significantly different from one another.

A positive regulator of anabolic function that is also directly activated by mTOR is S6K1, which phosphorylates its downstream target rpS6 when activated. rpS6 activation (Figure 3.5) appears to be tightly coupled to the muscle mass and muscle protein synthesis presented in Section II. HU and HU+REC+HU have lower expression, while content of this important factor is similar to control in the recovery groups (HU+REC = HU+REC+HU+REC = CON).

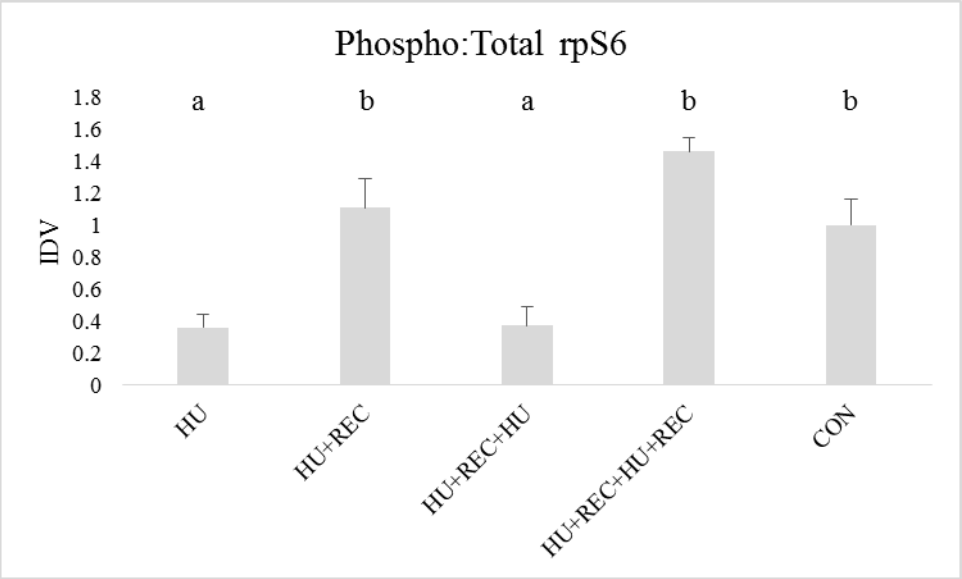

Fig. 3.5. Study II Expression of rpS6 (Ser235/Ser236). Immunoblot of the anabolic protein rpS6 in the gastrocnemius. Assessed as phosphorylated protein to total. Values are means ± SE. Bars displaying similar letters in each graph are not significantly different from one another.

eIF4E, a protein whose availability may be the best-characterized regulatory step of mRNA translation at the level of peptide chain initiation, is presented in Figure 3.6 with its phosphorylation and total expression ratio. While no statistically significant differences were detected, HU and HU+REC+HU were found to have expression values of 62.4% and 65.6% of CON (p = 0.16 and 0.26, respectively).

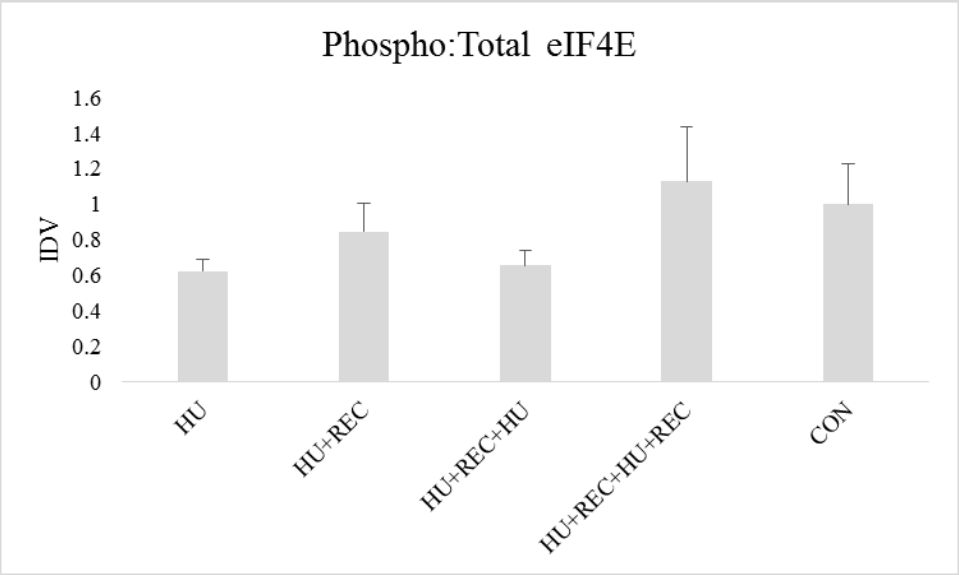

Fig. 3.6. Study II Expression of eIF4E (Ser209). Immunoblot of the anabolic protein eIF4E in the gastrocnemius. Assessed as phosphorylated protein to total. Values are means ± SE. Bars displaying similar letters in each graph are not significantly different from one another.

Largely independent of the P13K-Akt-mTOR signaling pathway, the MAP kinase signaling cascade has been purported to support anabolism under some conditions (65), particularly as it involves the extracellular-regulatable kinases ERK1/2. No differences were observed for the phosphor/total ratio among groups in this study (Figure 3.7), but HU and HU+REC+HU activity appeared lower than CON ($p \geq 0.05$).

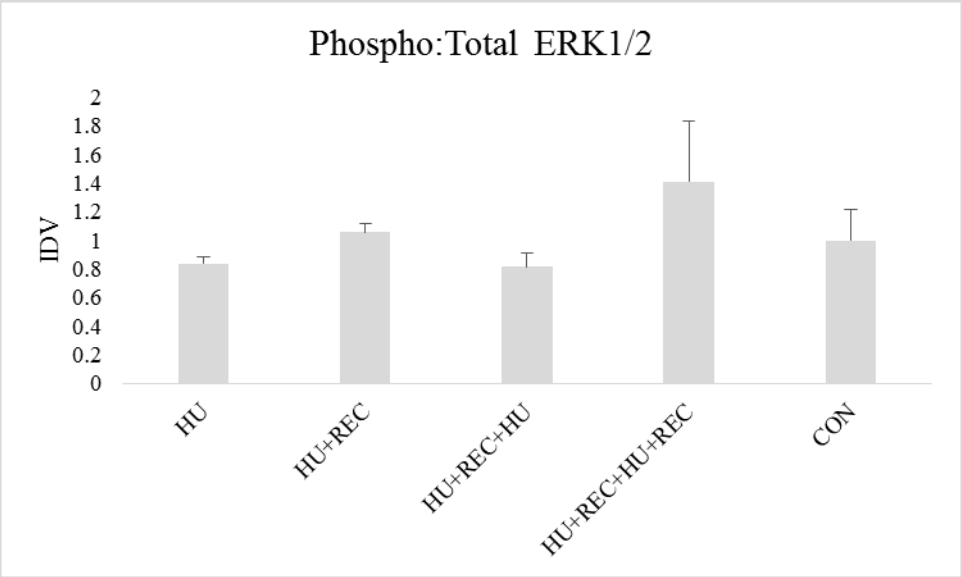

Fig. 3.7. Study II Expression of ERK1/2 (Thr202/Tyr204). Immunoblot of the anabolic protein ERK1/2 in the gastrocnemius. Assessed as phosphorylated protein to total. Values are means ± SE. Bars displaying similar letters in each graph are not significantly different from one another.

Protein Expression of Regulators of mRNA Translation Peptide Chain Elongation

The ratios of phosphorylated to total eEF2k are presented in Figure 3.8, and its downstream target- eEF2, is shown in Figure 3.9. Significant differences were not detected among groups in either protein, when assessed as a ratio of phosphorylated to total protein content.

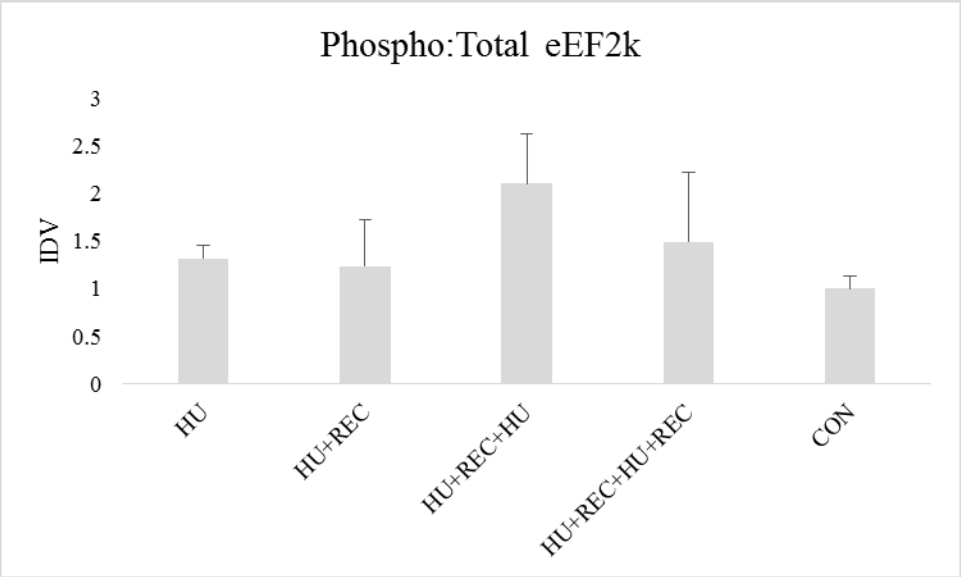

Fig. 3.8. Study II Expression of eEF2k (Ser366). Immunoblot of the elongation protein eEF2k in the gastrocnemius. Assessed as phosphorylated protein to total. Values are means ± SE. Bars displaying similar letters in each graph are not significantly different from one another.

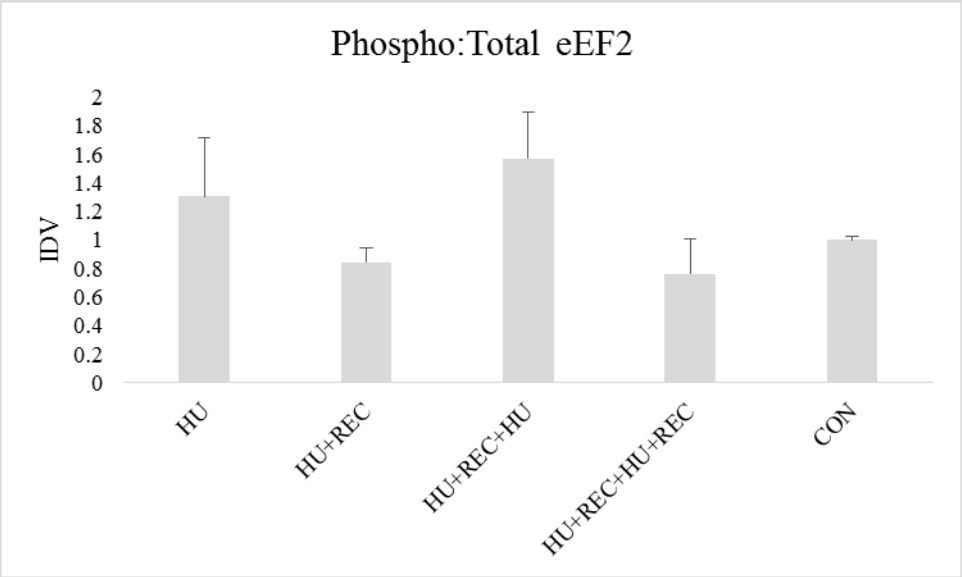

Fig. 3.9. Study II Expression of eEF2 (Thr56). Immunoblot of the elongation protein eEF2 in the gastrocnemius. Assessed as phosphorylated protein to total. Values are means ± SE. Bars displaying similar letters in each graph are not significantly different from one another.

Expression of Regulators of Catabolism

Four markers associated with catabolism (ubiquitin, FoxO3a, MuRF1, and MAFbx) are presented in Figures3.10-13, respectively. No differences were detected among groups in Ubiquitin, FoxO3a, or MAFbx. However, MuRF1 expression was lower in the HU group when compared to control. That difference was not detected in HU+REC+HU.

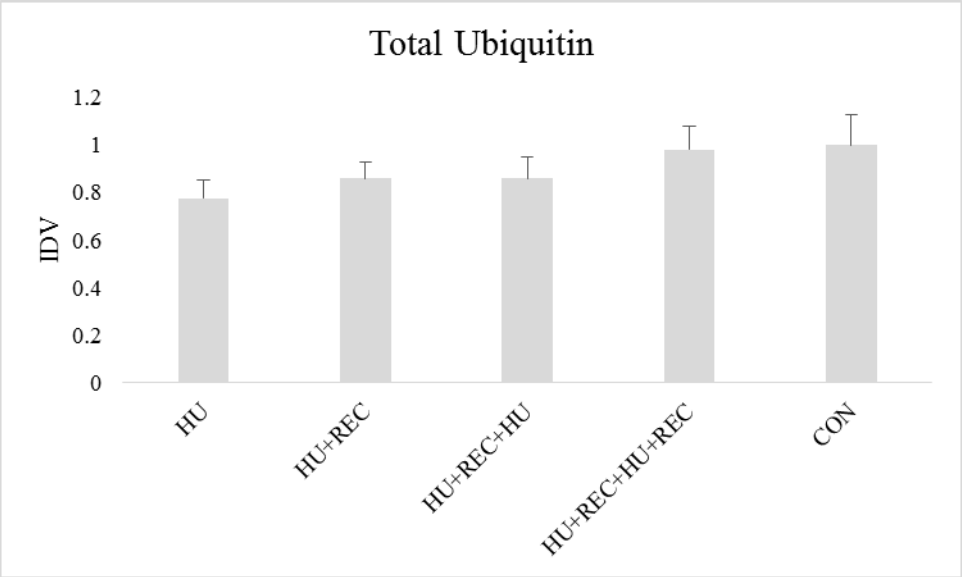

Fig. 3.10. Study II Expression of Ubiquitin. Immunoblot of the catabolism protein ubiquitin in the gastrocnemius. Assessed as total protein. Values are means ± SE. Bars displaying similar letters in each graph are not significantly different from one another.

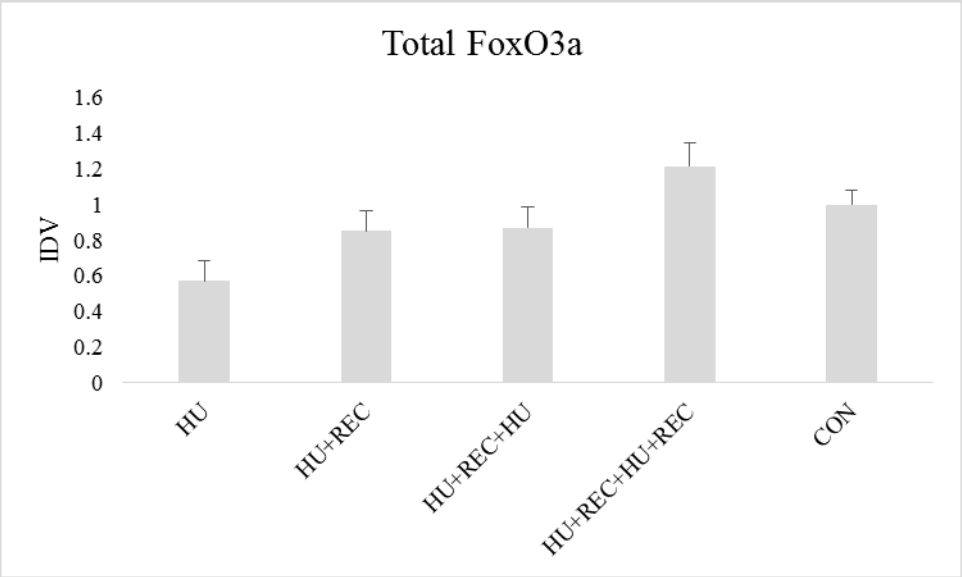

Fig. 3.11. Study II Expression of FoxO3a. Immunoblot of the catabolic protein FoxO3a in the gastrocnemius. Assessed as total protein. Values are means ± SE. Bars displaying similar letters in each graph are not significantly different from one another.

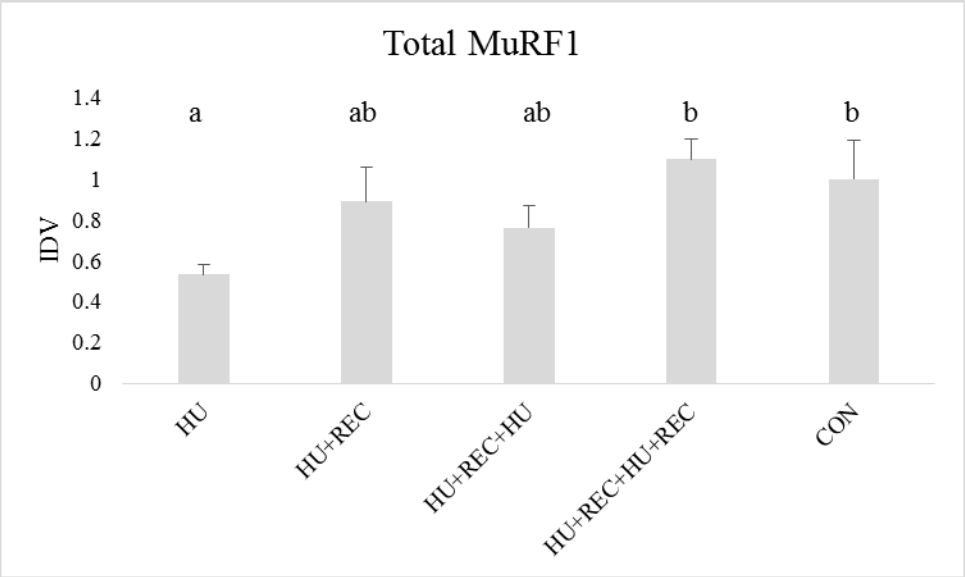

Fig. 3.12. Study II Expression of MuRF1. Immunoblot of the catabolic protein MuRF1 in the gastrocnemius. Assessed as total protein. Values are means ± SE. Bars displaying similar letters in each graph are not significantly different from one another.

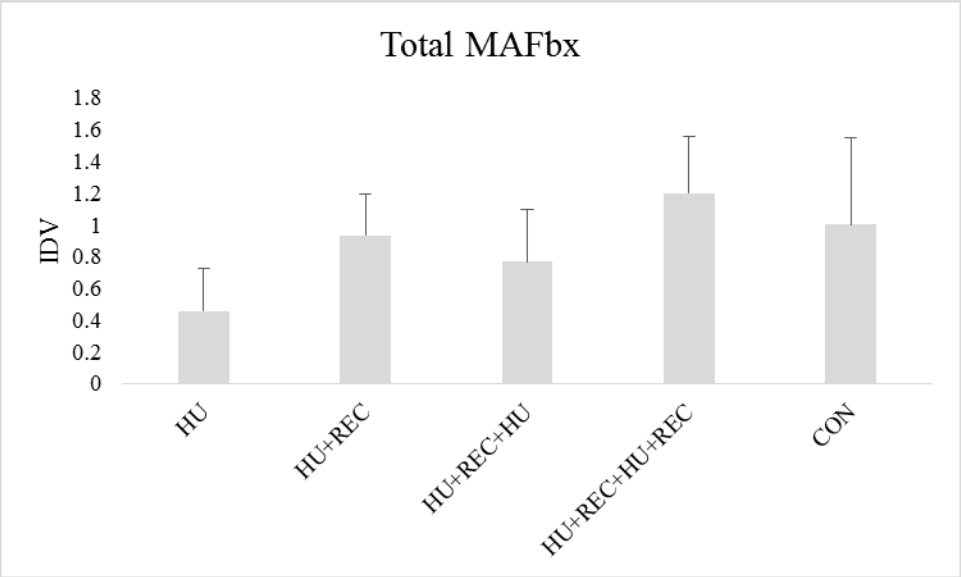

Fig. 3.13. Study II Expression of MAFbx. Immunoblot of the catabolic protein MAFbx in the gastrocnemius. Assessed as total protein. Values are means ± SE. Bars displaying similar letters in each graph are not significantly different from one another.

Expression of Apoptotic Markers

The apoptotic markers of Bcl-2 (Figure 3.14) and Bax (Figure 3.15) were assessed as prominent proteins involved with cellular apoptosis. While HU appears to have higher Bcl-2 expression, no statistical differences were detected. Conversely, Bax expression appears to be closely tied to loading conditions, as lower content was observed in HU and HU+REC+HU, while content in HU+REC and HU+REC+HU+REC was higher. None of the groups differed from CON.

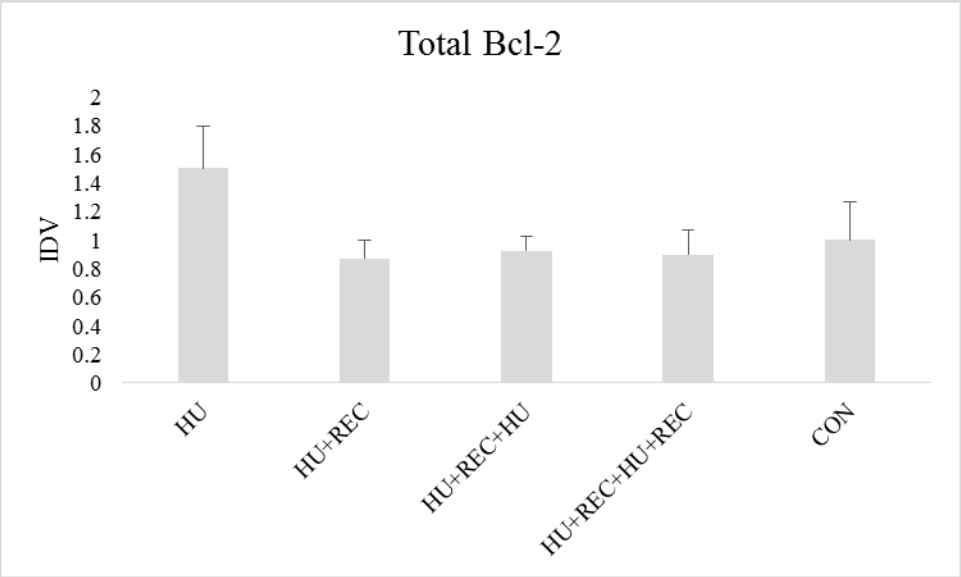

Fig. 3.14. Study II Expression of Bcl-2. Immunoblot of the apoptotic protein Bcl-2 in the gastrocnemius. Assessed as total protein. Values are means ± SE. Bars displaying similar letters in each graph are not significantly different from one another.

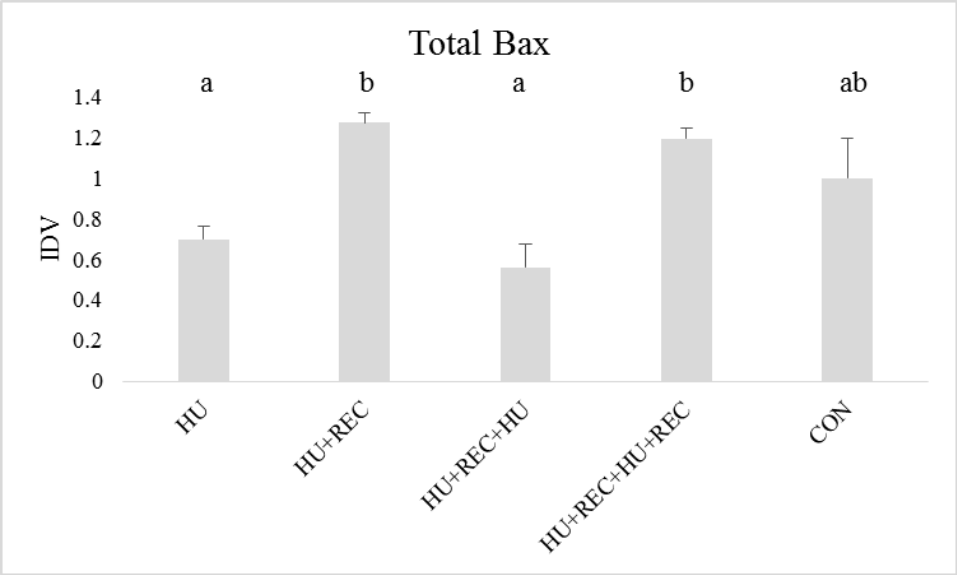

Fig. 3.15. Study II Expression of Bax. Immunoblot of the apoptotic protein Bax in the gastrocnemius. Assessed as total protein. Values are means ± SE. Bars displaying similar letters in each graph are not significantly different from one another.

Discussion

This work sought to expand upon the studies detailed in Section II, in which we determined that muscle plasticity (namely muscle anabolism and subsequently muscle mass) in response to changes in mechanical unloading and reloading appears to be replicable over a serial repeat in loading changes. We report that skeletal muscle plasticity has a biological resilience and repeatability that allows for it to rapidly and substantially alter its form and function due to changes in mechanical stimuli. In the current study, we utilized immunoblotting to visualize the upstream signaling of mRNA translation for peptide chain initiation and elongation, markers of the ubiquitin proteasome and autophagy/lysosomal catabolic systems, and apoptotic proteins. For the

first time we demonstrate that the repeatable alterations in muscle anabolism at the completion of long-duration unloading and recovery appear to be supported by changes of protein expression. We acknowledge that each of our time points is at the completion of either a 28 d unloading period or 56 d recovery, so while we may not capture the more robust signaling changes present at the onset of altered mechanical load, we believe we adequately represent the newly established steady-state levels for unloading (HU & HU+REC+HU) and their apparent return to control values following recovery (HU+REC & HU+REC+HU+REC = CON).

Muscle mRNA Translation Peptide Chain Initiation Signaling Coincides with Mechanical Loading Status

Recent work has suggested that total mTOR content may be indicative of muscle protein synthesis (130), and is consistent with findings of the present study (Figure 3.3) since total mTOR was reduced (vs. CON) in both disuse groups when FSR and muscle mass were both reduced. A reduction in total mTOR with unloading is also consistent with the work from Dreyer et al., who reported a reduction in total mTOR content in paraplegic Sprague-Dawley rats (47). Unfortunately, protein synthesis was not measured in that study. Although the models are not similar between the present study and the work by others (47), it supports the notion that total mTOR content plays a role in the anabolic potential of skeletal muscle. We should note that previously published data appears to contradict that notion (167), but that study only carried out unloading for 14 d and recovery for 7 d, and total mTOR was assessed via unconventional blotting

methods. As the unloaded muscle may not have reached steady-state disuse, total mTOR may not be the ideal marker for assessing anabolism in that study (167).

Protein synthesis is impeded by the eIF4E binding protein 1 (4E-BP1), which represses mRNA translation initiation by competitively inhibiting to eIF4E, preventing the assembly of eIF4F (For Review; (116)), which is critical for peptide chain initiation to occur. The phosphorylation of 4E-BP1 not only relieves its inhibition on eIF4E, but also renders it as an inhibitor for other eIF4E complexes, so reduced ratios of phosphorylated:total expression of this important repressor may indicate reduced protein synthesis (19). And while no statistical significance was determined for eIF4E, the apparent 25% reduction observed in each unloading group may indicate reduced polysome formation, and suggests that even subtle alterations in this ration (significant or otherwise) may have a profound influence on overall anabolic potential. Additional work should determine if polysome density is affected in the HU and HU+REC+HU groups, and determine the prevalence of 4E-BP1-eIF4E complexes in this experimental design.

Ribosomal protein S6 (rpS6) is a known positive regulator of protein synthesis. More often analyzed in exercise studies than disuse conditions, rpS6 has repeatedly been found with higher phosphorylation status following resistance exercise (35, 79, 154), but has also been shown to be reduced by 14 d of hindlimb unloading in (137). Figure 3.5 clearly shows that rpS6 activity is closely associated with mechanical loading status and its signaling is reproducible, even with serial/subsequent changes in loading status. In their review, Chaillou et al. postulate that rpS6 phosphorylation modifies ribosome

function and may actually alter myofibrillar protein synthesis by preferentially translating mRNAs for contractile proteins (34). Further research is necessary to discern if the disconnect of unloading on myofibrillar protein synthesis by muscle type discussed in the previous Section (Figure 2.9) is supported by rpS6 phosphorylation status in the soleus muscle.

While phosphorylation of eIF4E at Ser209 is not believed to directly contribute to ribosome formation (146), another study reported that Ser209 phosphorylation after formation of the 80s initiation complex may allow eIF4F to detach during elongation and more quickly become available for additional recruitment of the next initiation complex, even if it will be associated with different transcripts (186). Therefore, our data may be the first to suggest that mechanical disuse, as observed in our HU and HU+REC+HU animals, contributes to a subtle ($p = 0.16$ and $p = 0.26$) reduction eIF4E activity, which may suggest less efficient mRNA translation (Figure 3.6).

In 2006 we demonstrated that the MAPK (ERK) pathway is partially responsible for load-dependent changes in FSR, and its anabolic regulation seems to be independent of mTOR (65). Phosphorylation of Thr202/Tyr204 activates ERK1/2 and contributes to formation of the translation initiation complex and protein synthesis. While we failed to detect significant differences in ERK1/2 activity among loading conditions (Figure 3.7), we acknowledge this may be due to the fiber composition of the gastrocnemius. In work by Dupont et al. in which rats were subjected to 7, 14, and 28 d of hindlimb suspension, a number of anabolic and catabolic signaling proteins were assessed in the soleus and extensor digitorum longus muscles. While the phosphorylation of ERK1/2 was

decreased by mechanical unloading in the soleus, activity in the fast-twitch EDL was not significantly different than control at any time point (53). It should be noted that the EDL does not atrophy during unloading due to its position on the tibia. Therefore, we postulate that soleus muscles from this experiment may have significant reductions in ERK1/2 activity in the unloading groups, and that this may elucidate some of the rationale as to why the soleus muscle exhibits greater relative losses of mass (-54.4% and -54.1% vs. CON) than the gastrocnemius (-28.2% and -23.7% vs. CON) during HU and HU+REC+HU, respectively (Figure 2.2D). Of potential interest, it has been shown that 10 d of casting followed by 30 d of recovery failed to alter ERK1/2 signaling at any point (36), which, when viewed in total, may suggest MAPK signaling during atrophy may be dependent on the type of disuse and subsequent signaling mechanisms. While MAPK signaling may be a key modulator of muscle protein synthesis during normal or overloading conditions, this work may highlight the value of tissue-specific and atrophy source-specific differences in MAPK signaling during muscle atrophy due to mechanical unloading.

eEF2 Relative Expression, but not eEF2k Relative Expression, Suggests that Translation Elongation Signaling may Correlate with Mechanical Load

Translation elongation is regulated by eEF2, and is inactivated by hyperphosphorylation by its kinase, eEF2k. In turn, the phosphorylation of eEF2k inactivates the kinase, allowing for the decoding of the mRNA and the corresponding polypeptide assembly by the polysome. In this study, neither eEF2k (Figure 3.8) nor

eEF2 (Figure 3.9) demonstrated statistically significant differences among groups in the gastrocnemius, suggesting that elongation may not be a highly-regulated component of mRNA translation. eEF2k activity appears to be fairly consistent with control activity, with HU+REC+HU being inexplicably higher than CON ($p \geq 0.05$). However, the +30.3% in eEF2 activity observed in the HU animals (vs. CON) and +56.9% increase in HU+REC+HU animals ($p = 0.13$) may indicate that eEF2 activity may correlate more strongly with muscle protein synthesis values during mechanical unloading and reloading. There remains a paucity of information on the effects of microgravity or mechanical unloading on elongation factor phosphorylation relative to its total content, but the present study indicates that further investigation may be warranted.

Long-duration Unweighting and Recovery Overcomes the Reported Robust Changes in Catabolic Signaling Markers at the Onset of Unloading and Reloading

While not directly associated with muscle protein anabolism, per se, there appears to be a growing belief that the Ser473 site of Akt (activating Rictor and mTORC2) may play an important role in repressing the FoxO class of transcription factors, which in turn regulate ubiquitin ligases MuRF1 and MAFbx (184, 204). Phosphorylation of Akt at Ser473 has been studied in various atrophic models, demonstrating reduced phosphorylated:total expression following 10 d of hindlimb suspension, and an elevated ratio on Day 3 and Day 10 of recovery from disuse (141). In a paraplegic model, 10 wk of spinal denervation had a non-significant increase in Akt activity (47). The elevated values in all groups observed in Figure 3.2 may indicate that

Rictor activity is maintained during disuse, or may be attempting to repress catabolic activity or remodeling.

Total FoxO3a is presented in Figure 3.11 with no differences among groups detected. Total FoxO3a protein content was unchanged in the vastus lateralis of healthy men subjected to 20 d of ULLS (179). Total FoxO3a was reduced with 14 d in rat soleus in one study (87), but was accompanied by greater reductions in the phosphorylation state of FoxO3a, resulting in greater ubiquitin signaling and increased atrophy. Similar results (decreased phosphorylated FoxO3a) were recently found by Lawler et al., in which they saw a 50% reduction in the rat soleus within 54 h of hindlimb unloading (126). Therefore, future efforts should be made to quantify alterations of phosphorylation status of FoxO3a under long-duration unloading and recovery as well as their potential impact on muscle protein anabolism.

Phosphorylation of FoxO3a by Akt (when activated by phosphorylation at Ser473) results in FoxO3a's association with 14-3-3 proteins and its expulsion from the nucleus and confinement to the cytosol (25). This prevents its ability to initiate ubiquitin ligase activity, including the muscle-specific E3 ubiquitin ligases MuRF1 and MAFbx (For Review; (16)). Figure 3.12 and Figure 3.13 present the protein expression of MuRF1 and MAFbx, respectively, in the gastrocnemius muscle. Total muscle content for ubiquitin was measured and presented in Figure 3.10. Surprisingly MuRF1 was 47% lower than control values in the HU group ($p < 0.05$), but was only 24% lower in the HU+REC+HU tissues ($p \geq 0.05$), possibly suggesting a disconnect in muscle plasticity and repeatability. No changes were detected among MAFbx groups or total

muscle ubiquitin protein content, demonstrating that these signals are not different among groups during steady-state disuse or complete recovery from disuse. We postulate that our values may be altered had shorter unloading periods been assessed, as 3 d rodent immobilization (casting) studies have demonstrated nearly 5-fold increases in MuRF1 and 4-fold increases in MAXbx mRNA expression, and increases in overall ubiquitin protein levels (179). In a 20 d bed rest study in healthy men, total ubiquitin was 4-fold higher than pre-bed rest values, while MuRF1 displayed non-significant increases (~70%) and significant increases in MAFbx (~100%) (158). MurF1 and MAFbx protein expression were also elevated in 14 d unloading studies in rat (87). Together with the work presented in this present study, it suggests the increases in catabolism during disuse are only prevalent in early-stage unloading, and do not appear to persist through 28 d unloading, which we discuss throughout the Dissertation as steady-state disuse. Future directives should seek to verify and discern the data presented in this study to determine the impact of long-duration disuse and recovery, and evaluate whether repeat exposures alter these effects.

Apoptotic Signaling During Steady-state Mechanical Unloading is not Explained by Early-Stage Unloading Signaling

The protein content for the anti-apoptotic Bcl-2 and the pro-apoptotic Bax are displayed in Figure 3.14 and Figure 3.15, respectively. Fourteen day hindlimb suspension of young rats (6 m) resulted in increased Bax mRNA and protein content, with no changes observed in Bcl-2 mRNA but an increase in Bcl-2 protein content in the

gastrocnemius (198). These findings differ from those reported in our study, in which Bcl-2 was not changed (although HU observed a 50% increase; $p = 0.25$ vs. CON) and Bax protein content was actually decreased during HU and HU+REC+HU when compared to recovery groups and control. The increased Bax protein and decreased Bcl-2 protein published by Siu et al. was corroborated by Propst et al., who found +117% increases in Bax protein and -18% reductions in Bcl-2 expression in the soleus of rats after 2 d of hindlimb suspension (165). Interestingly, the same study actually saw a reversal of protein signaling as measured at Day 2 vs. Day 28 of hindlimb unloaded animals. Bax exhibited a -30% decrease and Bcl-2 a +95% gain. They concluded that apoptotic signaling during mechanical unloading is biphasic, with pro-apoptotic signaling rising early and then declining with prolonged disuse. If the transition occurs in the rat after Day 14 of hindlimb unloading, and knowing that apoptosis is correlated with muscle protein breakdown (131) , this notion strongly agrees with the findings of Thomason et al. (Fig. 2; (214)), that claim muscle protein degradation is rampantly increased from Day 0 to Day 14 in unloaded muscle, and then reduces to control levels by Day 21 of unloading and remains at a steady-state for the duration of the chronic unweighting. Therefore, if apoptosis and protein degradation are reversed/slowed in steady-state disuse (> 14 d unloading), this supports most of the protein expression detailed in our study, but not consistent with the Bcl-2 protein content in the HU+REC+HU animals of the present study, which may force us to question whether adaptations occuring with a single exposure to muscle atrophying events are reproducible with subsequent unloading periods. To our knowledge, there are few data

published regarding degradation and apoptosis in unloading models lasting 28 d or more, so additional studies are needed to further characterize the impact of long-duration unloading, and perhaps to attempt to elucidate the timing and impetus for the switch from high apoptosis/high degradation to low apoptosis/low degradation states.

Conclusion

The present study expanded on prior work on changes of muscle mass by exploring the signaling details taking place during serial bouts of long-duration unloading and reloading, and determine if the protein expression and/or activation (as predicted by phosphorylation state) supported the alterations in anabolism and mass featured in Section II. In summary, muscle mass after 28 d of unloading seems to be strongly dependent on muscle protein synthesis, which is supported by diminished expression or activation of key anabolic signaling markers, rather than increased catabolism or degradation. Remarkably, these signals are reversed at the completion of 56 d of recovery from disuse when passive reambulation-no exercise recovery intervention was employed. We highlight an apparent inverse relationship between apoptotic signaling and steady-state unloading, but more work is warranted to determine if protein homeostasis is normalized with prolonged exposure. When biological repeatability of muscle protein signaling was tested, HU+REC+HU often responded similarly to the results of HU, and HU+REC+HU+REC mimicked the protein contents of HU+REC and CON (with few exceptions). This study clearly demarcates the notion of muscle plasticity under changes in mechanical unloading and reloading, and future

studies should invoke mechanical overload (i.e. resistance exercise) to enhance the breadth of current work to date.

IV. RESISTANCE EXERCISE DOES NOT IMPROVE RECOVERY FROM DISUSE OR PREVENT FUTURE UNLOADING ALTERATIONS

Synopsis

Skeletal muscle homeostasis is directly tied to the stimuli acting upon it. Mechanical unloading and reloading have been shown to contribute to marked changes in muscle size, function, and composition, and our previous work has demonstrated that these effects are repeatable when exposed to additional bouts of disuse or recovery, which we consider important to understanding muscle biology and a novel finding. In this study we supplemented our recovery group after 28 d disuse with a long-term resistance exercise program in an attempt to boost muscle recovery above that observed after passive reloading, and to determine which, if any, muscle responses to a second period of 28 d of unloading can be mitigated by pre-disuse exercise training. Male Sprague-Dawley rats (n = 44) were normalized by size and placed in one of the following groups: 1) a 28 d unloading group that was followed by 56 d of recovery supplemented by resistance training (HU+EX), 2) animals undergoing long-duration unloading and training recovery prior to a second 28 d disuse period (HU+EX+HU), and 3) a control group (CON). At the end of the study muscles of the lower limb were removed and subjected to a variety of measures pertinent to muscle protein turnover and compared to the findings presented in early Sections. Interestingly, the exercise prescription (compared to passive ambulation recovery) resulted in reduced gastrocnemius muscle weights and muscle cross-sectional area that was not wholly explained by protein anabolism measures. In addition, there appeared to be no

improvements to muscle outcomes during a second period of disuse when preceded by resistance exercise training. We conclude by commenting on the efficacy of the training program used, detail possible rationales for the data observed, and make suggestions on how future strategies may be able to better improve recovery from disuse.

Introduction

The previous Sections have outlined the effects of mechanical unloading and reloading on muscle plasticity (ability for muscle to rapidly and specifically adapt to stimuli), and sought to establish biological resilience (capacity for change to stimuli) and biological repeatability (ability to replicate previous changes) as facets of plasticity. In order to expand our characterization of biological repeatability, it was imperative to add a component of hyper-mechanotransduction (overload) to compare to the aforementioned unload and reload measures.

Observations during initial exercise studies have largely shaped our understanding of exercise physiology and responses to training (41, 81, 98, 182). We know that some acute adaptations to exercise training include improved anabolic signaling immediately post-exercise (11, 20, 230) that can culminate in hypertrophy with chronic training (89, 92, 212), but are completely lost upon the cessation of continued training (102, 202). There is less information regarding exercise training following disuse or injury. In one study, 12 weeks of strength training following long-term disuse resulted in improved quadriceps area and strength over standard rehabilitation practices

(205), but another study indicated that muscle may be predisposed to training-induced injury after long-duration atrophy (163).

The purpose of this study was to include resistance exercise to muscle recovering from long-term disuse, to examine how it would compare to normal ambulation recovery, as well as what impact it may have on an additional period of weightlessness. Using our rodent model of resistance exercise (66) to execute an exercise paradigm known to improve bone outcomes 1) after 28 d disuse and 2) mitigate losses in bone in a second 28 d unloading period (197), we hypothesize that a moderate-intensity, moderate-volume resistance exercise program will improve muscle mass above that of passive recovery alone, but will not prove to have protective effects on a subsequent disuse period.

Materials and Methods

Animals

All procedures described herein were approved by and conducted in accordance with the Institutional Animal Care and Use Committee of Texas A&M University. Forty-four male Sprague-Dawley rats (Harlan Laboratories Inc, Houston, Texas) were selected for this study and obtained at 5.5 months of age. Animals were group-housed for 2 wk in a standard environment (23ºC ± 2ºC, 12:12 h dark/light cycle) and given water and standard rodent chow *ad libitum*. Following transport recovery and acclimation, all animals were singly-housed, normalized by body weight, and assigned to one of the following groups: 1) 28 d of constant hindlimb unloading immediately

followed by a 56 d recovery bout of normal ambulation supplemented with resistance exercise (HU+EX, *n* = 14), 2) 28 d of HU with a 56 d EX recovery period, followed by a second 28 d unloading period (HU+EX+HU, *n* = 18), and 3) an age- and housing-matched control group (CON, *n* = 14). Figure 4.1 demonstrates the groups added in this study and how they coincide with the experimental groups detailed in Section II.

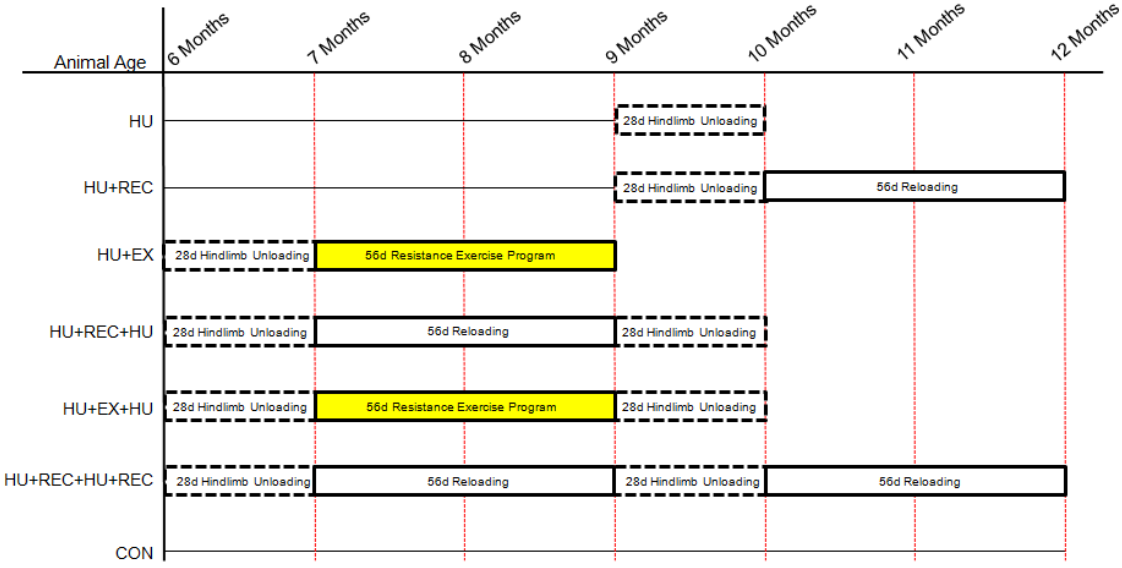

Fig. 4.1. Study III Experimental Study Design. Hindlimb Unloading (HU) was achieved via a tail suspension harness and carried out continuously for 28 d, and Reloading (REC) was carried out by 56 d passive recovery through normal cage ambulation or with Reloading supplemented with Resistance Exercise (EX) performed 21 times over the 56 d recovery period.

Body weights were recorded weekly, and twice-daily health checks were carried out to ensure each animal was healthy and loaded appropriately. In order to prevent any effects

due to altered food consumption (proven to affect body and muscle masses), all control animals were pair-fed to HU rats during the first week of each unloading period.

At the conclusion of the study, each animal was anesthetized with ketamine/xylazine (100 $mg \cdot kg^{-1}$ & 10 $mg \cdot kg^{-1}$, respectively) prior to tissue harvest. Cardiac puncture was used to draw approximately 2 - 4 ml of whole blood under anesthesia, using a Serum Separator Tube (Becton, Dickinson and Company, Franklin Lakes, New Jersey) and was immediately followed by euthanasia via decapitation, and removal of the tibia as well as the gastrocnemius, soleus, and plantaris muscle of each hindlimb. Blood samples were gently inverted five times to activate clotting, allowed to rest at room temperature for 30 min, centrifuged at 1,200 g for 30 min in order to collect blood serum, which was then stored at -80 °C. Tibiae were cleaned of soft tissue and stored in 70% ethanol at 4 °C. The gastrocnemius, soleus, and plantaris muscles were excised, cleaned of extraneous blood, fat, and connective tissue, weighed and recorded, and finally snap-frozen in liquid nitrogen before -80 °C storage.

Hindlimb Unloading

Simulated microgravity was accomplished through the use of hindlimb unloading (HU), a well-published ground-based analog to spaceflight (For Review; (149)) commonly utilized by our group to study muscle atrophy (50, 63, 64, 118). Tail harnesses were attached 24 h prior to each suspension period and removed for each recovery bout. Animals were briefly anesthetized with 2% isofluorane (US Pharmacopia, Rockville, Maryland) in order to attach the custom tail harness. A thin

layer of non-irritant adhesive (Amazing Goop, Eclectic Products, Los Angeles, California) was generously applied around the base of the tail, and was firmly attached to porous athletic tape (Kendall, Mansfield, Massachusetts) and allowed to dry. The athletic tape attached to the base of the tail (~2.54 cm of contact) on each lateral side and extended ~15.24 cm distally, where each end of the tape connected and joined a paper clip. The animal was allowed to recover from anesthesia and wore the harness while ambulating normally. On Day 0 of each unloading period the paper clip of the harness was then attached to a swivel apparatus overhead that was connected to a steel bar bisecting the top of the custom-built 45.72 cm x 45.72 cm x 45.72 cm cage. When attached, the animal's hindquarters would be elevated high enough that they could not come in contact with the floor of the cage, resulting in a 30° head-down tilt and complete disuse of the hindlimbs. The steel bar allowed for nearly complete movement about the cage with the forelimbs, but prevented the animal from resting its rear quarters on the walls. This system did not inhibit the rats' ability to feed, drink, or groom.

Upon completing their first unloading period (HU+EX & HU+EX+HU), animals were anesthetized, had their harnesses removed, and allowed full ambulation throughout their 56 d recovery and exercise training before being harvested (HU+EX) or subjected to a second unloading (HU+EX+HU). On Day 28 of their second unloading bout, HU+EX+HU animals were anesthetized, removed from HU, and subjected immediately to tissue harvest before undesired weight-bearing of the hindlimbs could occur. Any animal found out of its harness during a health check was immediately removed from the

study, as were animals facing any sort of health concern. Overall, the study maintained a 95% success rate in completing each 28 d HU bout.

Resistance Exercise Training

Following their first unloading bout, animals were given 7 d of ambulatory recovery and then began the resistance exercise program previously employed in our lab (67, 74, 156). Training occurred in a custom-built upright acrylic box (21 cm length x 21 cm width x 35 cm height) fitted with an illuminated lever situated above the animal's head. The rat was operant conditioned to recognize the activation of the light bulb and attempt to depress the overhead lever, which required full extension of the lower body. When necessary, a brief foot shock was administered to encourage an exercise repetition. Three operant conditioning sessions (0 g; 50 repetitions/session) were given to train the animal for the program, with 48 h rest between sessions. Following operant conditioning, resistance was increased through the addition of lead weights to a small vest affixed to the animal. Training three times per week (48 h rest between sessions) for 7 wk, intensity was progressively increased from 80 g to 270 g load, a protocol proven to improve several aspects of skeletal parameters above normal ambulatory reloading when invoked after steady-state disuse atrophy (197). Twenty-four hours after the final exercise session HU+EX animals were harvested and HU+EX+HU animals were placed in their second suspension bout.

Peripheral Quantitative Computed Tomography

Peripheral Quantitative Computed Tomography (pQCT) scans were carried out immediately prior to tissue harvest, and allowed for both *in vivo* measures and *ex vivo* supporting data. Under the aforementioned ketamine/xylazine anesthesia, animals were firmly secured and had their left lower limbs scanned on a Stratec XCT Research-M device (Norland Corp., Fort Atkinson, Wisconsin) calibrated with a hydroxyapatite standard cone phantom. A custom 3D-printed brace (ABS polymer) was used to prevent movement of the lower limb during the scanning procedure. Total tibia length was first recorded by the machine, and then the left lower hindlimb was scanned *in vivo* at a rate of 2.5 $mm \cdot s^{-1}$ with a voxel resolution of 100 μm^2 and a scanning beam thickness of 500 µm. Two slices were scanned at 50% tibia length (middiaphysis), 1 mm apart, and assessed for total limb cross-sectional area (CSA_{TOT}), muscle tissue CSA (CSA_{MM}), and fat (both subcutaneous and intramuscular) CSA and percentage. Excised tibiae were scanned *ex vivo* when necessary to determine tibia length for normalized mass analyses (see Results).

Scan images were analyzed using Stratec software (ver. 6.00, Norland Corp., Fort Atkinson, Wisconsin). The software, originally designed for bone research and clinical assessments, was adjusted to allow for skeletal muscle measurements using methods revised from other works (174). Standardized analysis schemes were utilized for all muscle acquisitions. A region of interest was established around the entire limb circumference, and specific values were discerned through image filters and density thresholds available with the XCT550 software. Limb cross-sectional area (CSA_{TOT}) of

the midshaft was determined with a Calcbd analysis (outer threshold of -101 $mg \cdot cm^{-3}$, contour mode 1, peel mode 2, inner threshold of 40 $mg \cdot cm^{-3}$, and visualized with filter F03F05F05), which the software determined as the total area assessed, and additional analyses allowed for the determination of the muscle cross-sectional area (CSA_{MM}) and fat cross-sectional area (CSA_{FAT}). The software computes a "trabecular area" (all tissues with densities < 40 $mg \cdot cm^{-3}$) in this case representing fat and bone marrow area ($CSA_{FAT\&MARROW}$) and "cort-subcort area" (all tissues with densities > 40 $mg \cdot cm^{-3}$) indicative of bone, muscle, and skin area. Additional analyses were used to remove the bone, marrow, and skin values. Bone and marrow ($CSA_{BONE\&MARROW}$) was calculated (outer threshold of 710 $mg \cdot cm^{-3}$, inner threshold of 710 $mg \cdot cm^{-3}$), with "trabecular" values representing marrow total area (CSA_{MARROW}) and "cort-subcort" determined bone tissue area of the tibia and fibula of each slice (CSA_{BONE}). Finally, skin area (CSA_{SKIN}) was isolated from CSA_{TOT} with a Cortbd analysis (outer threshold of -101 $mg \cdot cm^{-3}$, separation mode 4, inner threshold of 2000 $mg \cdot cm^{-3}$). Collectively, these analyses provided the following data:

CSA_{TOT}, CSA of the entire limb at the midshaft of the tibia

$$CSA_{MM} = CSA_{TOT} - (CSA_{FAT\&MARROW} + CSA_{BONE} + CSA_{SKIN})$$

$$CSA_{FAT} = CSA_{FAT\&MARROW} - CSA_{MARROW}$$

$$\%_{FAT} = CSA_{FAT} / CSA_{TOT}$$

Each slice was analyzed individually and then averaged for each animal.

Collagen

Collagen concentration was measured by quantification of the collagen-specific amino acid hydroxyproline via High Performance Liquid Chromatography (HPLC) using previously published methods (33, 166). Approximately 10 mg of pulverized gastrocnemius muscle was carefully cleaned of extraneous collagen fibers, weighed, freeze-dried for 36 h and then reweighed to provide a dry weight and water concentration measure. Samples were derivatized and injected onto an HPLC (LC-20AB and SIL-20, Shimadzu Scientific Instruments, Columbia, Maryland) and separated on an XTerra RP 18 column (Waters Corporation, Milford, Massachusetts). Hydroxyproline samples were normalized to an internal standard and compared with a standard curve (33). Unless otherwise noted, all chemicals were obtained from Sigma Aldrich (St. Louis, Missouri).

Intramuscular Amino Acid Concentration

Individual concentrations of 29 amino acids commonly found in the skeletal muscle cytosolic pool were assessed with ultra-performance liquid chromatography (UPLC) using techniques previously described (27). In short, 500 mg of pulverized gastrocnemius tissues were homogenized using a Polytron (Brinkmann Lab Equipment, Westbury, New York) in 3 ml 1.5 M perchloric acid, vortexed, and centrifuged until pelleted. The supernatants (containing the cytosolic pool) were neutralized with 2 M potassium carbonate (1:1 v/v) and lipid extracted with diethyl ether (1:3 v/v), vortexed, and the ether layer removed. The lipid-free samples were filtered through 0.2 μm

polycarbonate syringe filters and derivatized with o-phtaldialdehyde before analyzed on a UPLC (Waters Corporation, Milford, Massachusetts). Identification and quantification of amino acids was accomplished using external standards. Samples were analyzed in triplicate.

Measurement of Protein Synthesis

Twenty-four hour fractional synthesis rates (FSR) for the mixed (total) and myofibrillar (contractile) fractions were assessed in the gastrocnemius, soleus, and plantaris muscles using deuterium oxide (^2H_2O) incorporation techniques well-described by our lab (76, 156). Animals were given a bolus dose of 99.9% deuterium oxide (Cambridge Isotopes, Andover, Massachussetts) in a saline solution (0.9% NaCl) via intraperitoneal injection (20µl·g^{-1} body weight) 24 h prior to tissue harvest. The priming bolus was supplemented with 4% ^2H_2O drinking water provided *ad libitum* to maintain enrichment during the final 24 h of the study. FSR was determined by measuring the levels of ^2H incorporation into the muscle protein and the precursor pool, described in detail below. To isolate the myofibrillar subfraction for FSR and the cytosolic subfraction for immunoblotting, differential centrifugation was employed using methods detailed elsewhere (156). Pulverized skeletal muscle (~60 mg) was homogenized with a Polytron in a 0.4 ml Norris buffer (25 mM Hepes, 25 mM benzamidine, 10 mM magnesium chloride ($MgCl_2$), 5 mM β-glycerophosphate, 4 mM EDTA, 2 mM phenylmethanesulfonylfluoride (PMSF), 0.2 mM ATP, 0.5% protease inhibitor cocktail P8340 (v/v), 0.1% Triton-X 100 (v/v), 10 mM activated sodium orthovanidate

(Na_3VO_4), and 100 mM sodium fluoride (NaF); pH 7.4). Each sample rested on ice for 1 h before centrifugation at 30,000 g for 30 min at 4 °C. The pellet, containing the myofibrillar subfraction, was then prepared identically to the mixed fraction samples. The supernatant (the cytosolic-rich fraction) was decanted and saved for determining protein expression via immunoblotting.

Sample preparation for total protein FSR was determined in the mixed subfraction as previously described by our lab (76). Both pulverized mixed muscle tissues (~30 mg) and myofibrillar pellets were homogenized with a Polytron in 0.3 ml of 10% (w/v) trichloroacetic (TCA) acid. Samples were centrifuged at 5,000 g for 15 min at 4 °C, the supernatant (containing free, unbound amino acids) was decanted and removed, 0.3 ml TCA added to the pellet and vortexed until broken down, and the wash-spin step repeated two additional times. After the third and final wash step the protein-bound pellet was dissolved in 0.4 ml of 6 N hydrochloric acid for 24 h at 100 °C. 100 µl of the hydrolysate was dried down and derivatized with 100 µl of a 3:2:1 (v/v/v) solution of methyl-8 (N,N-Dimethylformamide dimethyl acetal, Thermo Fisher Scientific, Waltham, Massachusetts), methanol, and acetonitrile for 1 h at 70ºC. Derivatized samples were injected into a GCMS (Agilent 7890 GC & 5975 VL MSD, Agilent Technologies, Santa Clara, California) using previously described parameters (74, 75). All muscle samples were analyzed in triplicate and calculated from a linear regression formula generated by known ^{2}H-alanine standards (0-2.0% ^{2}H-alanine:alanine) prepared identically to the sample procedure.

Deuterium (^2H) enrichment of the available precursor pool was determined by quantifying ^2H_2O-enriched serum based on a linear regression formula generated by deuterium standards identically prepared. A 20 µl serum sample was allowed to react with 2 µl of 10 N sodium hydroxide and 4 µl of a 5% (v/v) acetone in acetonitrile solution at room temperature for 24 h. Then, ~0.5 g sodium sulfate decahydrate was added as a drying agent, and 0.6 ml chloroform was introduced to the sample to stop the isotopic exchange between ^2H_2O-enriched serum samples and acetone. A small aliquot (1 µl) was injected into the GCMS, volatilized, separated, and detected using methods detailed in earlier publications by our lab (74, 75, 156). All serum samples were prepared and measured in duplicate, and the average value used in FSR calculations.

FSR was calculated using the following equation:

$$FSR = E_A \cdot [E_{BW} \times t(\text{d}) \times 3.7)^{-1} \times 100,$$

where E_A represents the amount of protein-bound ^2H-alanine (mole percent excess), E_{BW} is the quantity of ^2H_2O in the precursor pool (mole percent excess), t(d) designates the total time of incorporation (in days), and 3.7 represents the exchange coefficient of ^2H between body water and alanine (e.g. 3.7 of 4 carbon-bound hydrogens of alanine exchange with water (49)).

Immunoblotting

A small (10 µl) aliquot was used to determine protein concentration quantification via bicinchoninic acid (BCA) assay (199), and 60 µg of protein was

selected for each sample to ensure even loading and qualitative analyses. Samples were randomly selected and blocked by gel to ensure a minimum *n*=2 for each group was represented on each gel, and location within each gel was randomized to minimize any potential bias. Samples were added to 4x Laemmli buffer (123) and denatured at 100 °C before being loaded onto 4-15% gradient polyacrylamide gels (Lonza, Switzerland) for protein separation via 1 h SDS-PAGE (40 mA in standard electrode buffer [25 mM Tris, 19.2 mM glycine, 0.1% SDS (w/v)]) and a 45 min semi-dry transfer (350 mA) onto a nitrocellulose membrane, 5% (w/v) non-fat dry milk in tris-buffered saline (m-TBS) was used to block the membrane before primary antibody incubation. MuRF1 and MAFbx were acquired from ECM Biosciences (Versailles, Kentucky), and all remaining antibodies described herein were purchased from Cell Signaling Technology (Beverly, Massachusetts). The following proteins were assess for total content, and when applicable, for phosphorylation content of key sites: Akt (phosphorylated at Ser473), mTOR, rpS6 (Ser235/236), 4E-BP1 (Thr 37/46), eIF4E (Ser209), ERK1/2 (Thr202/Tyr204), eEF2k (Ser366), eEF2 (Thr56), Ubiquitin, FoxO3a, MuRF1, MAFbx, Bcl-2, and Bax. Membranes were incubated in the appropriate antibody dilution (typically 1:1000) in m-TBS overnight with gentle agitation at 4 °C. Membranes were washed three times in 1x TBS for 5 min each, then incubated in the appropriate (anti-rabbit or anti-mouse) secondary antibody (1:2000) in m-TBS for 1 h with gentle agitation at room temperature. Blots were washed a second time, followed by a 5 min incubation with enhanced chemiluminescence (Thermo Fisher Scientific), and were detected using an Alpha Innotech (San Leandro, California) imaging system. Bands

were developed with a CCD camera and optical densities were determined using Alpha Innotech's AlphaEase FC software, which was automatically set to remove non-specific binding from densitometry values. Groups were run on membranes representing all study groups from this project as well as the groups detailed in Section III (minimum n = 2 per blot). All bands were normalized by the average density of the CON animals' content to allow qualitative comparisons between membranes, and when necessary Ponceau S staining was used as a loading control (178), arguably a stronger correction method (2). Ubiquitin was assessed as the entire band to capture total ubiquitination levels. All values are displayed as Integrated Density Values (IDV) to provide qualitative comparisons.

Statistical Analysis

All analyses were carried out using SigmaStat v3.5 (Systat Software Inc., San Jose, California) to determine differences among groups in this study as well as in the groups discussed in Section II & Section III. A one-way analysis of variance (ANOVA) was used to compare groups, and when significant F-ratios were present a Student-Newman-Keuls (SNK) post hoc procedure was used to test differences among group means. Significance levels were predetermined at $p < 0.05$. For all results described in this study, groups sharing a similar letter are not significantly different ($p \geq 0.05$) and exact p values may be included for results that warrant highlighting and discussion, even if deemed not statistically significant.

Results

The findings of the non-exercised groups (HU, HU+REC, HU+REC+HU, & HU+REC+HU+REC) are discussed in great detail in Section II and Section III. They are included in the following results to allow comparisons to be made to the exercise groups (HU+EX & HU+EX+HU). In this cross-sectional study design, HU+REC is best compared to HU+EX to make inferences on the impact of passive versus active recovery from long-duration unloading, and HU+EX+HU may be considered as a pre-unloading exercise conditioning group (vs. HU+REC+HU).

Muscle Mass, Area, and Composition

Absolute muscle mass (Figure 4.2) and muscle weights normalized by tibia length (Figure 4.4) in the gastrocnemius and plantaris agree with the findings observed in total (Figure 4.5A) and muscle (Figure 4.5B) CSA, in which we actually observed a significant ($p < 0.05$) decline in muscle mass with our exercise paradigm (HU+EX vs. HU+REC). Soleus was not different in these Figures when considering the impact the exercise prescription during recovery on mass. In Figure 4.3, mass is normalized by body weight, and gastrocnemius and soleus relative masses were elevated (HU+EX vs. HU+REC), while plantaris was not, and was likely due to the considerable losses of body weight (Figure 4.3D) and relative limb fat (Figure 4.5C) during exercise training. In all aforementioned figures, no differences were detected between HU+EX+HU and HU+REC+HU, suggesting that our chronic resistance exercise paradigm, at least during

recovery, does not act to preserve muscle mass or area after a subsequent 28 d suspension period.

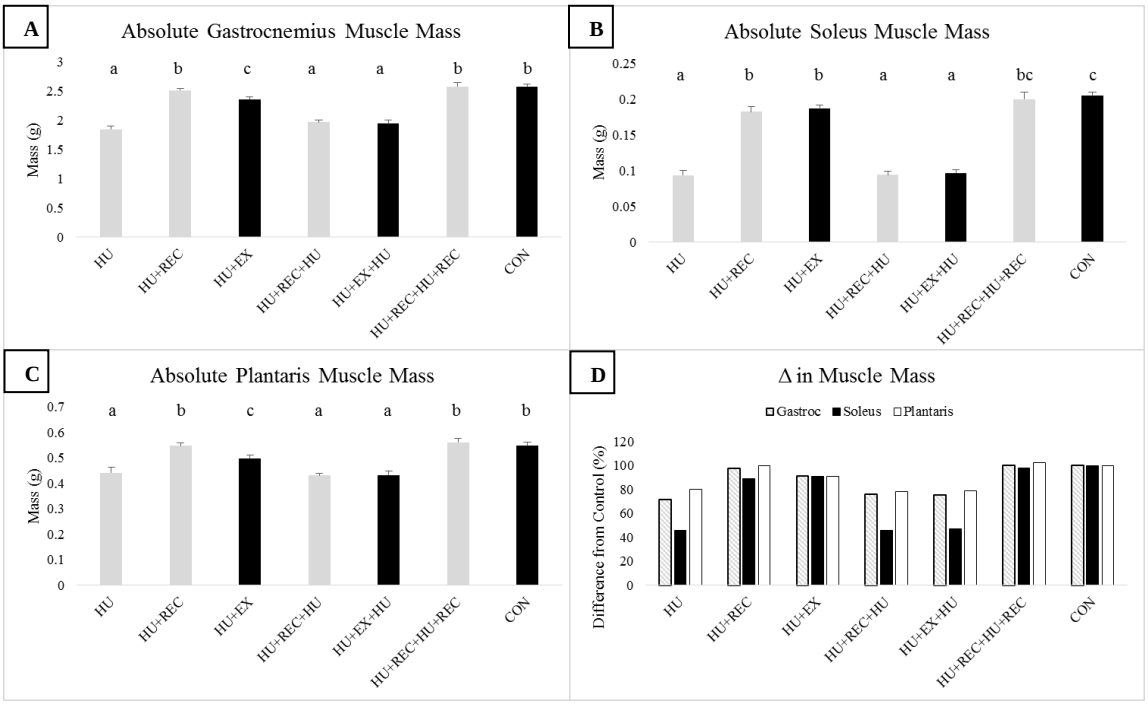

Figure 4.2. Study III Muscle Mass (Absolute). Muscle wet mass for the (A) gastrocnemius, (B) soleus, and (C) plantaris tissues, as well as (D) percent change from control for each tissue type. Values are means ± SE. Bars displaying similar letters in each graph are not significantly different from one another.

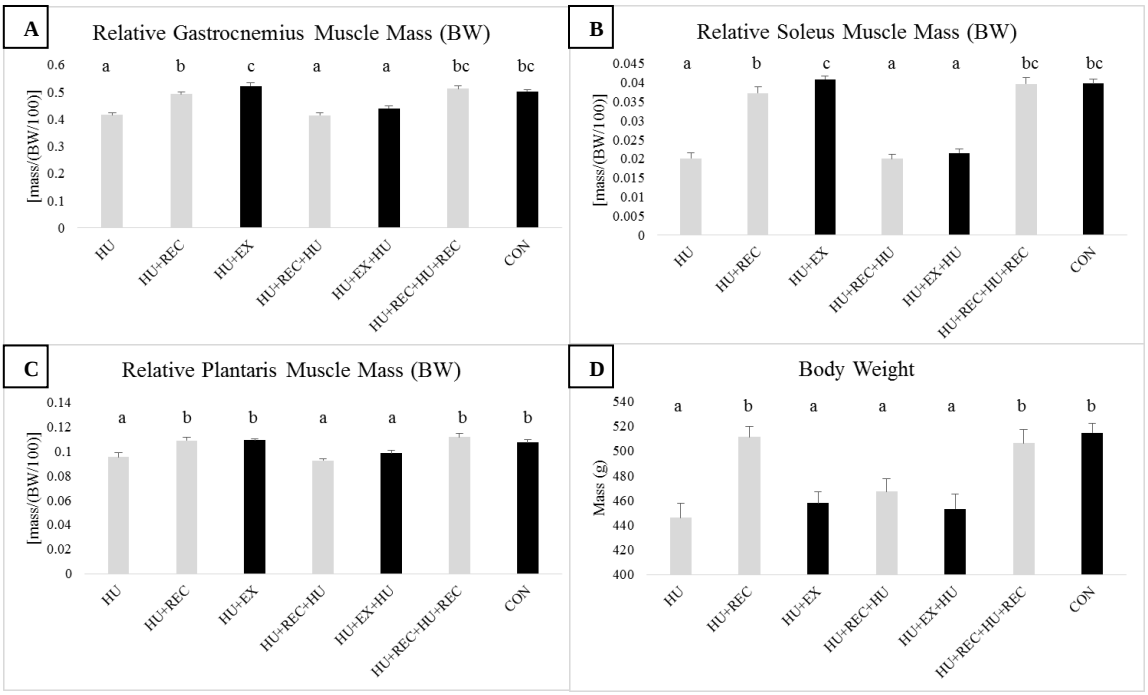

Figure 4.3. Study III Muscle Mass (Relative to body weight). Endpoint data for muscle mass normalized by body weight (g muscle · g body weight^{-1}) for the (A) gastrocnemius, (B) soleus, and (C) plantaris tissues, when assessed by (D) body weight (g). Values are means ± SE. Bars displaying similar letters in each graph are not significantly different from one another.

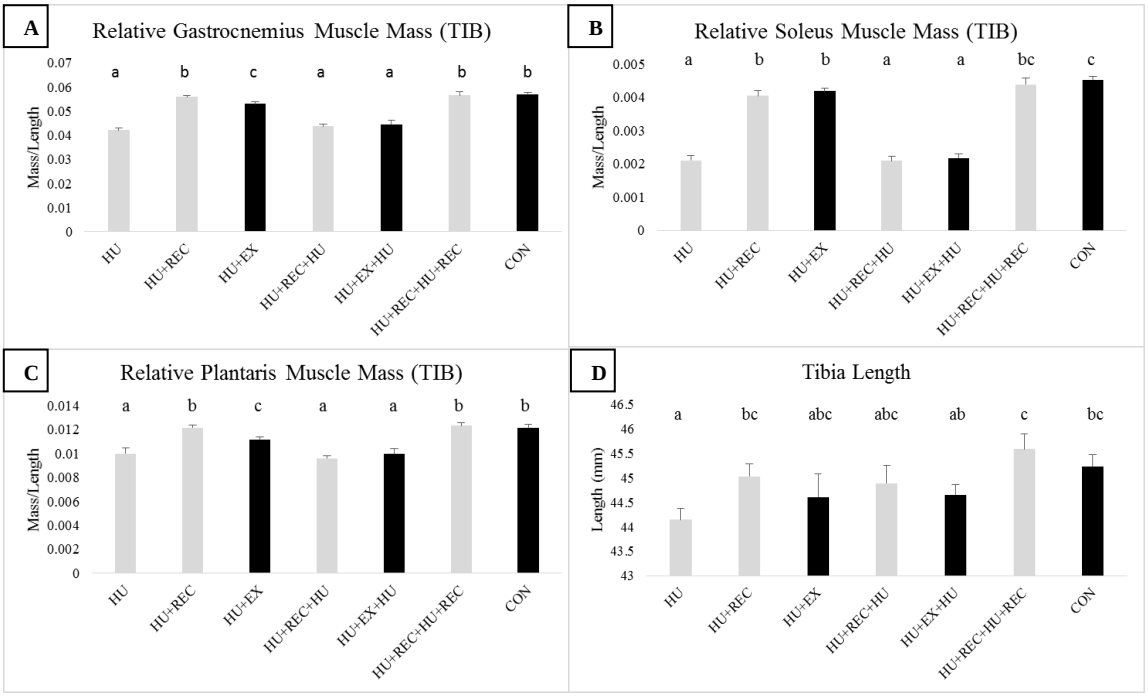

Fig. 4.4. Study III Muscle Mass (Relative to tibia length). Endpoint data for muscle mass normalized by bone length (g muscle· mm tibia length^{-1}) for the (A) gastrocnemius, (B) soleus, and (C) plantaris tissues, as well as (D) *in vivo* tibia lengths. Values are means ± SE. Bars displaying similar letters in each graph are not significantly different from one another.

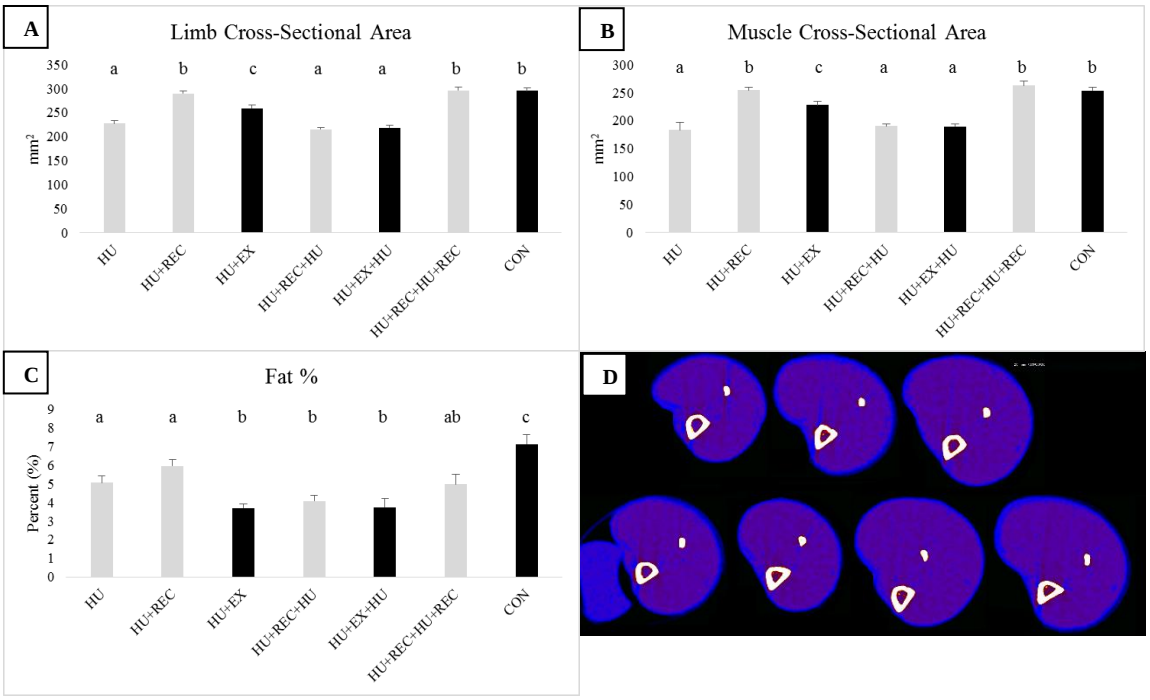

Fig. 4.5. Study III Peripheral Quantitative Computed Tomography (pQCT) Morphometry. *In vivo* assessments of the lower limb (at 50% tibia length) were taken just prior to sacrifice and evaluated for (A) limb CSA, (B) Muscle CSA, and (C) Fat Percent, Figure (D) poses representative scans of experimental groups (top line: HU, HU+REC, HU+EX; bottom line: HU+REC+HU [with brace], HU+EX+HU, HU+REC+HU+REC, and CON). Values are means ± SE. Bars displaying similar letters in each graph are not significantly different from one another.

No differences were found in muscle water percentage (Figure 4.6) when scrutinizing for exercise-generated effects.

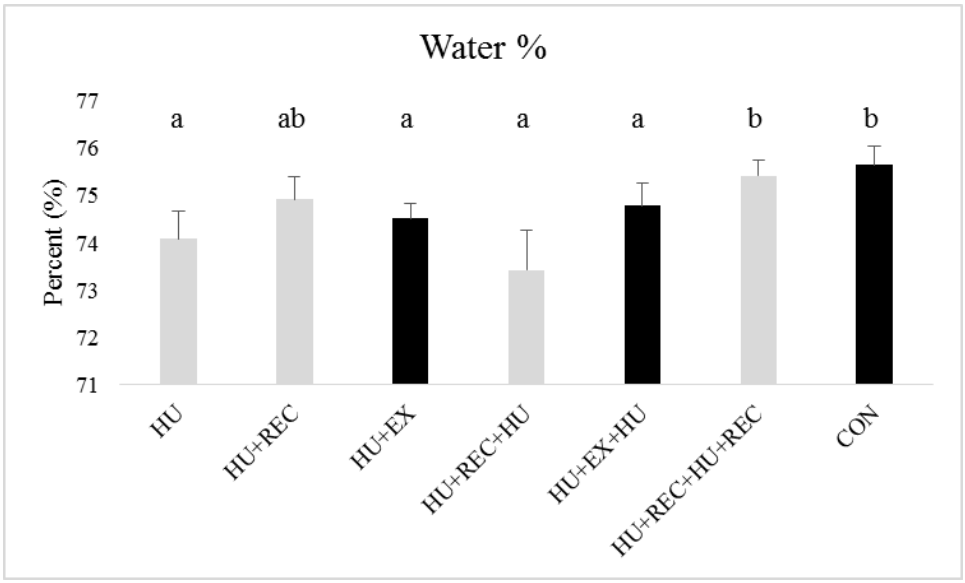

Fig 4.6. Study III Muscle Water Content. Muscle weights were taken before and after desiccation to determine water concentration. Values are means ± SE. Bars displaying similar letters in each graph are not significantly different from one another.

Exercise had no effect on muscle collagen content during recovery (HU+EX vs. HU+REC), which was assessed by hydroxyproline detection (Figure 4.7). However, resistance exercise appears to play a role in reducing the increase in muscle collagen observed in a second unloading bout, as HU+EX+HU was not different from CON ($p \geq 0.05$).

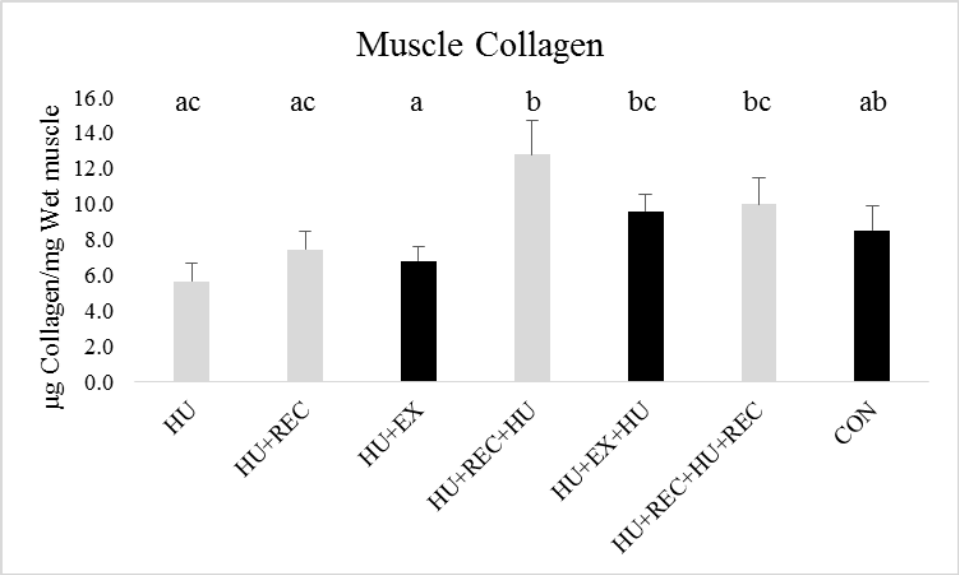

Fig. 4.7. Study III Gastrocnemius Collagen Concentration. Collagen concentration was determined via HPLC quantification of hydroxyproline concentration per mg wet muscle. Values are means ± SE. Bars displaying similar letters in each graph are not significantly different from one another.

Gastrocnemius Cytosolic Amino Acid Profile

Individual concentrations of 29 amino acids were measured in the free pool of the gastrocnemius as an indication of amino acid availability and to investigate which (if any) essential amino acids appeared to rate-limit muscle anabolism during mechanical overload (Table 4.1). No branched-chain amino acids (BCAA) were altered in HU+EX (vs. HU+REC), though essential amino acid (EAA) phenylalanine was reduced vs. HU+REC, but was not different than CON, and non-essential amino acids aspartate and proline were elevated. Interestingly, HU+EX+HU concentrations of all three BCAAs (isoleucine, leucine, and valine) were elevated above CON, but not to the values that HU

and HU+REC+HU observed. HU+EX+HU also had reduced lysine (EAA), alanine and arginine (non-essential), and 3-methylhistidine (vs. HU+REC+HU & CON).

	HU	HU+REC	HU+EX	HU+REC+HU	HU+EX+HU	HU+REC+HU+REC	CON
BCAA							
Isoleucine	0.1657 ± 0.0246^{a}	0.0934 ± 0.0045^{b}	0.0742 ± 0.0026^{b}	0.1544 ± 0.0082^{a}	0.1087 ± 0.0067^{c}	0.0819 ± 0.0085^{b}	0.0850 ± 0.0041^{b}
Leucine	0.2929 ± 0.0439^{a}	0.1520 ± 0.0066^{b}	0.1173 ± 0.0041^{b}	0.2729 ± 0.0161^{a}	0.1863 ± 0.0116^{c}	0.1348 ± 0.0104^{b}	0.1420 ± 0.0066^{b}
Valine	0.3204 ± 0.0392^{a}	0.1993 ± 0.0071^{b}	0.1984 ± 0.0070^{b}	0.3016 ± 0.0180^{a}	0.2321 ± 0.0111^{c}	0.1885 ± 0.0120^{b}	0.1871 ± 0.0076^{b}
EAA							
Histidine	0.1535 ± 0.0138	0.1717 ± 0.0076	0.1450 ± 0.0133	0.1614 ± 0.0079	0.1342 ± 0.0071	0.1532 ± 0.0103	0.1594 ± 0.0100
Lysine	0.2528 ± 0.0445^{ab}	0.2910 ± 0.0194^{a}	0.3017 ± 0.0254^{a}	0.2553 ± 0.0313^{a}	0.1721 ± 0.0076^{b}	0.2975 ± 0.0328^{a}	0.2647 ± 0.0266^{a}
Methionine	0.0439 ± 0.0082	0.0296 ± 0.0034	0.0300 ± 0.0030	0.0380 ± 0.0024	0.0259 ± 0.0044	0.0281 ± 0.0045	0.0248 ± 0.0031
Phenylalanine	0.1022 ± 0.0166^{a}	0.0719 ± 0.0038^{b}	0.0514 ± 0.0052^{c}	0.0982 ± 0.0063^{a}	0.0691 ± 0.0039^{bc}	0.0593 ± 0.0062^{bc}	0.0690 ± 0.0041^{bc}
Threonine	0.3514 ± 0.0801	0.3776 ± 0.0175	0.3523 ± 0.0150	0.3593 ± 0.0223	0.3104 ± 0.0140	0.3932 ± 0.0336	0.3784 ± 0.0256
Tryptophan	N/A	N/A	N/A	N/A	N/A	N/A	N/A
Other Common							
Alanine	2.1768 ± 0.1937^{a}	2.2515 ± 0.0923^{a}	2.0778 ± 0.1050^{a}	2.0905 ± 0.1146^{a}	1.8267 ± 0.0887^{b}	2.1624 ± 0.1591^{a}	2.3031 ± 0.1205^{a}
Arginine	0.1130 ± 0.0273^{a}	0.1073 ± 0.0057^{a}	0.1364 ± 0.0100^{a}	0.1137 ± 0.0146^{a}	0.0924 ± 0.0080^{b}	0.1099 ± 0.0145^{a}	0.0944 ± 0.0098^{a}
Asparagine	0.2977 ± 0.0327	0.4832 ± 0.1594	0.3289 ± 0.0160	0.5618 ± 0.2710	0.2468 ± 0.0148	0.4206 ± 0.0933	0.4548 ± 0.1467
Aspartate	0.0726 ± 0.0047^{a}	0.0725 ± 0.0043^{a}	0.1158 ± 0.0091^{b}	0.0495 ± 0.0068^{c}	0.0750 ± 0.0051^{a}	0.0791 ± 0.0073^{a}	0.0786 ± 0.0041^{a}
Cysteine	N/A	N/A	N/A	N/A	N/A	N/A	N/A
Glutamate	0.4634 ± 0.0148^{a}	0.5649 ± 0.0300^{b}	0.6600 ± 0.0521^{b}	0.6040 ± 0.0533^{ab}	0.5097 ± 0.0428^{ab}	0.5158 ± 0.0483^{ab}	0.4366 ± 0.0240^{a}
Glutamine	4.3383 ± 0.2829	4.7407 ± 0.2745	5.6772 ± 0.3195	4.7276 ± 0.4532	4.6911 ± 0.25563	4.9578 ± 0.3956	4.8488 ± 0.4000
Glycine	2.8103 ± 0.2395	2.4545 ± 0.1025	2.8358 ± 0.1873	2.8013 ± 0.1810	2.5400 ± 0.1436	2.4735 ± 0.1844	2.4305 ± 0.1862
Proline	0.2355 ± 0.0246^{a}	0.2928 ± 0.0099a^{b}	0.3197 ± 0.0148^{b}	0.2309 ± 0.0142^{a}	0.2300 ± 0.0122^{a}	0.2733 ± 0.0194^{ab}	0.2703 ± 0.0135^{ab}
Serine	0.4917 ± 0.0360	0.5577 ± 0.0217	0.6274 ± 0.0285	0.5413 ± 0.0311	0.4969 ± 0.0203	0.5614 ± 0.0408	0.5581 ± 0.0422
Tyrosine	0.1014 ± 0.0125^{ab}	0.0954 ± 0.0044^{ab}	0.0709 ± 0.0031^{b}	0.1046 ± 0.0066^{a}	0.0815 ± 0.0040^{b}	0.0885 ± 0.0075^{ab}	0.0867 ± 0.0048^{b}
All Other							
3-Methylhistidine	0.0632 ± 0.0096^{ab}	0.0643 ± 0.0049^{ab}	0.0722 ± 0.0059^{a}	0.0560 ± 0.0089^{ab}	0.0402 ± 0.0032^{b}	0.0685 ± 0.0098^{a}	0.0650 ± 0.0057^{a}
α-Aminobutyric Acid	0.5510 ± 0.0388	0.4763 ± 0.0241	0.4521 ± 0.0426	0.5513 ± 0.0515	0.5005 ± 0.0297	0.5155 ± 0.0507	0.4904 ± 0.0292
Anserine	10.6103 ± 0.8998^{a}	7.4142 ± 0.3011^{b}	7.224 ± 0.3769^{b}	10.1498 ± 0.6731^{a}	9.0763 ± 0.5187^{ab}	7.0908 ± 0.4397^{b}	7.7005 ± 0.3310^{b}
β-Alanine	0.1384 ± 0.0089^{ab}	0.1298 ± 0.0039^{ab}	0.1175 ± 0.0035^{b}	0.1511 ± 0.0069^{a}	0.1296 ± 0.0063^{ab}	0.1235 ± 0.0031^{ab}	0.1284 ± 0.0052^{ab}
Carnosine	2.1357 ± 0.1699	2.3507 ± 0.1015	2.5280 ± 0.1184	2.3833 ± 0.1192	2.4783 ± 0.1599	2.3497 ± 0.156	1.9775 ± 0.0758
Citrulline	0.2080 ± 0.0226	0.2368 ± 0.0108	0.3002 ± 0.0310	0.2182 ± 0.0172	0.2119 ± 0.0113	0.2455 ± 0.0202	0.2335 ± 0.0145
Ethanolamine	0.0707 ± 0.0070^{a}	0.0556 ± 0.0025^{ab}	0.0393 ± 0.0045^{b}	0.0667 ± 0.0037^{a}	0.0439 ± 0.0032^{bc}	0.0508 ± 0.0035^{ac}	0.0530 ± 0.0035^{ac}
Hydroxyproline	0.1171 ± 0.0182^{ab}	0.1122 ± 0.0074^{ab}	0.1343 ± 0.0083^{ab}	0.1056 ± 0.0092^{ab}	0.1026 ± 0.0087^{ab}	0.0634 ± 0.0086^{b}	0.123 ± 0.0090^{ab}
Ornithine	0.0168 ± 0.0029^{a}	0.0249 ± 0.0013^{ab}	0.0285 ± 0.0016^{b}	0.0170 ± 0.0016^{ab}	0.0178 ± 0.0016^{a}	0.0227 ± 0.0023^{ab}	0.0228 ± 0.0020^{ab}
Phosphoethanolamine	0.0698 ± 0.0107^{a}	0.0444 ± 0.0038^{b}	0.0469 ± 0.0060^{b}	0.0651 ± 0.0080^{a}	0.0646 ± 0.0060^{a}	0.0378 ± 0.0035^{b}	0.0446 ± 0.0042^{b}
Taurine	17.9230 ± 1.5208	15.5782 ± 0.6011	14.1913 ± 0.6466	16.8416 ± 0.8655	14.9615 ± 0.5941	14.3525 ± 1.0718	14.6455 ± 0.7223

Table 4.1. Study III Gastrocnemius Cytosolic Amino Acid Profile. Amino acid composition was assessed in the gastrocnemius free pool via UPLC. Values are means ± SE. Data displaying different letters within each amino acid are significantly different.

Muscle Protein Synthesis

Total muscle protein synthesis was evaluated during the final 24 h of each study group (Figure 4.8A-C).

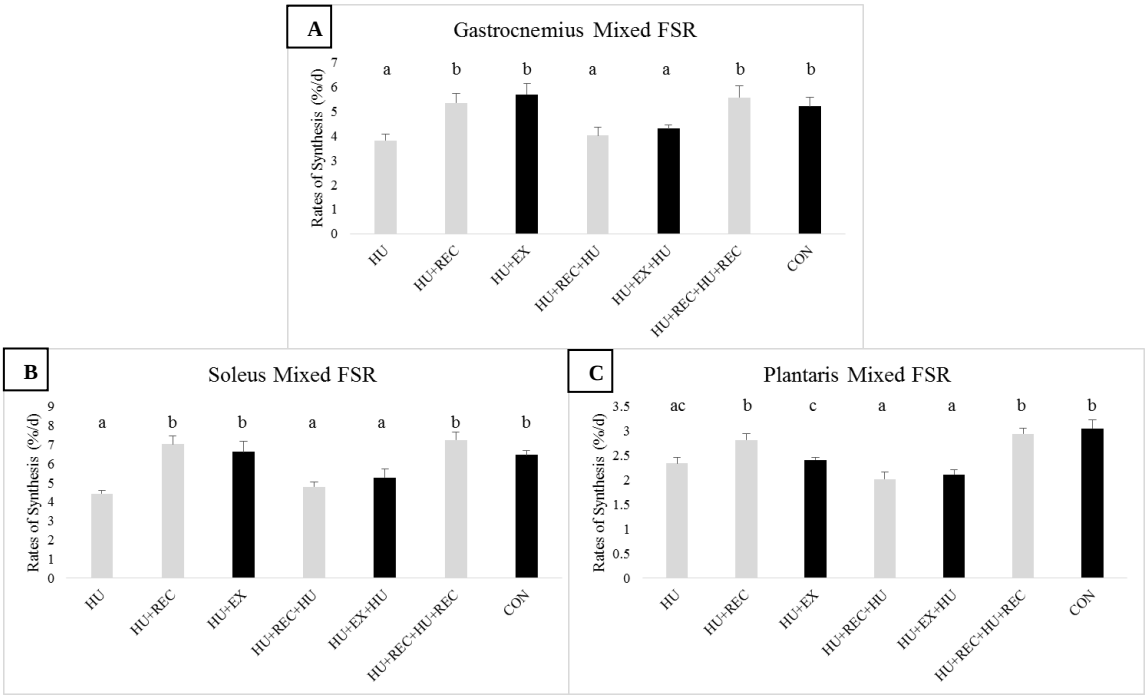

Fig. 4.8. Study III 24 h Mixed Fractional Synthesis Rates. Twenty-four hour cumulative mixed FSR in the (A) gastrocnemius, (B) soleus, and (C) plantaris muscles. Values are means ± SE. Bars displaying similar letters in each graph are not significantly different from one another.

Mixed FSR was unchanged due to exercise in the gastrocnemius and soleus muscle (vs. HU+REC), and the exercise prescription had no preserving/rescuing effect on synthesis rates in the HU+EX+HU group (vs. HU+REC+HU). Plantaris FSR measured at 56 d after HU was actually reduced by the exercise protocol,

yielding only 85.4% of the muscle anabolism displayed by passive recovery measures. Resistance exercise did not produce any changes in contractile muscle protein synthesis (Figure 4.9).

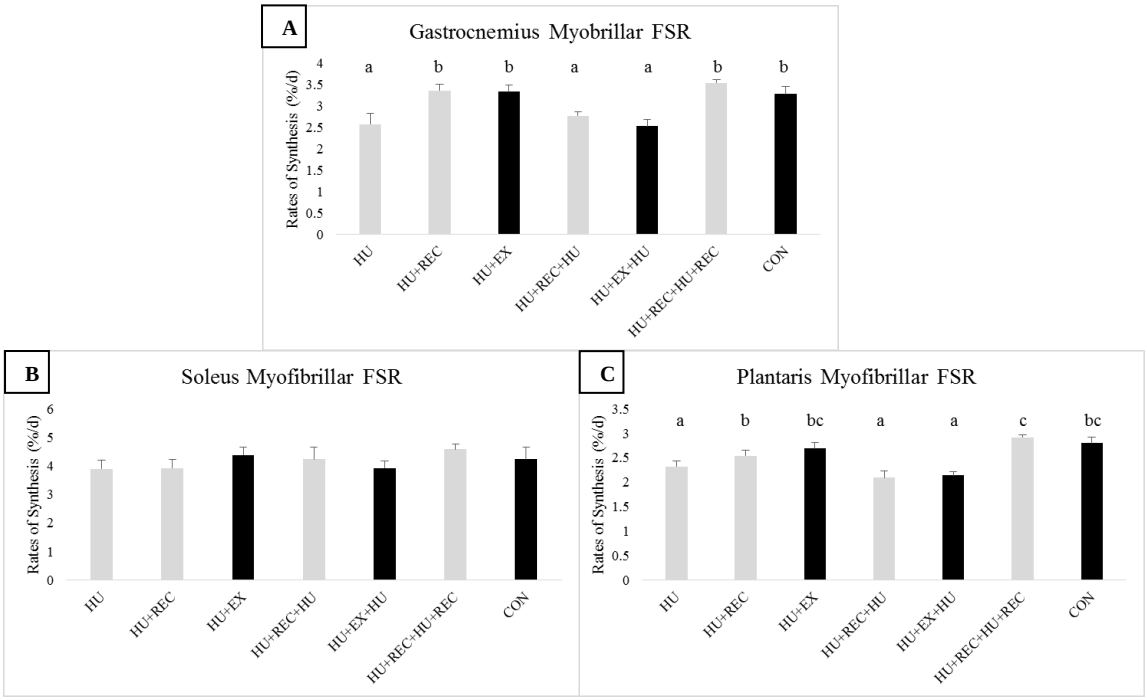

Fig. 4.9. Study III 24 h Myofibrillar Fractional Synthesis Rates. Twenty-four hour cumulative myofibrillar FSR in the (A) gastrocnemius, (B) soleus, and (C) plantaris muscles. Values are means ± SE. Bars displaying similar letters in each graph are not significantly different from one another.

Expression of Anabolic Markers

Exercise did not alter (HU+EX vs. HU+REC and/or HU+EX+HU vs. HU+REC+HU; $p \geq 0.05$) protein expression (displayed as phosphorylated:total content unless specified otherwise) in any of the following signaling proteins: Akt(Ser473), rpS6

(Ser235/236), or ERK1/2 (Thr202/Tyr204), although their findings can be found in Figures 4.10, 4.13, and 4.15, respectively. Total mTOR protein (Figure 4.11) was increased in HU+EX animals above CON values (+66.5%; $p < 0.05$), but was not different than HU+REC ($p \geq 0.05$). Exercise generated robust elevations in relative 4E-BP1 phosphorylation (Figure 4.12) and subtle increases in eIF4E phosphorylation (Figure 4.14) with HU+EX, but did not alter HU+EX+HU expression relative to HU+REC+HU.

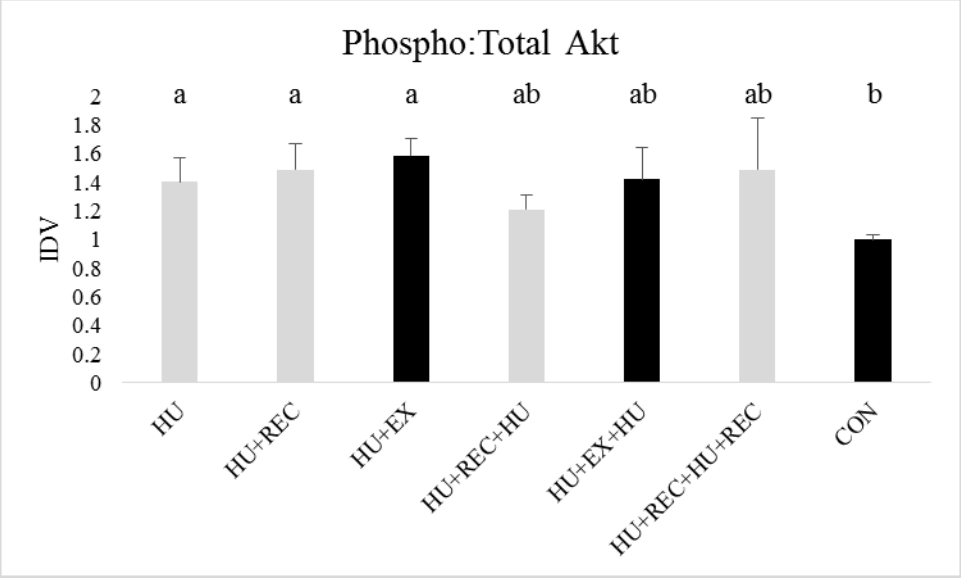

Fig. 4.10. Study III Expression of Akt (Ser473). Immunoblot of the anabolic protein Akt in the gastrocnemius. Assessed as phosphorylated protein to total. Values are means ± SE. Bars displaying similar letters in each graph are not significantly different from one another.

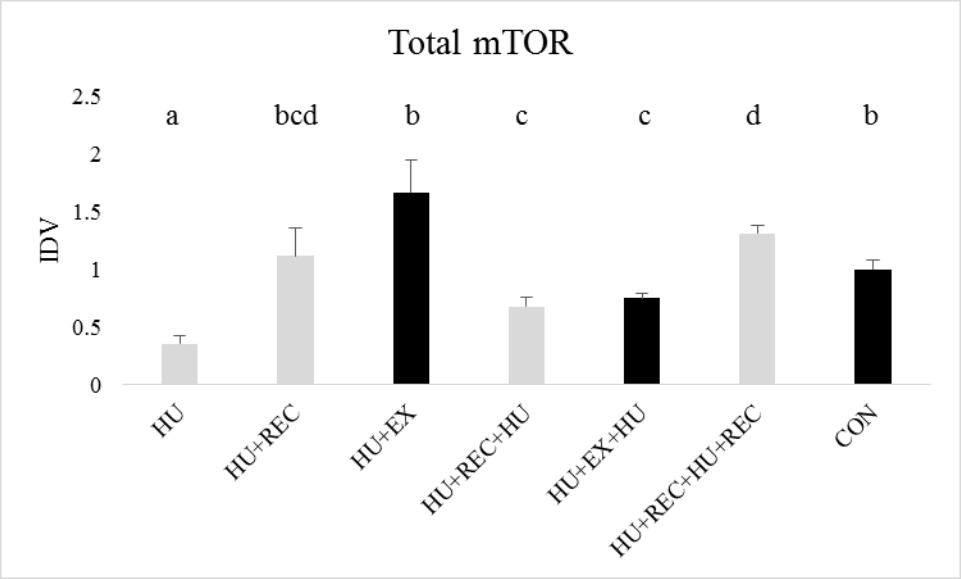

Fig. 4.11. Study III Expression of Total mTOR. Immunoblot of the anabolic protein mTOR in the gastrocnemius. Assessed as total protein. Values are means ± SE. Bars displaying similar letters in each graph are not significantly different from one another.

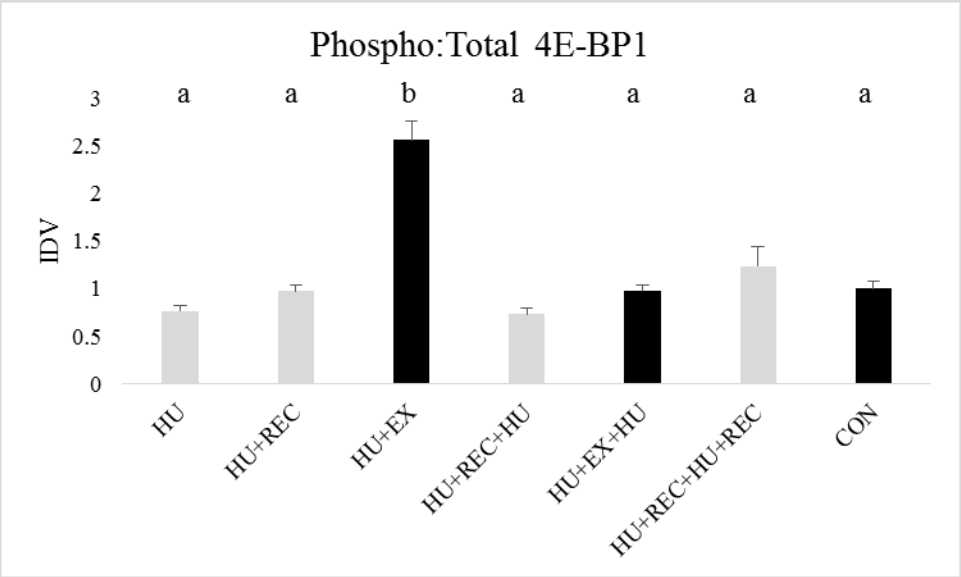

Fig. 4.12. Study III Expression of 4E-BP1 (Thr37/46). Immunoblot of the anabolic protein 4E-BP1 in the gastrocnemius. Assessed as phosphorylated protein to total. Values are means ± SE. Bars displaying similar letters in each graph are not significantly different from one another.

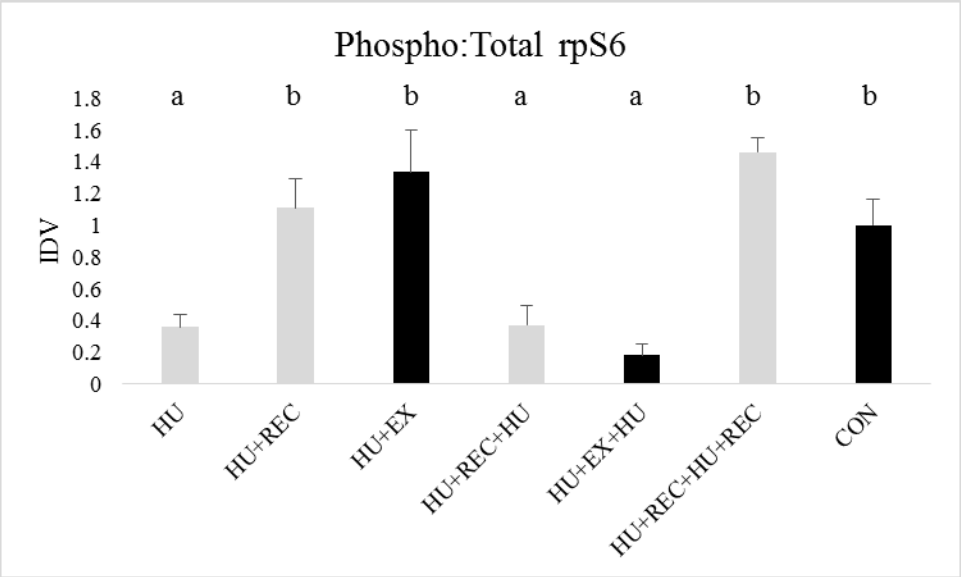

Fig. 4.13. Study III Expression of rpS6 (Ser235/Ser236). Immunoblot of the anabolic protein rpS6 in the gastrocnemius. Assessed as phosphorylated protein to total. Values are means ± SE. Bars displaying similar letters in each graph are not significantly different from one another.

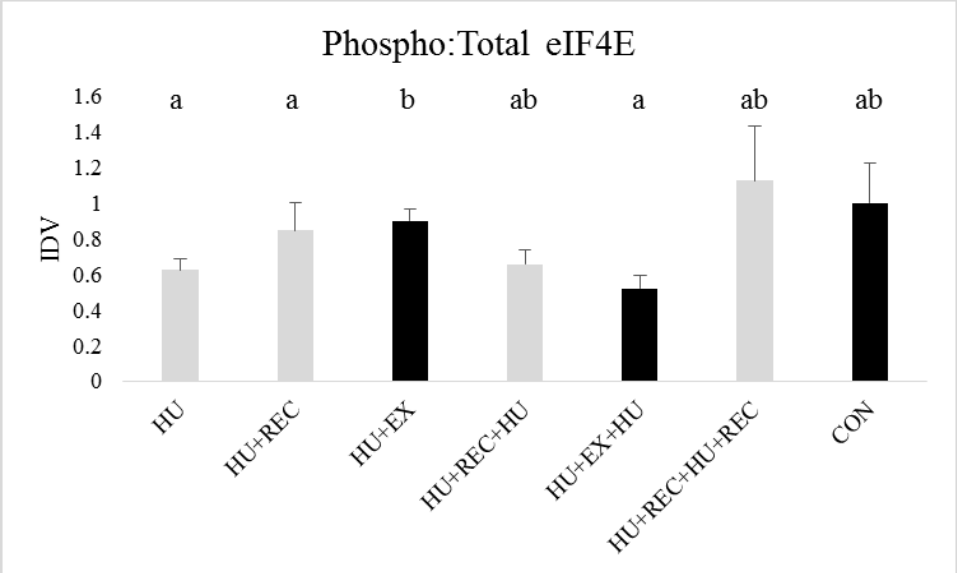

Fig. 4.14. Study III Expression of eIF4E (Ser209). Immunoblot of the anabolic protein eIF4E in the gastrocnemius. Assessed as phosphorylated protein to total. Values are means ± SE. Bars displaying similar letters in each graph are not significantly different from one another.

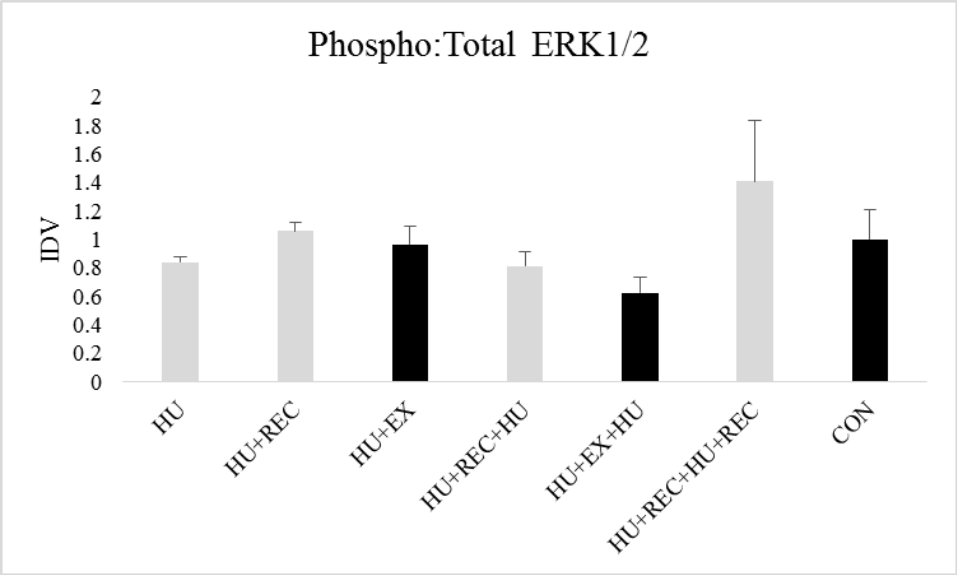

Fig. 4.15. Study III Expression of ERK1/2 (Thr202/Tyr204). Immunoblot of the anabolic protein ERK1/2 in the gastrocnemius. Assessed as phosphorylated protein to total. Values are means ± SE. Bars displaying similar letters in each graph are not significantly different from one another.

Expression of Regulators of mRNA Translation Elongation

The ratios of phosphorylated to total eEF2k is presented in Figure 4.16, and its downstream target- eEF2, is shown in Figure 4.17. Significant differences were not detected among groups in the inhibitory kinase, while HU+EX relative phosphorylation of eEF2 (Figure 4.17A) was the lowest of any group (-37.3% vs. CON; $p < 0.05$). The only other group to express reduced eEF2 was HU+EX+HU (-26% vs CON; $p < 0.05$), though this effect may be due to substantial increases in total eEF2 content due to exercise (Figure 4.17B).

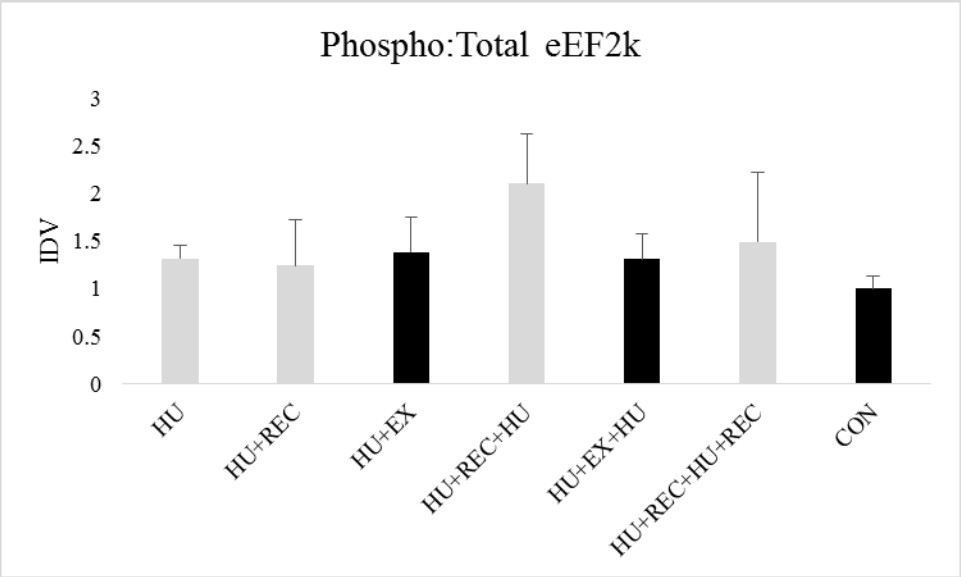

Fig. 4.16. Study III Expression of eEF2k (Ser366). Immunoblot of the elongation protein eEF2k in the gastrocnemius. Assessed as phosphorylated protein to total. Values are means ± SE. Bars displaying similar letters in each graph are not significantly different from one another.

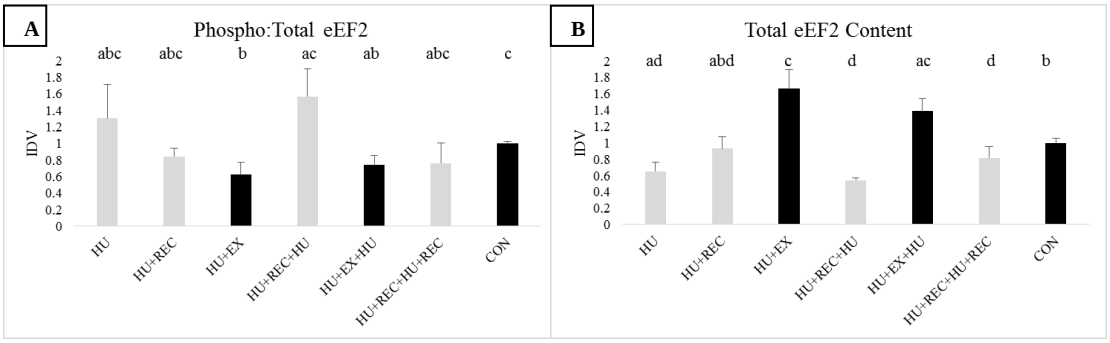

Fig. 4.17. Study III Expression of eEF2. Data is present as (A) a ratio of phosphorylated eEF2 (Thr56) to total expression, and (B) Total eEF2 content alone. Values are means ± SE. Bars displaying similar letters in each graph are not significantly different from one another.

Expression of Regulators of Catabolism

Four markers associated with catabolism (ubiquitin, FoxO3a, MuRF1, and MAFbx) are presented in Figures 4.18-21, respectively. Ubiquitin content was not different among loading conditions, and MuRF1 was not different among exercise groups and their sedentary counterparts. Total FoxO3a expression (Figure 4.19) was elevated in HU+EX and HU+EX+HU (vs. HU+REC and HU+REC+HU, respectively), while MAFbx demonstrated nonsignificant increases due to exercise during recovery (HU+EX was +74.6%; $p = 0.27$).

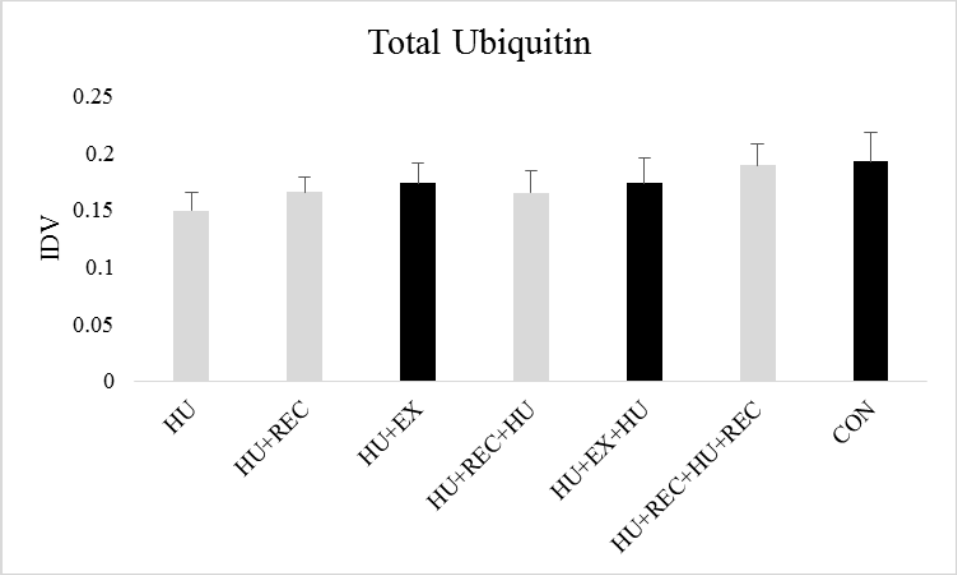

Fig. 4.18. Study III Expression of Ubiquitin. Immunoblot of the catabolic protein ubiquitin in the gastrocnemius. Assessed as total content. Values are means ± SE. Bars displaying similar letters in each graph are not significantly different from one another.

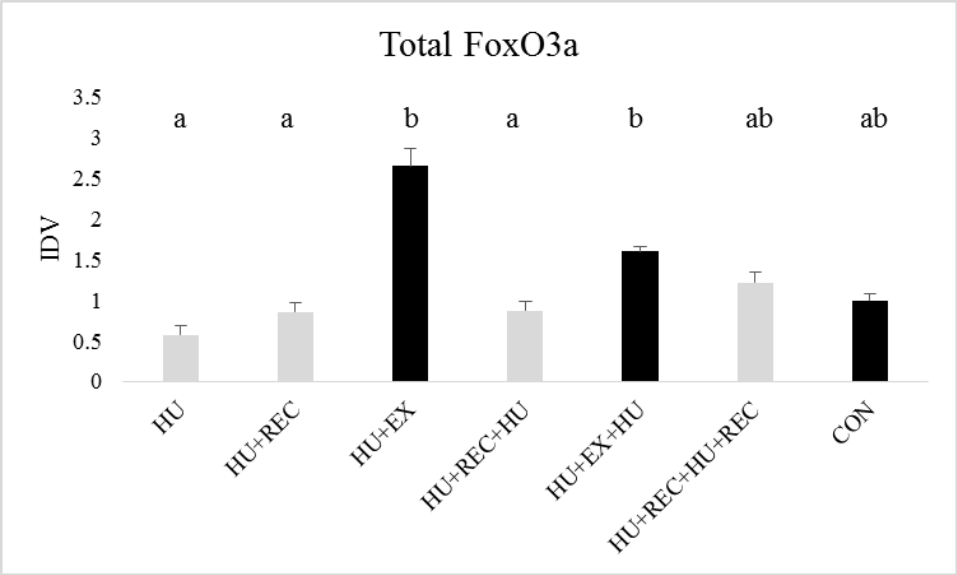

Fig. 4.19. Study III Expression of FoxO3a. Immunoblot of the catabolic protein FoxO3a in the gastrocnemius. Assessed as total content. Values are means ± SE. Bars displaying similar letters in each graph are not significantly different from one another.

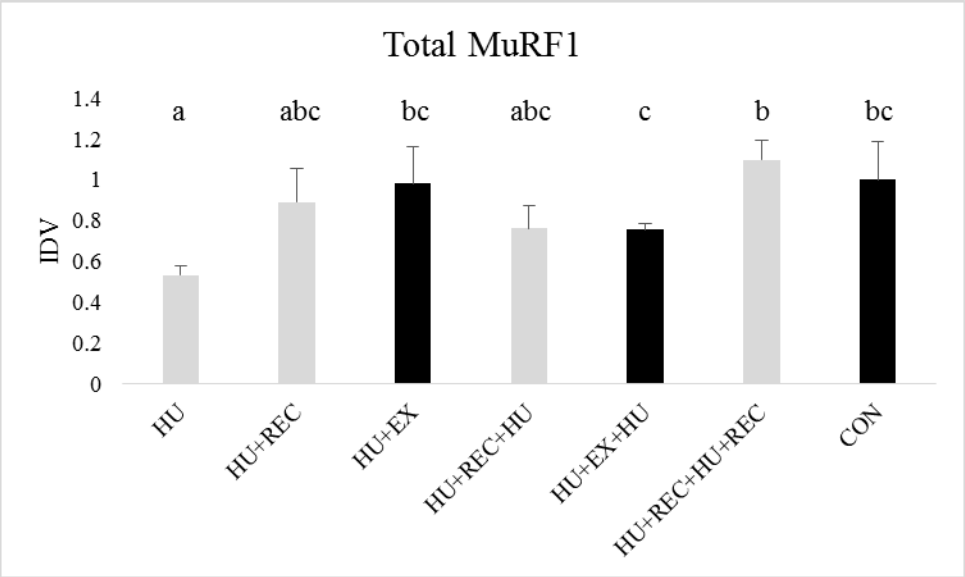

Fig. 4.20. Study III Expression of MuRF1. Immunoblot of the catabolic protein MuRF1 in the gastrocnemius. Assessed as total content. Values are means ± SE. Bars displaying similar letters in each graph are not significantly different from one another.

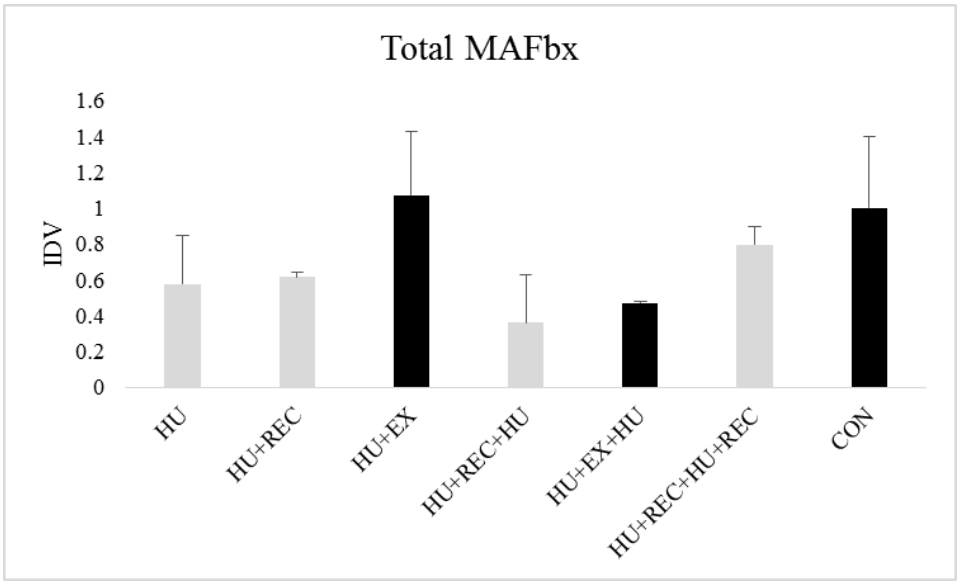

Fig. 4.21. Study III Expression of MAFbx. Immunoblot of the catabolic protein MAFbx in the gastrocnemius. Assessed as total content. Values are means ± SE. Bars displaying similar letters in each graph are not significantly different from one another.

Expression of Apoptotic Markers

Lastly, the apoptotic markers Bcl-2 (Figure 4.22) and Bax (Figure 4.23) are provided below. There were slight, albeit insignificant, increases in both exercise groups compared to their passive recovery groups in Bcl-2 protein content, and Bax signaling was identical (EX vs. REC groups).

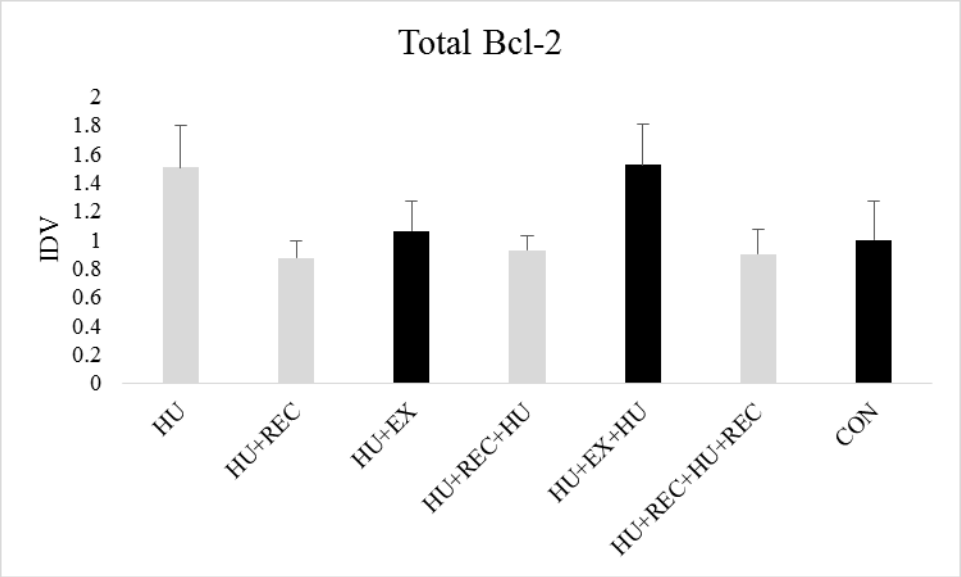

Fig. 4.22. Study III Expression of Bcl-2. Immunoblot of the apoptotic protein Bcl-2 in the gastrocnemius. Assessed as total content. Values are means ± SE. Bars displaying similar letters in each graph are not significantly different from one another.

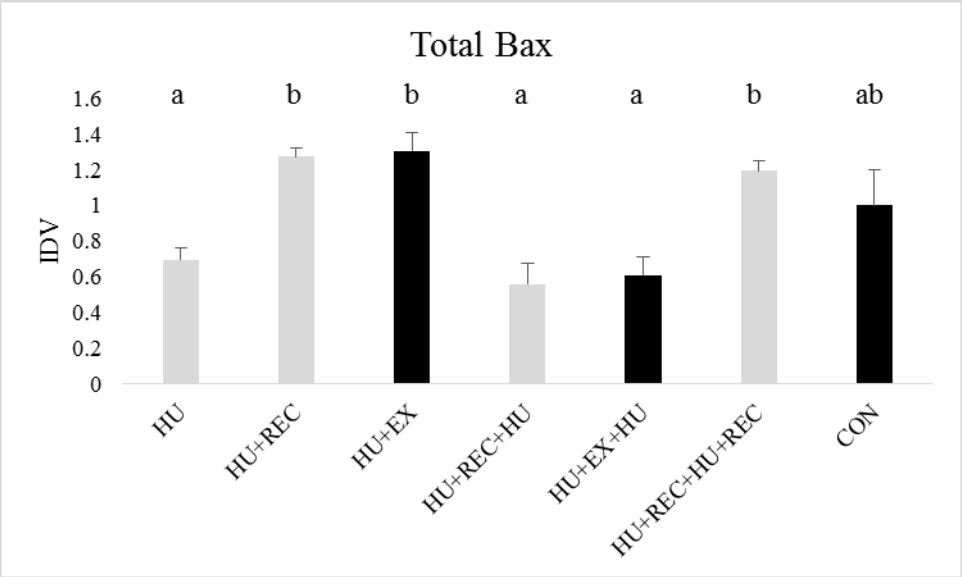

Fig. 4.23. Study III Expression of Bax. Immunoblot of the apoptotic protein Bax in the gastrocnemius. Assessed as total content. Values are means ± SE. Bars displaying similar letters in each graph are not significantly different from one another.

Discussion

The breadth and depth of skeletal muscle physiology research is nearly immeasurable, as the tissue is constantly being driven by countless factors to determine or alter cell size, function, nuclear status, energy state, and several other components of the locomotive tissue, even when considering only protein homeostatic balance. Muscle's influences as an endocrine organ have led to considerable efforts in investigating muscle's interaction with several other organs or disease states. Many of these changes contribute to the notion of muscle plasticity- the tissue's ability to rapidly change according to the specific mode and magnitude of various stimuli. The work described herein wanted to characterize biological repeatability (the ability for muscle

plasticity to be reversed as well as replicated under cyclical changes in opposing stimuli) as a component of plasticity, with a focus on mechanical load status. And while the literature describes the short- (61, 129, 213, 238) and long-term (125, 128, 203) effects of disuse on skeletal muscle function, structure, and biology, as well as muscle's ability to recover following disuse (with passive (23, 232) and active (105, 163) rehabilitation), no work to date can truly delineate if muscle's plasticity and biological repeatability is influenced by successive bouts of unloading or reloading, nor the impact of overload on these conditions.

This study adopted a resistance exercise prescription that was proven to increase skeletal parameters beyond those of passive recovery following long-duration hindlimb unloading, and to mitigate some of the negative effects of a second bout of mechanical unloading (197). Overall, it appears that the exercise prescription required for robust skeletal changes during recovery and as a preventer of future losses may be considerably lower than the changes needed to elicit changes in muscle protein anabolism and overall changes in mass. While some anabolic signaling supported the effects of the resistance training protocol, our findings suggest that the moderate-intensity, moderate-volume program employed was either insufficient to stimulate hypertrophy or was performed in tissue that was pre-damaged by the unloading and therefore unprepared for an intervention of this intensity and/or frequency. These concepts are more elaborately discussed in Section V.

The Resistance Exercise Paradigm Employed did not Elicit Hypertrophy

The observed changes in body weight and fat % after the exercise recovery period, and overall reductions in gastrocnemius and plantaris muscle masses, corroborated by decreases in limb and muscle CSA at the middiaphysis, demonstrate that our exercise regimen was not properly prescribed to facilitate an anabolic recovery from disuse. The slight increases of relative muscle mass (normalized by body weight) suggest that non-muscular tissue, likely fat tissue, was lost at a slightly greater rate than muscle as opposed to better 'maintaining' of muscle mass in the face of atrophying conditions.

Mixed muscle FSR was not increased in any muscle in the 24 h following the final exercise bout in any of the studied tissues, confirming the ineffectiveness of this exercise protocol as an appropriate therapy following long-duration disuse as a means to improve muscle mass recovery above passive reloading alone. In fact, FSR was lower in the plantaris muscle of HU+EX animals. As food intake was not found to differ between HU+EX and HU+REC, it would appear that the diminished FSR in the plantaris was caused by ineffective anabolic signaling or an increase in catabolic or apoptotic factors. Exercise did not alter myofibrillar FSR when compared against the non-exercise load-matched group (HU+EX vs. HU+REC; HU+EX+HU vs. HU+REC+HU).

It is difficult to judge the anabolic signaling cascades responsible for controlling muscle protein synthesis in our study, as the samples are harvested 24 h after the final exercise session. If we consider mTOR to be the primary regulator of the PI3K/Akt/mTOR pathway, and that pathway to be the predominant regulator of muscle

anabolism, then a 24-h measure is far too late to capture most of the signaling changes that occur due to resistance exercise (20, 230). While the signaling discussed in Section III is useful as it provides insight to the regulation of steady-state disuse and full recovery, our model simply fails to capture the signaling response (if any) to our resistance exercise paradigm. The one signaling activity that was increased in our HU+EX group was 4E-BP1. The increased phosphorylation-to-total expression of 4E-BP1 prevents its binding to eIF4E, thereby allowing for mRNA translation initiation complex formation (71). This increased phosphorylation does not imply increased anabolism, but simply the removal of an inhibitory regulator of translation. Our exercise program may provide increased elongation efficiency, evidenced by our eIF4E phosphorylation (186) and reduced eEF2 phosphorylation (113), but this alteration did not contribute to improved anabolism. Of interest is that the increase of total eEF2 content following resistance exercise persisted even after 28 d of unloading (HU+EX+HU), which resulted in a relative lowering of phosphorylation that should prove to be conducive to anabolism. More research is necessary to determine why protein content is maintained at higher levels in response to exercise even after 28 d of unloading. Our data suggests that primary culprits altering anabolism are upstream of the elongation process of protein synthesis.

Resistance Exercise Elevated FOXO3a Content, but No Downstream Catabolic or Apoptotic Markers

Resistance exercise demonstrated higher total FOXO3a expression in HU+EX animals compared to their HU+REC counterparts, which agrees with similar 24 h post-exercise work by others (136) in protein but may not be supported by transcription work (135). It should be noted, however, that measures of transcript and protein are not always consistent. Increased FOXO3a expression did not result in increases in its downstream targets MuRF1 or MAFbx, which has been characterized elsewhere in steady-state atrophy (184) but no works measuring the 24 h post-exercise protein expression are known to the authors. Our HU+EX animals did not display any differences in apoptotic signaling vs. HU+REC, and no catabolic or apoptotic measures were altered in HU+EX+HU compared to HU+REC+HU.

Skeletal Muscle may not be Prepared for Resistance Exercise Therapies After Unloading

One possible concern is that the muscle is weakened during long-duration unloading, perhaps predisposing it to increased damage during recovery that is exacerbated by the onset of a resistance exercise regimen. Research has demonstrated increased interstitial regions, mononuclear invasion, and lesions are specific to the recovery after unloading and not the disuse condition alone (121, 122), and exercise recovery work has shown muscle to be particularly sensitive to pliometric exercises (163). This may be due to losses of contractile fibers during unloading (168, 171, 172), which renders muscle unprepared for the return of full weight-bearing loads, or the

overload posed by this exercise intervention. We may have created substantial muscular injury during the early-stage exercise, in which operant conditioning began only 7 d after the cessation of unloading, and was arguably the most damaging exercise during the early portion of the training, when the highest number of repetitions (lowest weights) were invoked. If our exercise regimen was similar to overtraining syndrome in athletes, it may have similar effects, which include elevated degradation and decreased synthesis (187). This is wildly different than passive recovery from exercise, in which synthesis rates return to control values in the first 6 h after cessation of disuse, remain at basal levels for 2 d, then significantly increased on Day 4 (221). If we impeded early stage recovery, and had exercise conditions induced an overtraining state, it would be no surprise that our masses were lower than those of HU+REC animals. Future studies should detail the efficacy of the training paradigm on healthy, non-unloaded animals to determine if any hypertrophic effect can be obtained from the prescribed training, as well as detail the early time-point effects of this training on recovering muscle with emphasis on muscle protein turnover as well as morphological impacts.

Conclusion

This work highlights the challenges of preventing muscle atrophy during disuse or recovering after long-duration unweighting, as a similar exercise prescription not only resulted in improved recovery in bone, but also mitigated several outcomes of skeletal physiology during subsequent unloading (197), but in these current studies exacerbated recovery in muscle compared to passive recovery. Whether the lack of hypertrophy via

exercise during recovery from disuse is due to a lack of exercise intensity remains to be seen. Post-disuse exercise prescriptions studies should highlight two critical values: at what time post-unloading is muscle no longer susceptible to increased myodamage, especially during eccentric resistance exercise, and is an exercise prescription proven in non-unloaded animals (normal starting values) sufficient to improve muscle mass following steady-state disuse. Our findings determine that resistance exercise programs sufficient to rescue and improve bone outcomes may contribute to improved recovery in muscle (vs. passive recovery), but the rationale remains to be elucidated.

V. DEPTOR EXPRESSION AND REGULATION IS ALTERED BY MECHANICAL LOAD

Synopsis

Recent interest in the protein DEPTOR, a negative regulator of mTOR, has demonstrated its potential as a therapeutic target in maintaining muscle mass during atrophy *in vitro*. In this final study, we explore the extent to which DEPTOR and one of its regulatory proteins are expressed in comparison to mechanical loading states. Male Sprague-Dawley rats (n = 108) from the studies described in the previous Sections were placed in one of the following groups: 28 d unloading (HU), 28 d unloading with 56 d recovery with either passive ambulation reloading (HU+REC) or chronic resistance training (HU+EX), groups exposed to 28 d unloading, one of the recovery strategies, and then a second 28 d unweighting period (HU+REC+HU & HU+EX+HU), animals undergoing two unloading and two passive recovery cycles (HU+REC+HU+REC), or control (CON). At the end of the study, the gastrocnemius muscles from each animal were removed and assessed for DEPTOR and RBX1 protein content via immunoblotting. This information was presented, along with key data from earlier Sections, to explore the mechanistic regulation of DEPTOR on muscle mass via tight manipulations of muscle anabolism. Results include the first known data demonstrating steady-state unloading is accompanied by elevated DEPTOR expression (and concomitantly lower RBX1 content) that is reversed with mechanical reloading or overloading. We also demonstrate that mixed muscle FSR highly correlates with DEPTOR content in an inverse relationship, posing its potential as a surrogate for

quantifiable muscle protein synthesis measures. Overall, we close out the Dissertation with this study to highlight a currently unexplored opportunity to exploit muscle anabolism regulation and possibly determine a realistic target for anti-atrophy countermeasures.

Introduction

The Sections above have characterized the reactions to steady-state atrophy from mechanical unloading, the efficacy of recovery from disuse using a moderate-intensity, moderate-volume voluntary resistance exercise training program vs. passive reloading, and sought to establish biological repeatability (ability to repeatedly respond to specific stimuli with similar reactions) and biological resilience (instances where muscle's capacity for change was exceeded) as functions of muscle plasticity (ability to change to specific stimuli based on its magnitude and type. In this final study we delve into a more mechanistic marker of muscle homeostasis.

mTOR has been widely regarded as the keystone signaling protein for muscle anabolism (17). With downstream targets to increase formation of the initiation translation complex (thereby allowing for mRNA translation into polypeptides) as well as prevent the formation of said ribosomal complex (For Review; (190)), and upstream control via mechanotransduction (20), amino acid influx (46), insulin (167), growth hormone (97), hypoxia (24), stress (37), or countless other stimuli have established mTOR as a mainstay target of muscle biology in striving to understand the control of muscle mass.

The protein mTOR is just one component that compromises the anabolic regulator mTOR-complex 1 (mTORC1), which differs from the cytoskeleton- and cell survival-regulating mTORC2 due to the inclusion of either Raptor or Rictor, respectively. One protein found in both complexes is the DEP domain-containing mTOR-interacting protein (DEPTOR), which acts as a potent endogenous inhibitor of mTOR. Its role has traditionally focused in tumorogenesis, as its potential overexpression could result in minimal (or non-existent protein synthesis of cancer cells (160, 224, 236, 237). It wasn't until the work by Kazi et al. that DEPTOR was considered for the opposite of its target for cancer therapies: targeting DEPTOR suppression in order to drive muscle protein synthesis through rescued or improved mTOR signaling (115). Their work demonstrated that *in vitro* suppression of DEPTOR maintained anabolism and muscle weights through 3 d of casting disuse. Our lab's work generated the first known physiological alterations in DEPTOR content, as we observed reduced DEPTOR expression following an acute session of resistance exercise, as well as similarly-suppressed DEPTOR content during sarcopenic obesity in both exercised and sedentary subjects, suggesting its potential role in anabolic resistance (155). We therefore turn our attention to further examining this protein during conditions known to affect muscle anabolism and mass to understand the mechanisms involved in mTOR-driven muscle homeostasis.

Based on our previous findings (155), we hypothesized that DEPTOR protein expression would closely and inversely mimic muscle anabolism (mixed muscle FSR). As our exercise paradigm was not overtly successful at generating a hypertrophic effect,

we did not anticipate DEPTOR content to be noticeably lower in our exercised group (compared to passive recovery alone). We also investigated expression of Ring-box protein 1 (RBX1), a component of the SCF complex known to downregulate DEPTOR content (237). We expected to see RBX1 total content to be associated with changes in loading conditions, as its knockdown was recently proven to result in an accumulation of DEPTOR and subsequent inhibition of mTOR-mediated cell growth (233). Lastly, we sought to objectively test the relationship between our 24 h FSR measures and DEPTOR content. Tying into our central aim of this Dissertation, we hypothesized that DEPTOR content would respond in a similar fashion and intensity in subsequent repeated bouts of similar loads, i.e., muscle plasticity and repeatability would be reflected in DEPTOR protein expression in relation to mechanical unloading, reloading, and overload.

Materials and Methods

Animals

All procedures described herein were approved by and conducted in accordance with the Institutional Animal Care and Use Committee of Texas A&M University. Male Sprague-Dawley rats (Harlan Laboratories Inc, Houston, Texas) were selected for this study and obtained at 5.5 months of age. Animals were group-housed for 2 wk in a standard environment (23ºC ± 2ºC, 12:12 h dark/light cycle) and given water and standard rodent chow *ad libitum*. Following transport recovery and acclimation, all animals were singly-housed, normalized by body weight, and assigned to one of the following groups: 1) 28 d of constant hindlimb unloading (HU, n = 16), 2) 28 d HU

session immediately followed by a 56 d recovery bout of normal ambulation (HU+REC, *n* = 16), 3) 28 d of constant hindlimb unloading immediately followed by a 56 d recovery bout of normal ambulation supplemented with resistance exercise (HU+EX, *n* = 14), 4) two HU cycles of 28 d with a 56 d recovery bout between unloadings (HU+REC+HU, *n* = 16), 5) two unloading cycles with a 56 d EX program during recovery period between unloadings (HU+EX+HU, *n* = 18), 6) two alternating cycles of 28 d HU and 56 d recovery (HU+REC+HU+REC, *n* = 14), and 7) an age- and housing-matched control group (CON, *n* = 14). Figure 5.1 illustrates the experimental design.

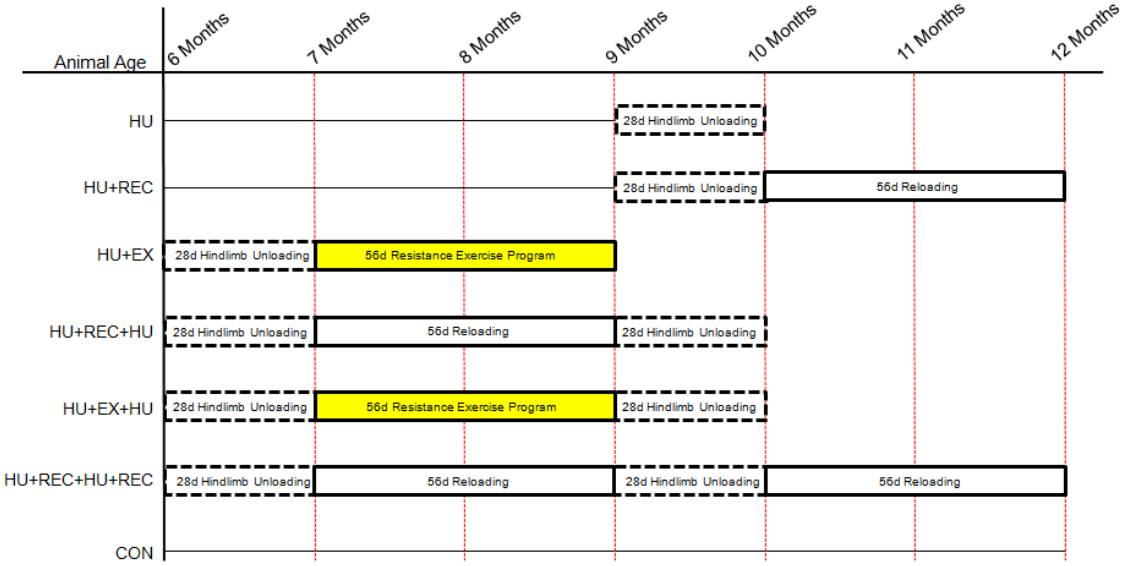

Fig. 5.1. Study IV Experimental Study Design. Hindlimb Unloading (HU) was achieved via a tail suspension harness and carried out continuously for 28 d, and Reloading (REC) was carried out by 56 d passive recovery through normal cage ambulation or with Reloading supplemented with Resistance Exercise (EX) performed 21 times over the 56 d recovery period.

Body weights were recorded weekly, and twice-daily health checks were carried out to ensure each animal was healthy and loaded appropriately. In order to prevent any effects due to food consumption (proven to affect body and muscle masses), all animals were pair-fed during the first week of each unloading period.

At the conclusion of the study, each animal was anesthetized with ketamine/xylazine (100 $mg \cdot kg^{-1}$ & 10 $mg \cdot kg^{-1}$, respectively) prior to tissue harvest. Cardiac puncture was immediately followed by euthanasia via decapitation, and tissue removal. Whole blood was collected and spun to collect serum, which was then stored at -80 °C. The gastrocnemius muscles were excised, cleaned of extraneous blood, fat, and connective tissue, weighed and recorded, and finally snap-frozen in liquid nitrogen before -80 °C storage.

Hindlimb Unloading

Simulated microgravity was accomplished through the use of hindlimb unloading (HU), a well-published ground-based analog to spaceflight (For Review; (149)) commonly utilized by our group to study muscle atrophy (50, 63, 64, 118) (WIGGS). Tail harnesses were attached 24 h prior to each suspension period and removed for each recovery bout. Animals were briefly anesthetized with 2% isofluorane (US Pharmacopia, Rockville, Maryland) in order to attach the custom tail harness. A thin layer of non-irritant adhesive (Amazing Goop, Eclectic Products, Los Angeles, California) was generously applied around the base of the tail, and was firmly attached to porous athletic tape (Kendall, Mansfield, Massachusetts) and allowed to dry. The

athletic tape attached to the base of the tail (~2.54 cm of contact) on each lateral side and extended ~15.24 distally, where each end of the tape connected and joined a paper clip. The animal was allowed to recover from anesthesia and wore the harness while ambulating normally. On Day 0 of each unloading period the paper clip of the harness was then attached to a swivel apparatus overhead that was connected to a steel bar bisecting the top of the custom-built 45.72 cm x 45.72 cm x 45.72 cm cage. When attached, the animal's hindquarters would be elevated high enough that they could not come in contact with the floor of the cage, resulting in a 30° head-down tilt and complete disuse of the hindlimbs. The steel bar allowed for nearly complete movement about the cage with the forelimbs, but prevented the animal from resting its rear quarters on the walls. This system did not inhibit the rats' ability to feed, drink, or groom.

On Day 28 of HU, animals reaching their final time point (HU, HU+REC+HU, & HU+EX+HU) were anesthetized, removed from HU, and subjected immediately to tissue harvest. Animals that would continue on to a recovery bout were anesthetized, had their harnesses removed, and allowed full ambulation throughout their 56 d recovery session before being harvested (HU+REC, HU+EX, & HU+REC+HU+REC) or subjected to a second unloading (HU+REC+HU & HU+EX+HU). Any animal found out of its harness during a health check was immediately removed from the study, as were animals facing any sort of health concern. Overall, the study maintained a 95% success rate in completing each 28 d HU bout.

Resistance Exercise Training

Following their first unloading bout, animals were given 7 d of ambulatory recovery and then began the resistance exercise program previously employed in our lab (67, 74, 156). Training occurred in a custom-built upright acrylic box (21 cm length x 21 cm width x 35 cm height) fitted with an illuminated lever situated above the animal's head. The rat was be operant conditioned to recognize the activation of the light bulb and attempt to depress the overhead lever, which required full extension of the lower body. When necessary, a brief foot shock was administered to encourage an exercise repetition. Three operant conditioning sessions (0 g; 50 repetitions/session) was given to train the animal for the program, with 48 h rest between sessions. Following operant conditioning, resistance was increased through the addition of lead weights to a small vest affixed to the animal. Training three times per week (48 h rest between sessions) for 7 wk, intensity was progressively increased from 80g to 270g load, a protocol proven to improve several aspects of skeletal parameters above normal ambulatory reloading when invoked after steady-state disuse atrophy (197). Twenty-four hours after the final exercise session HU+EX animals were harvested and HU+EX+HU animals were placed in their second suspension bout.

Measurement of Protein Synthesis

Twenty-four hour fractional synthesis rates (FSR) for the mixed (total) fraction were assessed in the gastrocnemius using deuterium oxide (^2H_2O) incorporation techniques well-described by our lab (76, 156). Animals were given a bolus dose of

99.9% deuterium oxide (Cambridge Isotopes, Andover, Massachussetts) in a saline solution (0.9% NaCl) via intraperitoneal injection (20µl·g^{-1} body weight) 24 h prior to tissue harvest. The priming bolus was supplemented with 4% $^{2}H_2O$ drinking water provided *ad libitum* to maintain enrichment during the final 24 h of the study. FSR was determined by measuring the levels of ^{2}H incorporation into the muscle protein and the precursor pool, described in detail below. FSR was determined in the mixed subfraction as previously described by our lab (76). Pulverized mixed muscle tissues (~30 mg) were homogenized with a Polytron in 0.3 ml of 10% (w/v) trichloroacetic (TCA) acid. Samples were centrifuged at 5,000 g for 15 min at 4 °C, the supernatant (containing free, unbound amino acids) was decanted and removed, 0.3 ml TCA added to the pellet and vortexed until broken down, and the wash-spin step repeated two additional times. After the third and final wash step the protein-bound pellet was dissolved in 0.4 ml of 6 N hydrochloric acid for 24 h at 100 °C. 100 µl of the hydrolysate was dried down and derivatized with 100 µl of a 3:2:1 (v/v/v) solution of methyl-8 (N,N-Dimethylformamide dimethyl acetal, Thermo Fisher Scientific, Waltham, Massachusetts), methanol, and acetonitrile for 1 h at 70ºC. Derivatized samples were injected into a GCMS (Agilent 7890 GC & 5975 VL MSD, Agilent Technologies, Santa Clara, California) using previously described parameters (74, 75). All muscle samples were analyzed in triplicate and calculated from a linear regression formula generated by known ^{2}H-alanine standards (0-2.0% ^{2}H-alanine:alanine) prepared identically to the sample procedure.

Deuterium (^{2}H) enrichment of the available precursor pool was determined by quantifying $^{2}H_2O$-enriched serum based on a linear regression formula generated by

deuterium standards identically prepared. A 20 µl serum sample was allowed to react with 2 µl of 10 N sodium hydroxide and 4 µl of a 5% (v/v) acetone in acetonitrile solution at room temperature for 24 h. Then, ~0.5 g sodium sulfate decahydrate was added as a drying agent, and 0.6 ml chloroform was introduced to the sample to stop the isotopic exchange between $^{2}H_2O$-enriched serum samples and acetone. A small aliquot (1 µl) was injected into the GCMS, volatilized, separated, and detected using methods detailed in earlier publications by our lab (74, 75, 156). All serum samples were prepared and measured in duplicate, and the average value used in FSR calculations.

FSR was calculated using the following equation:

$$FSR = E_A \cdot [E_{BW} \times t(d) \times 3.7)^{-1} \times 100,$$

where E_A represents the amount of protein-bound ^{2}H-alanine (mole percent excess), E_{BW} is the quantity of $^{2}H_2O$ in the precursor pool (mole percent excess), t(d) designates the total time of incorporation (in days), and 3.7 represents the exchange coefficient of ^{2}H between body water and alanine (e.g. 3.7 of 4 carbon-bound hydrogens of alanine exchange with water (49)).

Immunoblotting

Immunoblotting was carried out in the cytosolic-rich fraction of the gastrocnemius muscle. To isolate this fraction we employed methods detailed elsewhere (155). Briefly, differential centrifugation was carried out in 60 mg of pulverized gastrocnemius muscle tissue. The sample was homogenized with a Polytron (Brinkmann Lab Equipment, Westbury, New York) in 0.4 ml ice-cold Norris buffer (25

mM Hepes, 25 mM benzamidine, 10 mM $MgCl_2$, 5 mM β-glycerophosphate, 4 mM EDTA, 2 mM PMSF, 0.2 mM ATP, 0.5% protease inhibitor cocktail P8340 (v/v), 0.1% Triton-x 100, 10 mM activated Na_3VO_4, and 100 mM NaF; pH 7.4). Samples were allowed to rest for 1 h on ice before centrifugation at 30,000 g for 30 min at 4ºC. The supernatant (cytosolic-rich fraction) was decanted and saved for determining protein expression. A small (10 µl) aliquot was used to determine protein concentration quantification via bicinchoninic acid (BCA) assay (199), and 60 µg of protein was selected for each sample to ensure even loading and qualitative analyses. Samples were randomly selected and blocked by gel to ensure a minimum $n = 2$ for each group was represented on each gel, and location within each gel was randomized to minimize any potential bias. Samples were added to 4x Laemmli buffer (123) and denatured at 100 °C before being loaded onto 4-15% gradient polyacrylamide gels (Lonza, Switzerland) for protein separation via 1 h SDS-PAGE (40 mA in standard electrode buffer [25 mM Tris, 19.2 mM glycine, 0.1% SDS (w/v)]) and a 45 min semi-dry transfer (350 mA) onto a nitrocellulose membrane, 5% (w/v) non-fat dry milk in tris-buffered saline (m-TBS) was used to block the membrane before primary antibody incubation. DEPTOR and RBX1 were acquired from Cell Signaling Technology (Beverly, Massachusetts). Membranes incubated in the appropriate antibody dilution (1:1000) in m-TBS overnight with gentle agitation at 4 °C. Membranes were washed three times in 1x TBS for 5 min each, then incubated in anti-rabbit secondary antibody (1:2000) in m-TBS for 1 h with gentle agitation at room temperature. Blots were washed a second time, followed by a 5 min incubation with enhanced chemiluminescence (Thermo Fisher Scientific), and were

detected using an Alpha Innotech (San Leandro, California) imaging system. Bands were developed with a CCD camera and optical densities were determined using Alpha Innotech's AlphaEase FC software, which was automatically set to remove non-specific binding from densitometry values. All bands were normalized by the average density of the CON animals' band (minimum n = 2 per blot) to allow qualitative comparisons between membranes, and when necessary Ponceau S staining was used as a loading control (178), arguably a stronger correction method (2).

Statistical Analysis

As the project employed a cross-section study design, none of the statistical analyses were considered with repeated measures. All analyses were carried out using SigmaStat v3.5 (Systat Software Inc., San Jose, California). A one-way analysis of variance (ANOVA) was used to compare groups, and a Student-Newman-Keuls (SNK) post hoc procedure was used to test differences among group means when significant F-ratios were present. Significance levels were predetermined at $p < 0.05$. For all results described in this study, groups sharing a similar letter are not significantly different ($p \geq 0.05$) and exact p values may be included for results that warrant highlighting and discussion, even if deemed not statistically significant.

Results

Gastrocnemius muscle mass (absolute) and synthesis rates were reported in previous Sections, but are provided in Figures 5.2A and 5.2B to make inferences on the

blotting data below. Briefly, each unloading period (HU, HU+REC+HU, & HU+EX+HU) demonstrated similar reductions in muscle mass, which is at least partly due to consistently lower rates of protein synthesis. Passive recovery (HU+REC & HU+REC+HU+REC) allowed for a complete rescuing of muscle mass and anabolism, returning to values that were not different from controls. However, when exercise was employed during recovery (HU+EX) muscle mass was found to be lower than passive recovery (-6.2% vs. HU+REC; $p < 0.05$), although this was not corroborated by mixed FSR (+6.4% vs. HU+REC; $p \geq 0.05$).

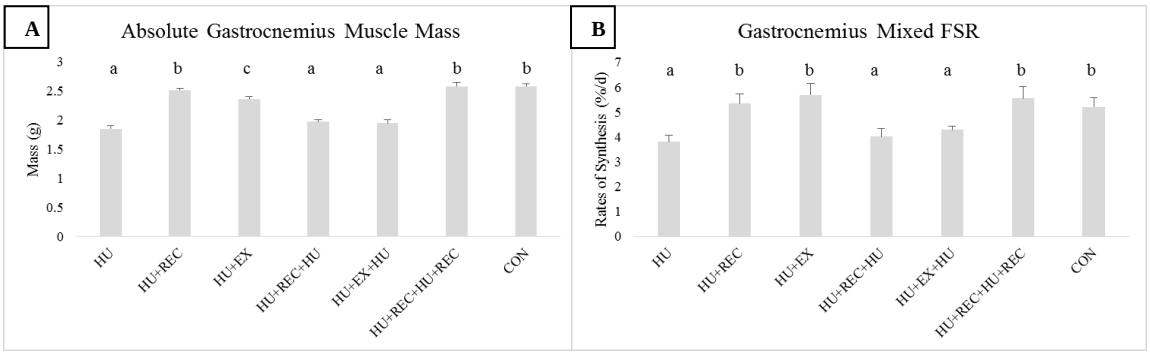

Figure 5.2. Study IV Gastrocnemius Mass & Anabolism. Data from previous Sections include (A) muscle wet mass and (B) mixed FSR for the gastrocnemius. Values are means ± SE. Bars displaying similar letters in each graph are not significantly different from one another within each Figure.

Protein expression for DEPTOR (Figure 5.3) was higher in unloaded groups, although HU+REC+HU (+18.2%) and HU+EX+HU (+30.6%) failed to achieve significance ($p \geq 0.05$) vs. CON. The loaded groups (HU+REC, HU+EX, & HU+REC+HU+REC) were similar to CON values.

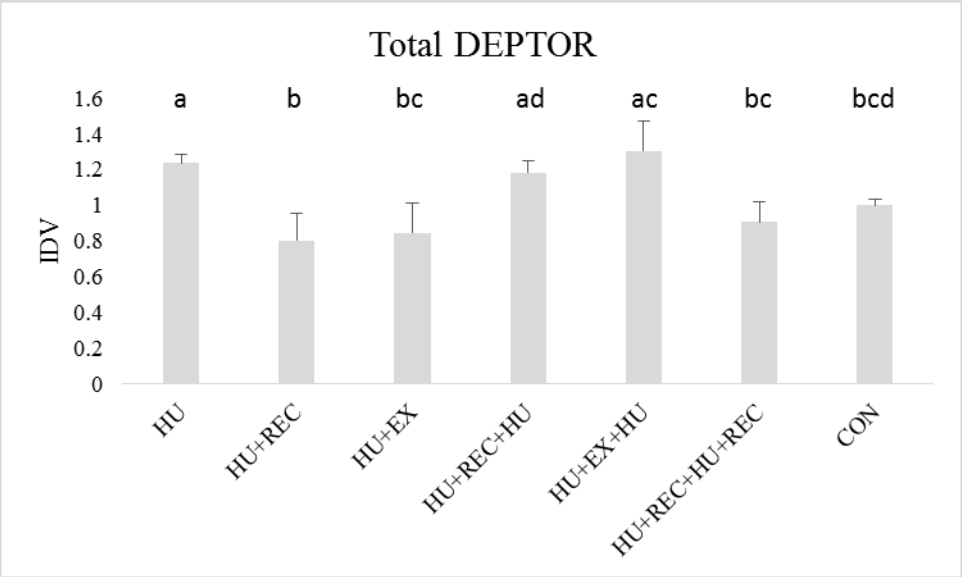

Fig. 5.3. Study IV Expression of Total DEPTOR. Immunoblot of the anabolic protein DEPTOR in the gastrocnemius. Assessed as total content. Values are means ± SE. Bars displaying similar letters in each graph are not significantly different from one another.

RBX1, a protein belonging to a specific ubiquitin ligase system that serves as a downstream regulator of DEPTOR through degradation of this inhibitor, is provided in Figure 5.4. RBX1 signaling generally appears to be tied to mechanical loading. Normal ambulation appears to increase RBX1 content above that observed in unloaded groups, with mixed statistical results. HU+EX expression was higher than all groups except CON. Unloaded animals were all lower than CON ($p < 0.05$).

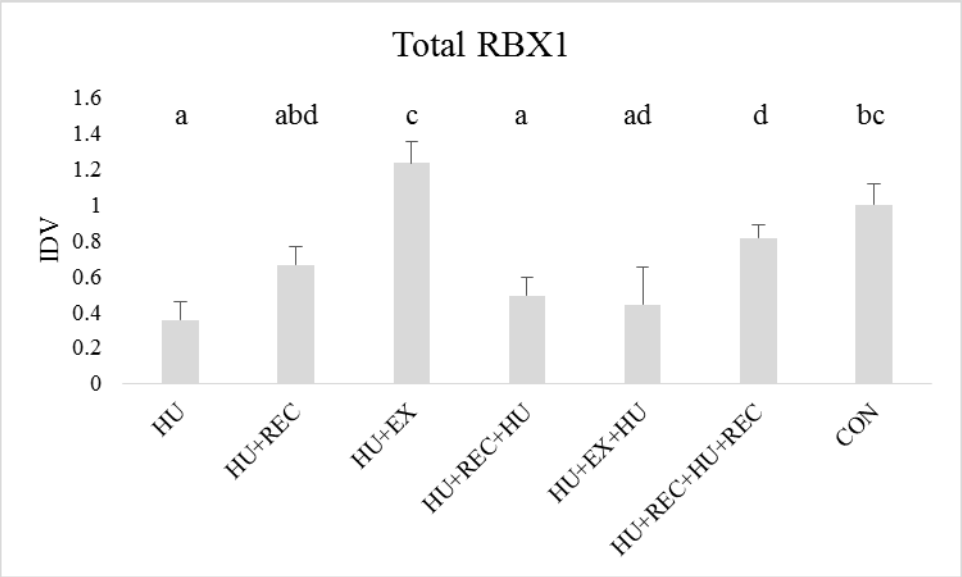

Fig. 5.4. Study IV Expression of Total RBX1. Immunoblot of the anabolic protein RBX1 in the gastrocnemius. Assessed as total content. Values are means ± SE. Bars displaying similar letters in each graph are not significantly different from one another.

Finally, DEPTOR content was compared to the corresponding mixed FSR for each group and displayed in Figure 5.5. DEPTOR content appears to correlate to mixed FSR in the gastrocnemius muscle in an inverse relationship (R = -0.9130)

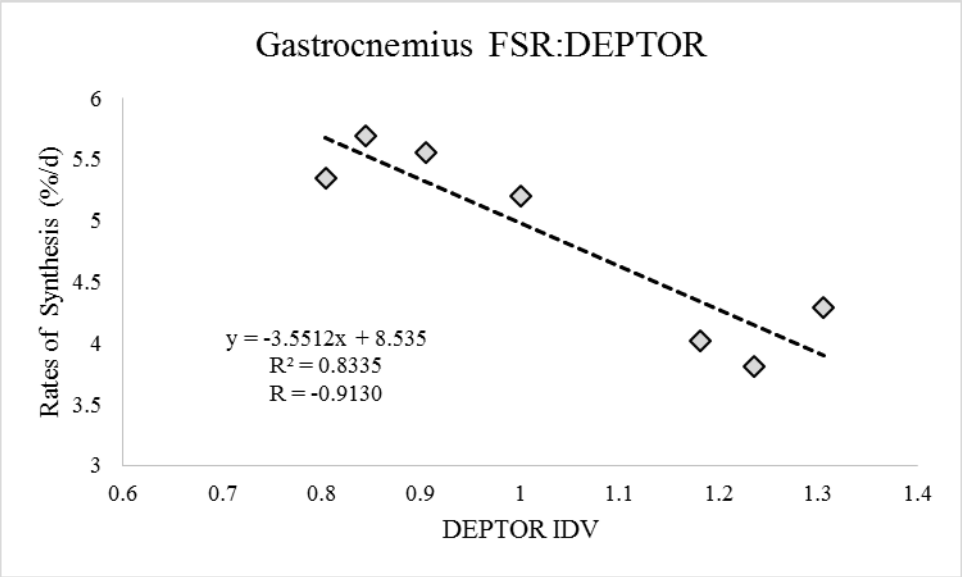

Fig. 5.5. Study IV FSR:DEPTOR Relationship. Gastrocnemius muscle comparing the mean values for the mixed FSR (y-axis) plotted against DEPTOR content (x-axis) for each group in the experimental design. No statistical comparisons made, but correlation coefficient was calculated.

Discussion

The relationship between mechanical loading conditions and muscle mass can be, in part, explained by muscle protein synthesis. This concept has been discussed extensively in the previous Sections, with particular attention being given to regulation of the PI3K/Akt/mTOR anabolic (rapamycin-sensitive) pathway. However, we have previously demonstrated that insulin and resistance exercise can alter muscle protein synthesis independent of a rapamycin-sensitive pathway (63). With the recent studies characterizing DEPTOR as a negative regulator of mTOR and some of its upstream signaling (160, 224, 237), DEPTOR was highlighted as a potential therapeutic for maintaining muscle in atrophic conditions. The first known work to assess DEPTOR

expression in skeletal muscle were by Kazi et al., in which they used DEPTOR knockdown via plasmids to eliminate mRNA and protein expression in C2C12s and saw an increase in protein synthesis over control cells (115). That study also demonstrated that DEPTOR suppression, in vivo, served as a therapy against atrophy during 3 d casting. Their use of *in vitro* DEPTOR reduction mitigated muscle wasting via maintained protein synthesis in the casting animals, but DEPTOR knockdown failed to produce a change in FSR or mass in ambulatory animals (115). Those studies proved DEPTOR is an important regulator of muscle protein metabolism and its downregulation could mitigate muscle atrophy. It was our work that published the first known physiological changes in DEPTOR, as its content was significantly lowered by resistance exercise versus control, postulating that it may be a regulator of the anabolic response to exercise in muscle (155). Nilsson et al. (155) was investigating the anabolic response to exercise in obese subjects, as it aimed to elucidate the anabolic resistance that occurs during sarcopenic obesity. Using acute resistance exercise with obese Zucker rats, we observed that muscle masses were reduced in obese animals (vs. lean littermates), but that the reductions of muscle mass could not be explained by diminished FSR. Our findings determined that obese rodents express lower DEPTOR, which may ultimately contribute to elevated protein synthesis at rest (vs. lean sedentary), but was not altered by resistance training, solidifying the notion that obese subjects have elevated basal rates of synthesis that is not further improved by exercise (anabolic resistance), and suggests that DEPTOR expression could be tied to insulin sensitivity (155).

Nilsson et al. (155) also demonstrated that, in normal rats, resistance exercise profoundly affected DEPTOR expression, indicative of an elevated anabolic response post-exercise. In the present study, we did not see an additive effect of resistance exercise on DEPTOR expression when compared to recovery alone, which is likely why we did not see an effect of exercise on muscle mass or FSR beyond what was observed in recovery without exercise. These results indicate that either our resistance exercise protocol was not sufficient to elicit reductions of DEPTOR expression or that the recovery process already maximized alterations of DEPTOR that could not be further altered by exercise, making these animals 'resistant' to further anabolic stimuli. To support that concept, we noticed DEPTOR expression appeared to closely associate with our 24 h protein synthesis data, and therefore, we examined if chronic changes in mechanical load altered DEPTOR content and the potential relationship between DEPTOR expression with FSR. The present work, to our knowledge, was the first to show that DEPTOR expression in skeletal muscle during various stages of mechanical unloading and recovery are associated with anabolic properties of muscle. More work is necessary to determine dose/response relationships for DEPTOR expression and protein synthesis.

DEPTOR was inversely tied to muscle mass, and its higher values in unloaded groups may be associated with reduced mTOR phosphorylation (activation) and subsequent formation of the ribosome, as DEPTOR's binding prevents downstream signaling by mTOR (160). While the exact signaling details for DEPTOR's removal during recovery have not been fully elucidated, DEPTOR has been recently shown to be

degraded by activation of, among others, RSK1 and S6K1 via mitogenic activation. S6K1 phosphorylates DEPTOR to allow for its degradation by SCF, an E3 ligase (237). As we present a correlation between DEPTOR content and FSR (Figure 5.4), even a small reduction of DEPTOR accumulation may result in improved mTOR activation, allowing for increased S6K1 activation, feeding forward to decrease DEPTOR expression even further. We postulate that the lack of mTOR signaling (i.e. during disuse) allows for a constituent accumulation of DEPTOR, which then inhibits translation initiation. Alternatively, it is possible that DEPTOR accumulation may (also) be a result of a diminished ability to degrade this inhibitory protein.

The E3 ligase responsible for DEPTOR ubiquitination and subsequent breakdown is the SCF complex, which is comprised of β-TrCP, CUL1, and RBX1. As *in vitro* reductions RBX1 induce accumulation of DEPTOR, ultimately leading to mTOR inactivation in cancer cells, it suggested that RBX1 content may at least partially account for DEPTOR content (233). To our knowledge, this work is the first to directly assess RBX1 content with mechanoloading in skeletal muscle. As our lowest RBX1 content was expressed in our unloaded groups, it shows promise that RBX1 overexpression could be a potential target for improving mRNA translation in muscle, and also implicates that overall DEPTOR expression, regardless of upstream signaling, may be dependent on the capacity of muscle to degrade this important protein. Further studies are necessary to characterize the nuances of RBX1 signaling in regards to DEPTOR/mTOR outcomes.

The relationship between muscle protein synthesis and DEPTOR content was plotted in Figure 5.4, to illustrate the strong negative correlation (R = -0.9130) between this measures. This apparent association highlights DEPTOR's possible role as a key regulator of protein synthesis in skeletal muscle. DEPTOR expression may be considered, at least quantitatively, a viable target for clinical efforts to assess muscle anabolism when traditional quantitative measures (GCMS, IRMS) are not available. It's potential as a surrogate marker for muscle anabolism is a novel finding we discussed in our previous work (155), but is reinforced by the work detailed in this Dissertation.

Conclusion

Our recent interest in DEPTOR signaling and its relation to muscle mass and anabolism has provided the first two *in vivo* studies to demonstrate physiological alterations of DEPTOR content in skeletal muscle (present study and (155)). Its expression is so closely tied to daily 24 h FSR measures that we feel its value in muscle physiology studies may exceed even that of publishing mTOR data, as its upstream activation and subsequent return to basal activity following resistance exercise is so brief (20), yet the impact of a single session of acute resistance exercise to elevate muscle protein synthesis lasts at least 24 h (138). Therefore, future exercise studies and clinical research looking into muscle anabolism should target DEPTOR expression to further elucidate the role this protein plays in balancing muscle mass.

VI. SUMMARY AND CONCLUSION

Muscle Plasticity in Response to Mechanical Unloading and Reloading

Greek philosopher Hippocrates is credited as the first to detail physiological adaptations to activity, saying *"That which is used- develops. That which is not used wastes away."* It was not until 1959 that the term 'plasticity' was used to describe muscle's inherent ability to substantially, swiftly, and specifically alter its form and function in response to a change in stimuli (55). An abundance of the muscle research field has been dedicated to understanding- and ideally regulating, the changes in muscle mass that occur during inactivity or in response to exercise training. And while the value in improving muscle mass and function in athletes and the general population is noted, the significance of preventing or reversing muscle atrophy in clinical conditions is immense- ramifications of severe muscle atrophy include decreased strength (77, 220), altered functional properties (30, 56, 238), and lean body mass has been inversely associated with mortality risk, even when accounting for fat mass and cardiovascular risks (200). Therapies to reverse the adaptations that result in decreased protein synthesis and/or increased protein breakdown could immediately improve quality of life and alleviate morbidities in at-risk populations of several muscle-wasting conditions (29, 54, 57, 108).

To elicit a substantial reduction in muscle mass (and as a consequence, muscle strength), we opted to utilized hindlimb unloading, a rodent model originally tested in skeletal muscle as a model of inactivity (152) that was later noted as a strong ground-based analog to spaceflight (150), as this model creates a cardiovascular fluid shift

similar to that observed during spaceflight (94) coupled with a substantial reduction of muscle activity in the lower limb (173). Space travel physiology, when considering the compounded risks of microgravity and the space radiation environment, affords us opportunities to inhabit (and therefore study the adaptations that occur in) arguably the most extreme conditions to ever exist on skeletal muscle. Therefore, countermeasures that prove effective in mitigating or preventing muscle atrophy in space are of mammoth value. It is for this reason that we adopted hindlimb unloading to serve as our model for disuse over casting or denervation. The soleus was found to face rapid losses of muscle mass immediately following the onset of hindlimb unloading, with the most rapid losses (~ -50% vs. Day 0) happening in the first 28 d, but full recovery of mass happened within 28 d of recovery (216). Work by our colleagues prior to our collaboration highlighted several bone parameters that were impacted by 28 d of hindlimb unloading were fully recovered with 2x recovery time of 1 g reloading (196), and so 56 d recovery periods were selected for the projects detailed in this Dissertation.

Muscle plasticity with single bouts of steady-state disuse and full recovery after unloading is discussed in portions of Section II, III, and IV. The soleus muscle was found to be the most affected by 28 d of unloading, compared to the gastrocnemius and plantaris, when considering alterations in mass. The nearly -55% change (vs. control) is consistent with the work of others (127, 196, 216), and is met with a concomitant reduction in muscle protein synthesis (-31% vs. CON) that is similar to the decreases observed with prolonged bed rest (58). With similar results in the gastrocnemius, we sought to discern if the changes in muscle protein synthesis rates during steady-state

atrophy were being driven by altered mRNA translation, and our signaling data provided insight that initiation and elongation may both be negatively impacted during hindlimb unloading, even after 28 d of chronic unweighting. Our catabolic markers were less clear in explaining our findings, but may coincide with concepts offered by Thomason et al., suggesting that catabolism is not dissimilar from basal values in steady-state atrophy during disuse (214). We also observed a decrease in the expression of the anti-apoptotic protein Bax, but found support for this finding with long-duration disuse (165). The anabolic signaling, protein synthesis rates, and mass were all restored in the 56 d recovery group (vs. control values), confirming that our model could sufficiently induce and restore mass, highlighting it as an effective model for plasticity and biological resilience. Collectively, this work established a baseline from which we could explore biological repeatability in muscle.

Muscle Repeatability to Alterations in Mechanical Loading Conditions

To our knowledge, there has been no work explicitly describing biological repeatability as a facet of muscle plasticity. The notion originated as a concern in bone health in astronauts, with NASA-funded projects discussing the impact of multiple spaceflight missions on the overall health of an astronaut (85, 86, 194, 195). The only muscle outcomes assessed, if any, were wet mass, but inspired us to explore repeatability as a concept for not only space-related research, but muscle biology in general. The experimental design allowed us, for the first time, to clearly demonstrate muscle mass changes through repeated bouts of disuse with full recovery, and to explore factors that

influence muscle protein turnover in this model. Overall, muscle mass was impacted similarly in the second disuse period as it was in the first, and was supported by similar muscle protein synthesis as well as similar anabolic, catabolic, and apoptotic signaling. All of these outcomes were once again reversed during passive recovery, strongly supporting that muscle plasticity is appropriately and similarly impacted each time when exposed to repeating stimuli. This poses relevant information to NASA, as it suggests that while muscle mass will be lost during long-duration space travel (without countermeasures), and muscle mass will be similarly lost during subsequent missions in veteran astronauts, there are two beneficial messages: 1) muscle is not further exacerbated by serial unloadings, so veterans are not at risk for higher levels of atrophy compared to first-time astronauts, and 2) the muscle is fully recovered with adequate time back in a 1 g environment. This information is similarly beneficial to numerous clinical populations that may go through repeated periods of lengthy bed rest (which occurs in numerous conditions of chronic illness). Only one of the measured outcomes was affected in a dissimilar fashion during repeated unloading and recovery; muscle collagen concentrations, which have been shown to compromise muscle function (83). The identification of this difference may be of immediate value to NASA and clinical situations, and poses the notion that not all muscle outcomes are fully repeatable. Future research in the field, when appropriate, should add cyclical stimuli to elucidate other aspects of muscle biology that are not repeatable.

Resistance Exercise During Recovery

We employed a resistance exercise paradigm proven to produce training-induced benefits in bone, as well as mitigate future insults during subsequent unloading periods (197). As discussed in Section IV, this moderate-intensity, moderate-volume voluntary resistance training during recovery from unloading was not beneficial, and appeared to contribute to lower gastrocnemius muscle mass (vs. passive ambulation alone). We highlighted possible explanations for these findings, and do not discourage future studies from invoking exercise to expedite or increase recovery, but rather suggest potential avenues for future works to consider. Clinicians already prescribe passive and active rehabilitation during hospital stays to expedite discharge, improve functionality, and improve mortality (28, 120) in ICU patients. The value in unanimous position papers detailing the mechanisms behind recovery and concise strategies for rehabilitation from long-duration disuse in otherwise healthy individuals is of immediate value to athletes, warfighters, first responders, and many portions of the general public who wish to return to normal activity after injury/illness/debilitation that results in muscle atrophy.

DEPTOR

Section V provides insight into a molecular mechanism for anabolic regulation of mTOR. In previous work we determined that DEPTOR, a negative regulator of mTOR, could be a valuable target in controlling the anabolic response to exercise in skeletal muscle (155). This Dissertation provides the first known evidence of DEPTOR's increase during steady-state disuse, and its correlation to mixed muscle protein synthesis

rates. As pharmacological manipulation of DEPTOR proved to mitigate early losses in muscle mass due to casting (115), its value as a possible countermeasure to long-duration disuse cannot be understated. Kazi et al. demonstrated that knockdown of DEPTOR mRNA did not improve muscle with hypertrophic gains above control, but was immensely beneficial in preventing loss in a catabolic condition. The manipulation of this protein is not without risks, as a non-specific inhibition of DEPTOR in many cancer cells would be catastrophic. Further examination of DEPTOR's control on anabolism, and other signaling cascades, is imperative if we wish to translate benchtop research to clinical value to conditions suffering the consequences of atrophied muscle, but muscle-specific therapies will be required to prevent further- possibly life-threatening, insults.

Final Thought

The impetus for this Dissertation was born out of need to examine, and seek to remedy for, the impact of spaceflight on bone health. The experimental design established for the initial aims of the project afforded an opportunity for muscle to also be assessed, with NASA also highlighting the need to better understand muscle's responses to spaceflight in an effort to avoid operational (even life-threatening) risks of muscle atrophy and reduced muscle function during long-duration missions (162). But the wider-reaching benefits of this work extends to the general field of muscle biology. The concept of biological repeatability deepens our understanding of plasticity, and provides insight to the adaptability of muscle to undulating stimuli involving catabolic

conditions. While most of the data provided supports repeatability, even one disagreement (muscle collagen) exposes a chink in one's armor if making blanket assumptions that muscle will always react similarly to repeat changes in stimuli. Exploring these inconsistencies may highlight serious risks in astronaut muscle function as well as countless other health risks that may arise when muscle plasticity is not consistent.

REFERENCES

1. Adams GR, Caiozzo VJ, and Baldwin KM. Skeletal muscle unweighting: spaceflight and ground-based models. *Journal of Applied Physiology* 95: 2185-2201, 2003.
2. Aldridge GM, Podrebarac DM, Greenough WT, and Weiler IJ. The use of total protein stains as loading controls: an alternative to high-abundance single-protein controls in semi-quantitative immunoblotting. *Journal of Neuroscience Methods* 172: 250-254, 2008.
3. Alford EK, Roy RR, Hodgson JA, and Edgerton VR. Electromyography of rat soleus, medical gastrocnemius, and tibialis anterior during hind limb suspension. *Experimental Neurology* 96: 635-649, 1987.
4. Allen DL, Bandstra ER, Harrison BC, Thorng S, Stodieck LS, Kostenuik PJ, Morony S, Lacey DL, Hammond TG, and Leinwand LL. Effects of spaceflight on murine skeletal muscle gene expression. *Journal of Applied Physiology* 106: 582-595, 2009.
5. Allen MR and Bloomfield SA. Hindlimb unloading has a greater effect on cortical compared with cancellous bone in mature female rats. *Journal of Applied Physiology* 94: 642-650, 2003.
6. Allen MR, Hogan HA, and Bloomfield SA. Differential bone and muscle recovery following hindlimb unloading in skeletally mature male rats. *Journal of Musculoskeletal and Neuronal Interaction* 6: 217-225, 2006.

7. Andrianjafiniony T, Dupré-Aucouturier S, Letexier D, Couchoux H, and Desplanches D. Oxidative stress, apoptosis, and proteolysis in skeletal muscle repair after unloading. *American Journal of Physiology-Cell Physiology* 299: C307-C315, 2010.

8. Antonutto G, Capelli C, Girardis M, Zamparo P, and Di Prampero P. Effects of microgravity on maximal power of lower limbs during very short efforts in humans. *Journal of Applied Physiology* 86: 85-92, 1999.

9. Arbogast S, Smith J, Matuszczak Y, Hardin BJ, Moylan JS, Smith JD, Ware J, Kennedy AR, and Reid MB. Bowman-Birk inhibitor concentrate prevents atrophy, weakness, and oxidative stress in soleus muscle of hindlimb-unloaded mice. *Journal of Applied Physiology* 102: 956-964, 2007.

10. Armstrong RB and Phelps RO. Muscle fiber type composition of the rat hindlimb. *American Journal of Anatomy* 171: 259-272, 1984.

11. Baar K and Esser K. Phosphorylation of p70S6kcorrelates with increased skeletal muscle mass following resistance exercise. *American Journal of Physiology-Cell Physiology* 276: C120-C127, 1999.

12. Bajotto G, Sato Y, Kitaura Y, and Shimomura Y. Effect of branched-chain amino acid supplementation during unloading on regulatory components of protein synthesis in atrophied soleus muscles. *European Journal of Applied Physiology* 111: 1815-1828, 2011.

13. Bamman MM, Clarke MS, Feeback DL, Talmadge RJ, Stevens BR, Lieberman SA, and Greenisen MC. Impact of resistance exercise during bed rest on skeletal

muscle sarcopenia and myosin isoform distribution. *Journal of Applied Physiology* 84: 157-163, 1998.

14. Berg H, Dudley G, Haggmark T, Ohlsen H, and Tesch P. Effects of lower limb unloading on skeletal muscle mass and function in humans. *Journal of Applied Physiology* 70: 1882-1885, 1991.

15. Bloomfield S, Allen M, Hogan H, and Delp M. Site-and compartment-specific changes in bone with hindlimb unloading in mature adult rats. *Bone* 31: 149-157, 2002.

16. Bodine SC and Baehr LM. Skeletal muscle atrophy and the E3 ubiquitin ligases MuRF1 and MAFbx/atrogin-1. *American Journal of Physiology-Endocrinology and Metabolism* 307: E469-E484, 2014.

17. Bodine SC, Stitt TN, Gonzalez M, Kline WO, Stover GL, Bauerlein R, Zlotchenko E, Scrimgeour A, Lawrence JC, Glass DJ, and Yancopoulos GD. Akt/mTOR pathway is a crucial regulator of skeletal muscle hypertrophy and can prevent muscle atrophy in vivo. *Nature Cell Biology* 3: 1014-1019, 2001.

18. Bohé J, Low A, Wolfe RR, and Rennie MJ. Human muscle protein synthesis is modulated by extracellular, not intramuscular amino acid availability: a dose-response study. *The Journal of Physiology* 552: 315-324, 2003.

19. Bolster DR, Crozier SJ, Kimball SR, and Jefferson LS. AMP-activated protein kinase suppresses protein synthesis in rat skeletal muscle through down-regulated mammalian target of rapamycin (mTOR) signaling. *Journal of Biological Chemistry* 277: 23977-23980, 2002.

20. Bolster DR, Kubica N, Crozier SJ, Williamson DL, Farrell PA, Kimball SR, and Jefferson LS. Immediate response of mammalian target of rapamycin (mTOR)-mediated signalling following acute resistance exercise in rat skeletal muscle. *The Journal of Physiology* 553: 213-220, 2003.

21. Booth F and Kelso J. Effect of hind-limb immobilization on contractile and histochemical properties of skeletal muscle. *Pflügers Archiv* 342: 231-238, 1973.

22. Booth F and Seider M. Early change in skeletal muscle protein synthesis after limb immobilization of rats. *Journal of Applied Physiology* 47: 974-977, 1979.

23. Booth FW and Seider MJ. Recovery of skeletal muscle after 3 mo of hindlimb immobilization in rats. *Journal of Applied Physiology* 47: 435-439, 1979.

24. Brugarolas J, Lei K, Hurley RL, Manning BD, Reiling JH, Hafen E, Witters LA, Ellisen LW, and Kaelin WG. Regulation of mTOR function in response to hypoxia by REDD1 and the TSC1/TSC2 tumor suppressor complex. *Genes & Development* 18: 2893-2904, 2004.

25. Brunet A, Bonni A, Zigmond MJ, Lin MZ, Juo P, Hu LS, Anderson MJ, Arden KC, Blenis J, and Greenberg ME. Akt promotes cell survival by phosphorylating and inhibiting a Forkhead transcription factor. *Cell* 96: 857-868, 1999.

26. Bruusgaard JC, Egner IM, Larsen TK, Dupre-Aucouturier S, Desplanches D, and Gundersen K. No change in myonuclear number during muscle unloading and reloading. *Journal of Applied Physiology* 113: 290-296, 2012.

27. Buentello JA, Pohlenz C, Margulies D, Scholey VP, Wexler JB, Tovar-Ramírez D, Neill WH, Hinojosa-Baltazar P, and Gatlin IIIDM. A preliminary study of

digestive enzyme activities and amino acid composition of early juvenile yellowfin tuna (Thunnus albacares). *Aquaculture* 312: 205-211, 2011.

28. Burtin C, Clerckx B, Robbeets C, Ferdinande P, Langer D, Troosters T, Hermans G, Decramer M, and Gosselink R. Early exercise in critically ill patients enhances short-term functional recovery. *Critical Care Medicine* 37: 2499-2505, 2009.

29. Cahill GF. Starvation in Man. *New England Journal of Medicine* 282: 668-675, 1970.

30. Caiozzo VJ, Baker MJ, Herrick RE, Tao M, and Baldwin KM. Effect of spaceflight on skeletal muscle: mechanical properties and myosin isoform content of a slow muscle. *Journal of Applied Physiology* 76: 1764-1773, 1994.

31. Carlson CJ, Booth FW, and Gordon SE. Skeletal muscle myostatin mRNA expression is fiber-type specific and increases during hindlimb unloading. *American Journal of Physiology-Regulatory, Integrative and Comparative Physiology* 277: R601-R606, 1999.

32. Caron AZ, Drouin G, Desrosiers J, Trensz F, and Grenier G. A novel hindlimb immobilization procedure for studying skeletal muscle atrophy and recovery in mouse. *Journal of Applied Physiology* 106: 2049-2059, 2009.

33. Carroll CC, Whitt JA, Peterson A, Gump BS, Tedeschi J, and Broderick TL. Influence of acetaminophen consumption and exercise on Achilles tendon structural properties in male Wistar rats. *American Journal of Physiology-Regulatory, Integrative and Comparative Physiology* 302: R990-R995, 2012.

34. Chaillou T, Kirby TJ, and McCarthy JJ. Ribosome biogenesis: emerging evidence for a central role in the regulation of skeletal muscle mass. *Journal of Cellular Physiology* 229: 1584-1594, 2014.

35. Chaillou T, Koulmann N, Simler N, Meunier A, Serrurier B, Chapot R, Peinnequin A, Beaudry M, and Bigard X. Hypoxia transiently affects skeletal muscle hypertrophy in a functional overload model. *American Journal of Physiology-Regulatory, Integrative and Comparative Physiology* 302: R643-R654, 2012.

36. Childs TE, Spangenburg EE, Vyas DR, and Booth FW. Temporal alterations in protein signaling cascades during recovery from muscle atrophy. *American Journal of Physiology-Cell Physiology* 285: C391-C398, 2003.

37. Corradetti MN, Inoki K, and Guan K-L. The stress-inducted proteins RTP801 and RTP801L are negative regulators of the mammalian target of rapamycin pathway. *Journal of Biological Chemistry* 280: 9769-9772, 2005.

38. Cureton KJ, Collins MA, Hill DW, and McElhannon Jr FM. Muscle hypertrophy in men and women. *Medicine & Science in Sports & Exercise* 20: 338-344, 1988.

39. De Boer MD, Selby A, Atherton P, Smith K, Seynnes OR, Maganaris CN, Maffulli N, Movin T, Narici MV, and Rennie MJ. The temporal responses of protein synthesis, gene expression and cell signalling in human quadriceps muscle and patellar tendon to disuse. *The Journal of Physiology* 585: 241-251, 2007.

40. de Boer MD, Seynnes OR, Di Prampero PE, Pišot R, Mekjavić IB, Biolo G, and Narici MV. Effect of 5 weeks horizontal bed rest on human muscle thickness and architecture of weight bearing and non-weight bearing muscles. *European Journal of Applied Physiology* 104: 401-407, 2008.

41. DeLorme TL. Restoration of muscle power by heavy-resistance exercises. *Journal of Bone & Joint Surgery* 27: 645-667, 1945.

42. DeRuisseau KC, Kavazis AN, Deering MA, Falk DJ, Van Gammeren D, Yimlamai T, Ordway GA, and Powers SK. Mechanical ventilation induces alterations of the ubiquitin-proteasome pathway in the diaphragm. *Journal of Applied Physiology* 98: 1314-1321, 2005.

43. Desaphy J-F, Pierno S, Liantonio A, De Luca A, Didonna MP, Frigeri A, Nicchia GP, Svelto M, Camerino C, Zallone A, and Camerino DC. Recovery of the soleus muscle after short- and long-term disuse induced by hindlimb unloading: effects on the electrical properties and myosin heavy chain profile. *Neurobiology of Disease* 18: 356-365, 2005.

44. Deschenes MR, Britt AA, and Chandler WC. A comparison of the effects of unloading in young adult and aged skeletal muscle. *Medicine & Science in Sports & Exercise* 33: 1477-1483, 2001.

45. Desplanches D, Kayar SR, Sempore B, Flandrois R, and Hoppeler H. Rat soleus muscle ultrastructure after hindlimb suspension. *Journal of Applied Physiology* 69: 504-508, 1990.

46. Dreyer HC, Drummond MJ, Pennings B, Fujita S, Glynn EL, Chinkes DL, Dhanani S, Volpi E, and Rasmussen BB. Leucine-enriched essential amino acid and carbohydrate ingestion following resistance exercise enhances mTOR signaling and protein synthesis in human muscle. *American Journal of Physiology-Endocrinology And Metabolism* 294: E392-E400, 2008.

47. Dreyer HC, Glynn EL, Lujan HL, Fry CS, DiCarlo SE, and Rasmussen BB. Chronic paraplegia-induced muscle atrophy downregulates the mTOR/S6K1 signaling pathway. *Journal of Applied Physiology* 104: 27-33, 2008.

48. Drummond MJ, Dreyer HC, Fry CS, Glynn EL, and Rasmussen BB. Nutritional and contractile regulation of human skeletal muscle protein synthesis and mTORC1 signaling. *Journal of Applied Physiology* 106: 1374-1384, 2009.

49. Dufner DA, Bederman IR, Brunengraber DZ, Rachdaoui N, Ismail-Beigi F, Siegfried BA, Kimball SR, and Previs SF. Using 2H2O to study the influence of feeding on protein synthesis: effect of isotope equilibration in vivo vs. in cell culture. *American Journal of Physiology-Endocrinology and Metabolism* 288: E1277-E1283, 2005.

50. Dupont-Versteegden EE, Fluckey JD, Knox M, Gaddy D, and Peterson CA. Effect of flywheel-based resistance exercise on processes contributing to muscle atrophy during unloading in adult rats. *Journal of Applied Physiology* 101: 202-212, 2006.

51. Dupont-Versteegden EE, Houlé JD, Gurley CM, and Peterson CA. Early changes in muscle fiber size and gene expression in response to spinal cord transection

and exercise. *American Journal of Physiology - Cell Physiology* 275: C1124-C1133, 1998.

52. Dupont-Versteegden EE, Murphy RJL, Houlé JD, Gurley CM, and Peterson CA. Mechanisms leading to restoration of muscle size with exercise and transplantation after spinal cord injury. *American Journal of Physiology - Cell Physiology* 279: C1677-C1684, 2000.

53. Dupont E, Cieniewski-Bernard C, Bastide B, and Stevens L. Electrostimulation during hindlimb unloading modulates PI3K-AKT downstream targets without preventing soleus atrophy and restores slow phenotype through ERK. *American Journal of Physiology-Regulatory, Integrative and Comparative Physiology* 300: R408-R417, 2011.

54. Eccles J. Investigations on muscle atrophies arising from disuse and tenotomy. *The Journal of Physiology* 103: 253-266, 1944.

55. Eccles J. Plasticity at the simplest levels of the nervous system. *The Centennial Lectures, ed Culbertson JT(Putnam, New York)*: 217-244, 1959.

56. Edgerton VR, Zhou MY, Ohira Y, Klitgaard H, Jiang B, Bell G, Harris B, Saltin B, Gollnick PD, Roy RR, and et a. Human fiber size and enzymatic properties after 5 and 11 days of spaceflight. *Journal of Applied Physiology* 78: 1733-1739, 1995.

57. Fearon KCH and Preston T. Body Composition in Cancer Cachexia. *Transfusion Medicine and Hemotherapy* 17(suppl 3): 63-66, 1990.

58. Ferrando AA, Lane HW, Stuart CA, Davis-Street J, and Wolfe RR. Prolonged bed rest decreases skeletal muscle and whole body protein synthesis. *American Journal of Physiology-Endocrinology And Metabolism* 270: E627-E633, 1996.

59. Ferrando AA, Tipton KD, Bamman MM, and Wolfe RR. Resistance exercise maintains skeletal muscle protein synthesis during bed rest. *Journal of Applied Physiology* 82: 807-810, 1997.

60. Fitts RH, Riley DR, and Widrick J. Physiology of a microgravity environment invited review: microgravity and skeletal muscle. *Journal of Applied Physiology* 89: 823-839, 2000.

61. Fitts RH, Riley DR, and Widrick JJ. Functional and structural adaptations of skeletal muscle to microgravity. *Journal of Experimental Biology* 204: 3201-3208, 2001.

62. Flück M and Hoppeler H. Molecular basis of skeletal muscle plasticity-from gene to form and function. In: *Reviews of Physiology, Biochemistry and Pharmacology*: Springer, 2003, p. 159-216.

63. Fluckey JD, Dupont-Versteegden EE, Knox M, Gaddy D, Tesch PA, and Peterson CA. Insulin facilitation of muscle protein synthesis following resistance exercise in hindlimb-suspended rats is independent of a rapamycin-sensitive pathway. *American Journal of Physiology-Endocrinology and Metabolism* 287: E1070-E1075, 2004.

64. Fluckey JD, Dupont-Versteegden EE, Montague DC, Knox M, Tesch P, Peterson CA, and Gaddy-Kurten D. A rat resistance exercise regimen attenuates losses of

musculoskeletal mass during hindlimb suspension. *Acta Physiologica Scandinavica* 176: 293-300, 2002.

65. Fluckey JD, Knox M, Smith L, Dupont-Versteegden EE, Gaddy D, Tesch PA, and Peterson CA. Insulin-facilitated increase of muscle protein synthesis after resistance exercise involves a MAP kinase pathway. *American Journal of Physiology-Endocrinology and Metabolism* 290: E1205-1211, 2006.

66. Fluckey JD, Kraemer WJ, and Farrell PA. Pancreatic islet insulin secretion is increased after resistance exercise in rats. *Journal of Applied Physiology* 79: 1100-1105, 1995.

67. Fluckey JD, Vary TC, Jefferson LS, and Farrell PA. Augmented insulin action on rates of protein synthesis after resistance exercise in rats. *American Journal of Physiology - Endocrinology And Metabolism* 270: E313-E319, 1996.

68. Frimel TN, Kapadia F, Gaidosh GS, Li Y, Walter GA, and Vandenborne K. A model of muscle atrophy using cast immobilization in mice. *Muscle & Nerve* 32: 672-674, 2005.

69. Fujino H, Ishihara A, Murakami S, Yasuhara T, Kondo H, Mohri S, Takeda I, and Roy R. Protective effects of exercise preconditioning on hindlimb unloading-induced atrophy of rat soleus muscle. *Acta physiologica* 197: 65-74, 2009.

70. Fujino H, Kohzuki H, Takeda I, Kiyooka T, Miyasaka T, Mohri S, Shimizu J, and Kajiya F. Regression of capillary network in atrophied soleus muscle induced by hindlimb unweighting. *Journal of Applied Physiology* 98: 1407-1413, 2005.

71. Fukuglta M, Hogan C, Peebles P, Kolb E, Turner M, Madore F, Freedman W, Jacoby G, Sandage A, and Tammann G. Insulindependent stimulation of protein synthesis by phosphorylation of a regulator of 5'-cap function. *Nature* 371: 762-767, 1994.

72. Gabriel DA, Kamen G, and Frost G. Neural adaptations to resistive exercise. *Sports Medicine* 36: 133-149, 2006.

73. Garlick P, Millward D, and James W. The diurnal response of muscle and liver protein synthesis in vivo in meal-fed rats. *Biochemical Journal* 136: 935-945, 1973.

74. Gasier H, Riechman S, Wiggs M, Buentello A, Previs S, and Fluckey J. Cumulative responses of muscle protein synthesis are augmented with chronic resistance exercise training. *Acta physiologica* 201: 381-389, 2011.

75. Gasier HG, Fluckey JD, Previs SF, Wiggs MP, and Riechman SE. Acute resistance exercise augments integrative myofibrillar protein synthesis. *Metabolism* 61: 153-156, 2012.

76. Gasier HG, Riechman SE, Wiggs MP, Previs SF, and Fluckey JD. A comparison of 2H2O and phenylalanine flooding dose to investigate muscle protein synthesis with acute exercise in rats. *American Journal of Physiology-Endocrinology and Metabolism* 297: E252-259, 2009.

77. Germain P, Güell A, and Marini JF. Muscle strength during bedrest with and without muscle exercise as a countermeasure. *European Journal of Applied Physiology* 71: 342-348, 1995.

78. Gibson J, Halliday D, Morrison W, Stoward P, Hornsby G, Watt P, Murdoch G, and Rennie M. Decrease in human quadriceps muscle protein turnover consequent upon leg immobilization. *Clinical Science* 72: 503-509, 1987.

79. Glover EI, Oates BR, Tang JE, Moore DR, Tarnopolsky MA, and Phillips SM. Resistance exercise decreases eIF2Bε phosphorylation and potentiates the feeding-induced stimulation of p70S6K1 and rpS6 in young men. *American Journal of Physiology-Regulatory, Integrative and Comparative Physiology* 295: R604-R610, 2008.

80. Glover EI, Phillips SM, Oates BR, Tang JE, Tarnopolsky MA, Selby A, Smith K, and Rennie MJ. Immobilization induces anabolic resistance in human myofibrillar protein synthesis with low and high dose amino acid infusion. *The Journal of Physiology* 586: 6049-6061, 2008.

81. Gollnick PD, Saltin B, Saubert CW, Armstron.Rb, and Piehl K. Enzyme-Activity and Fiber Composition in Skeletal-Muscle of Untrained and Trained Men. *Journal of Applied Physiology* 33: 312-&, 1972.

82. Gopalakrishnan R, Genc KO, Rice AJ, Lee S, Evans HJ, Maender CC, Ilaslan H, and Cavanagh PR. Muscle volume, strength, endurance, and exercise loads during 6-month missions in space. *Aviation, Space, and Environmental Medicine* 81: 91-104, 2010.

83. Gosselin LE, Adams C, Cotter TA, McCormick RJ, and Thomas DP. *Effect of exercise training on passive stiffness in locomotor skeletal muscle: role of extracellular matrix*. Journal of Applied Physiology 85(3), 1998.

84. Griffiths RD. Muscle mass, survival, and the elderly ICU patient. *Nutrition* 12: 456-458, 1996.

85. Gupta S, Manske SL, and Judex S. Increasing the number of unloading/reambulation cycles does not adversely impact body composition and lumbar bone mineral density but reduces tissue sensitivity. *Acta Astronautica* 92: 89-96, 2013.

86. Gupta S, Vijayaraghavan S, Uzer G, and Judex S. Multiple exposures to unloading decrease bone's responsivity but compound skeletal losses in C57BL/6 mice. *American Journal of Physiology-Regulatory, Integrative and Comparative Physiology* 303: R159-R167, 2012.

87. Gwag T, Lee K, Ju H, Shin H, Lee J-W, and Choi I. Stress and signaling responses of rat skeletal muscle to brief endurance exercise during hindlimb unloading: a catch-up process for atrophied muscle. *Cellular Physiology and Biochemistry* 24: 537-546, 2009.

88. Häggmark T, Eriksson E, and Jansson E. Muscle fiber type changes in human skeletal muscle after injuries and immobilization. *Orthopedics* 9: 181-185, 1986.

89. Håggmark T, Jansson E, and Svane B. Cross-sectional area of the thigh muscle in man measured by computed tomography. *Scandinavian Journal of Clinical and Laboratory Investigation* 38: 355-360, 1978.

90. Häkkinen K, Alen M, Kallinen M, Newton R, and Kraemer W. Neuromuscular adaptation during prolonged strength training, detraining and re-strength-training

in middle-aged and elderly people. *European Journal of Applied Physiology* 83: 51-62, 2000.

91. Häkkinen K, Alen M, and Komi P. Changes in isometric force-and relaxation-time, electromyographic and muscle fibre characteristics of human skeletal muscle during strength training and detraining. *Acta Physiologica Scandinavica* 125: 573-585, 1985.

92. Häkkinen K, Komi P, and Tesch P. Effect of combined concentric and eccentric strength training and detraining on force-time, muscle fiber and metabolic characteristics of leg extensor muscles. *Scandinavian Journal of Medicine and Science in Sports* 3: 50-58, 1981.

93. Hanson AM, Stodieck LS, Cannon CM, Simske SJ, and Ferguson VL. Seven days of muscle re-loading and voluntary wheel running following hindlimb suspension in mice restores running performance, muscle morphology and metrics of fatigue but not muscle strength. *Journal of Muscle Research and Cell Motility* 31: 141-153, 2010.

94. Hargens A, Steskal J, Johansson C, and Tipton C. Tissue fluid shift, forelimb loading, and tail tension in tail-suspended rats. NASA. 1984.

95. Hauer K, Specht N, Schuler M, Bärtsch P, and Oster P. Intensive physical training in geriatric patients after severe falls and hip surgery. *Age and Ageing* 31: 49-57, 2002.

96. Haus JM, Carrithers JA, Carroll CC, Tesch PA, and Trappe TA. Contractile and connective tissue protein content of human skeletal muscle: effects of 35 and 90

days of simulated microgravity and exercise countermeasures. *American Journal of Physiology-Regulatory, Integrative and Comparative Physiology* 293: R1722-R1727, 2007.

97. Hayashi AA and Proud CG. The rapid activation of protein synthesis by growth hormone requires signaling through mTOR. *American Journal of Physiology-Endocrinology and Metabolism* 292: E1647-E1655, 2007.

98. Holloszy JO and Coyle EF. Adaptations of skeletal muscle to endurance exercise and their metabolic consequences. *Journal of Applied Physiology* 56: 831-838, 1984.

99. Hornberger TA, Hunter RB, Kandarian SC, and Esser KA. Regulation of translation factors during hindlimb unloading and denervation of skeletal muscle in rats. *American Journal of Physiology-Cell Physiology* 281: C179-C187, 2001.

100. Hortobagyi T, Dempsey L, Fraser D, Zheng D, Hamilton G, Lambert J, and Dohm L. Changes in muscle strength, muscle fibre size and myofibrillar gene expression after immobilization and retraining in humans. *The Journal of Physiology* 524: 293-304, 2000.

101. Houston M, Froese E, St P V, Green H, and Ranney D. Muscle performance, morphology and metabolic capacity during strength training and detraining: a one leg model. *European Journal of Applied Physiology* 51: 25-35, 1983.

102. Houston ME, Bentzen H, and Larsen H. Interrelationships between skeletal muscle adaptations and performance as studied by detraining and retraining. *Acta Physiologica Scandinavica* 105: 163-170, 1979.

103. Hudson MB, Smuder AJ, Nelson WB, Wiggs MP, Shimkus KL, Fluckey JD, Szeto HH, and Powers SK. Partial Support Ventilation and Mitochondrial-Targeted Antioxidants Protect against Ventilator-Induced Decreases in Diaphragm Muscle Protein Synthesis. *PLoS One* 10: e0137693, 2015.

104. Hurst JE and Fitts RH. Hindlimb unloading-induced muscle atrophy and loss of function: protective effect of isometric exercise. *Journal of Applied Physiology* 95: 1405-1417, 2003.

105. Hvid L, Aagaard P, Justesen L, Bayer ML, Andersen JL, Ørtenblad N, Kjaer M, and Suetta C. Effects of aging on muscle mechanical function and muscle fiber morphology during short-term immobilization and subsequent retraining. *Journal of Applied Physiology* 109(6) 1628-34, 2010.

106. Ishihara A, Kawano F, Ishioka N, Oishi H, Higashibata A, Shimazu T, and Ohira Y. Effects of running exercise during recovery from hindlimb unloading on soleus muscle fibers and their spinal motoneurons in rats. *Neuroscience Research* 48: 119-127, 2004.

107. Jackman RW and Kandarian SC. The molecular basis of skeletal muscle atrophy. *American Journal of Physiology: Cell Physiology* 287: C834-843, 2004.

108. Janssen I, Heymsfield SB, and Ross R. Low Relative Skeletal Muscle Mass (Sarcopenia) in Older Persons Is Associated with Functional Impairment and Physical Disability. *Journal of the American Geriatrics Society* 50: 889-896, 2002.

109. Jaspers SR, Fagan JM, and Tischler ME. Biochemical response to chronic shortening in unloaded soleus muscles. *Journal of Applied Physiology* 59: 1159-1163, 1985.

110. Jaspers SR and Tischler ME. Atrophy and growth failure of rat hindlimb muscles in tail-cast suspension. *Journal of Applied Physiology* 57: 1472-1479, 1984.

111. Jiang B, Ohira Y, Roy RR, Nguyen Q, Ilyina-Kakueva EI, Oganov V, and Edgerton VR. Adaptation of fibers in fast-twitch muscles of rats to spaceflight and hindlimb suspension. *Journal of Applied Physiology* 73: S58-S65, 1992.

112. Kalu DN. The ovariectomized rat model of postmenopausal bone loss. *Bone and Mineral* 15: 175-191, 1991.

113. Kandarian S, O'Brien S, Thomas K, Schulte L, and Navarro J. Regulation of skeletal muscle dihydropyridine receptor gene expression by biomechanical unloading. *Journal of Applied Physiology* 72: 2510-2514, 1992.

114. Kasper C, White T, and Maxwell L. Running during recovery from hindlimb suspension induces transient muscle injury. *Journal of Applied Physiology* 68: 533-539, 1990.

115. Kazi A, Hong-Brown L, Lang SM, and Lang CH. Deptor Knockdown Enhances mTOR Activity and Protein Synthesis in Myocytes and Ameliorates Disuse Muscle Atrophy. *Moecularl Medicine* 17: 925-936, 2011.

116. Kimball SR, Farrell PA, and Jefferson LS. Invited Review: Role of insulin in translational control of protein synthesis in skeletal muscle by amino acids or exercise. *Journal of Applied Physiology* 93: 1168-1180, 2002.

117. Kimball SR and Jefferson LS. Signaling pathways and molecular mechanisms through which branched-chain amino acids mediate translational control of protein synthesis. *The Journal of Nutrition* 136: 227S-231S, 2006.

118. Knox M, Fluckey JD, Bennett P, Peterson CA, and Dupont-Versteegden EE. Hindlimb Unloading in Adult Rats Using an Alternative Tail Harness Design. *Aviation, Space, and Environmental Medicine* 75: 692-696, 2004.

119. Krawiec BJ, Frost RA, Vary TC, Jefferson LS, and Lang CH. Hindlimb casting decreases muscle mass in part by proteasome-dependent proteolysis but independent of protein synthesis. *American Journal of Physiology-Endocrinology and Metabolism* 289: E969-E980, 2005.

120. Kress JP. Clinical trials of early mobilization of critically ill patients. *Critical Care Medicine* 37: S442-S447, 2009.

121. Krippendorf BB and Riley DA. Distinguishing unloading. Versus reloading-induced changes in rat soleus muscle. *Muscle & Nerve* 16: 99-108, 1993.

122. Krippendorf BB and Riley DA. Temporal changes in sarcomere lesions of rat adductor longus muscles during hindlimb reloading. *The Anatomical Record* 238: 304-310, 1994.

123. Laemmli UK. Cleavage of structural proteins during the assembly of the head of bacteriophage T4. *Nature* 227: 680-685, 1970.

124. Lambert BS, Shimkus KL, Fluckey JD, Riechman SE, Greene NP, Cardin JM, and Crouse SF. Anabolic Responses To Acute And Chronic Resistance Exercise Are Enhanced When Combined With Aquatic Treadmill Exercise. *American*

Journal of Physiology-Endocrinology and Metabolism: ajpendo. 00689.02013, 2014.

125. Lambertz D, Pérot C, Kaspranski R, and Goubel F. Effects of long-term spaceflight on mechanical properties of muscles in humans. *Journal of Applied Physiology* 90(1):179-88, 2001.

126. Lawler JM, Kunst M, Hord JM, Lee Y, Joshi K, Botchlett RE, Ramirez A, and Martinez DA. EUK-134 ameliorates nNOSμ translocation and skeletal muscle fiber atrophy during short-term mechanical unloading. *American Journal of Physiology-Regulatory, Integrative and Comparative Physiology* 306: R470-R482, 2014.

127. Lawler JM, Song W, and Demaree SR. Hindlimb unloading increases oxidative stress and disrupts antioxidant capacity in skeletal muscle. *Free Radical Biology and Medicine* 35: 9-16, 2003.

128. LeBlanc A, Lin C, Shackelford L, Sinitsyn V, Evans H, Belichenko O, Schenkman B, Kozlovskaya I, Oganov V, and Bakulin A. Muscle volume, MRI relaxation times (T2), and body composition after spaceflight. *Journal of Applied Physiology* 89: 2158-2164, 2000.

129. LeBlanc A, Rowe R, Schneider V, Evans H, and Hedrick T. Regional muscle loss after short duration spaceflight. *Aviation, Space, and Environmental Medicine* 66: 1151-1154, 1995.

130. Lee DE, Brown JL, Rosa ME, Brown LA, Perry RA, Wiggs MP, Nilsson MI, Crouse SF, Fluckey JD, and Washington TA. microRNA-16 Is Downregulated

During Insulin Resistance and Controls Skeletal Muscle Protein Accretion. *Journal of Cellular Biochemistry*, 2016.

131. Lee SW, Dai G, Hu Z, Wang X, Du J, and Mitch WE. Regulation of muscle protein degradation: coordinated control of apoptotic and ubiquitin-proteasome systems by phosphatidylinositol 3 kinase. *Journal of the American Society of Nephrology* 15: 1537-1545, 2004.

132. Levine S, Nguyen T, Taylor N, Friscia ME, Budak MT, Rothenberg P, Zhu J, Sachdeva R, Sonnad S, and Kaiser LR. Rapid disuse atrophy of diaphragm fibers in mechanically ventilated humans. *New England Journal of Medicine* 358: 1327-1335, 2008.

133. Lexell J, Sjöström M, Nordlund A-S, and Taylor CC. Growth and development of human muscle: A quantitative morphological study of whole vastus lateralis from childhood to adult age. *Muscle & Nerve* 15: 404-409, 1992.

134. Liu J, Peng Y, Cui Z, Wu Z, Qian A, Shang P, Qu L, Li Y, Liu J, and Long J. Depressed mitochondrial biogenesis and dynamic remodeling in mouse tibialis anterior and gastrocnemius induced by 4-week hindlimb unloading. *IUBMB Life* 64: 901-910, 2012.

135. Louis E, Raue U, Yang Y, Jemiolo B, and Trappe S. Time course of proteolytic, cytokine, and myostatin gene expression after acute exercise in human skeletal muscle. *Journal of Applied Physiology* 103: 1744-1751, 2007.

136. Luo L, Lu A-M, Wang Y, Hong A, Chen Y, Hu J, Li X, and Qin Z-H. Chronic resistance training activates autophagy and reduces apoptosis of muscle cells by

modulating IGF-1 and its receptors, Akt/mTOR and Akt/FOXO3a signaling in aged rats. *Experimental Gerontology* 48: 427-436, 2013.

137. Lysenko E, Turtikova O, Kachaeva E, Ushakov I, and Shenkman B. Time course of ribosomal kinase activity during hindlimb unloading. *Doklady Biochemistry and Biophysics*. Springer, 2010, p. 223-226.

138. MacDougall JD, Gibala MJ, Tarnopolsky MA, MacDonald JR, Interisano SA, and Yarasheski KE. The time course for elevated muscle protein synthesis following heavy resistance exercise. *Canadian Journal of Applied Physiology* 20: 480-486, 1995.

139. Martin TP. Protein and collagen content of rat skeletal muscle following space flight. *Cell and Tissue Research* 254: 251-253, 1988.

140. Matuszczak Y, Arbogast S, and Reid MB. Allopurinol mitigates muscle contractile dysfunction caused by hindlimb unloading in mice. *Aviation, Space, and Environmental Medicine* 75: 581-588, 2004.

141. McClung J, Kavazis A, Whidden M, DeRuisseau K, Falk D, Criswell D, and Powers S. Antioxidant administration attenuates mechanical ventilation-induced rat diaphragm muscle atrophy independent of protein kinase B (PKB–Akt) signalling. *The Journal of Physiology* 585: 203-215, 2007.

142. McDonald KS, Delp MD, and Fitts RH. Effect of hindlimb unweighting on tissue blood flow in the rat. *Journal of Applied Physiology* 72: 2210-2218, 1992.

143. McDonald KS and Fitts RH. Effect of hindlimb unloading on rat soleus fiber force, stiffness, and calcium sensitivity. *Journal of Applied Physiology* 79: 1796-1802, 1995.

144. McGrath JA and Goldspink DF. Glucocorticoid action on protein synthesis and protein breakdown in isolated skeletal muscles. *Biochemical Journal* 206: 641, 1982.

145. McGuire DK, Levine BD, Williamson JW, Snell PG, Blomqvist CG, Saltin B, and Mitchell JH. A 30-year follow-up of the Dallas Bed Rest and Training Study I. Effect of age on the cardiovascular response to exercise. *Circulation* 104: 1350-1357, 2001.

146. McKendrick L, Morley SJ, Pain VM, Jagus R, and Joshi B. Phosphorylation of eukaryotic initiation factor 4E (eIF4E) at Ser209 is not required for protein synthesis in vitro and in vivo. *European Journal of Biochemistry* 268: 5375-5385, 2001.

147. Miller TA, Lesniewski LA, Muller-Delp JM, Majors AK, Scalise D, and Delp MD. Hindlimb unloading induces a collagen isoform shift in the soleus muscle of the rat. *American Journal of Physiology - Regulatory, Integrative and Comparative Physiology* 281: R1710-R1717, 2001.

148. Mitchell SL, Stott DJ, Martin BJ, and Grant SJ. Randomized controlled trial of quadriceps training after proximal femoral fracture. *Clinical Rehabilitation* 15: 282-290, 2001.

149. Morey-Holton E, Globus RK, Kaplansky A, and Durnova G. The hindlimb unloading rat model: literature overview, technique update and comparison with space flight data. *Advances in Space Biology and Medicine* 10: 7-40, 2005.

150. Morey-Holton ER and Globus RK. Hindlimb unloading rodent model: technical aspects. *Journal of Applied Physiology* 92: 1367-1377, 2002.

151. Munoz KA, Satarug S, and Tischler ME. Time course of the response of myofibrillar and sarcoplasmic protein metabolism to unweighting of the soleus muscle. *Metabolism* 42: 1006-1012, 1993.

152. Musacchia X, Deavers D, Meininger G, and Davis T. A model for hypokinesia: effects on muscle atrophy in the rat. *Journal of Applied Physiology* 48: 479-486, 1980.

153. Musacchia XJ, Steffen JM, Fell RD, and Dombrowski MJ. Skeletal muscle response to spaceflight, whole body suspension, and recovery in rats. *Journal of Applied Physiology* 69: 2248-2253, 1990.

154. Nader GA, von Walden F, Liu C, Lindvall J, Gutmann L, Pistilli EE, and Gordon PM. Resistance exercise training modulates acute gene expression during human skeletal muscle hypertrophy. *Journal of Applied Physiology* 116: 693-702, 2014.

155. Nilsson MI, Dobson JP, Greene NP, Wiggs MP, Shimkus KL, Wudeck EV, Davis AR, Laureano ML, and Fluckey JD. Abnormal protein turnover and anabolic resistance to exercise in sarcopenic obesity. *The FASEB Journal* 27: 3905-3916, 2013.

156. Nilsson MI, Greene NP, Dobson JP, Wiggs MP, Gasier HG, Macias BR, Shimkus KL, and Fluckey JD. Insulin resistance syndrome blunts the mitochondrial anabolic response following resistance exercise. *American Journal of Physiology-Endocrinology and Metabolism* 299: E466-474, 2010.

157. Ogasawara R, Yasuda T, Ishii N, and Abe T. Comparison of muscle hypertrophy following 6-month of continuous and periodic strength training. *European Journal of Applied Physiology* 113: 975-985, 2013.

158. Ogawa T, Furochi H, Mameoka M, Hirasaka K, Onishi Y, Suzue N, Oarada M, Akamatsu M, Akima H, and Fukunaga T. Ubiquitin ligase gene expression in healthy volunteers with 20-day bedrest. *Muscle & Nerve* 34: 463-469, 2006.

159. Ohira Y, Jiang B, Roy RR, Oganov V, Ilyina-Kakueva E, Marini J, and Edgerton V. Rat soleus muscle fiber responses to 14 days of spaceflight and hindlimb suspension. *Journal of Applied Physiology* 73: S51-S57, 1992.

160. Peterson TR, Laplante M, Thoreen CC, Sancak Y, Kang SA, Kuehl WM, Gray NS, and Sabatini DM. DEPTOR Is an mTOR Inhibitor Frequently Overexpressed in Multiple Myeloma Cells and Required for Their Survival. *Cell* 137: 873-886, 2009.

161. Phillips SM, Glover EI, and Rennie MJ. Alterations of protein turnover underlying disuse atrophy in human skeletal muscle. *Journal of Applied Physiology* 107: 645-654, 2009.

162. Ploutz-Snyder LL, Ryder JW, English KL, Haddad F, and Baldwin KM. NASA evidence report: Risk of Impaired Performance Due to Reduced Muscle Mass, Strength, and Endurance, 2015.

163. Ploutz-Snyder LL, Tesch PA, Hather BM, and Dudley GA. Vulnerability to dysfunction and muscle injury after unloading. *Archives of Physical Medicine and Rehabilitation* 77: 773-777, 1996.

164. Pocknee RC and Heaton FW. Changes in Organ Growth with Feeding Pattern. The Influence of Feeding Frequency on the Circadian Rhythm of Protein Synthesis in the Rat. *The Journal of Nutrition* 108: 1266-1273, 1978.

165. Propst GK, Kwak H-B, Kim J-H, Dalton RL, and Lawler JM. Hindlimb Unloading Induces a Biphasic Temporal Response of Bcl-2 Apoptotic Signaling in the Rat Soleus Muscle. *The FASEB Journal* 22: 1238.1220, 2008.

166. Ramos JE, Al-Nakkash L, Peterson A, Gump BS, Janjulia T, Moore MS, Broderick TL, and Carroll CC. The soy isoflavone genistein inhibits the reduction in Achilles tendon collagen content induced by ovariectomy in rats. *Scandinavian Journal of Medicine & Science in Sports* 22: e108-e114, 2012.

167. Reynolds TH, Bodine SC, and Lawrence JC. Control of Ser2448 phosphorylation in the mammalian target of rapamycin by insulin and skeletal muscle load. *Journal of Biological Chemistry* 277: 17657-17662, 2002.

168. Riley D, Ellis S, Slocum G, Sedlak F, Bain J, Krippendorf B, Lehman C, Macias M, Thompson J, and Vijayan K. In-flight and postflight changes in skeletal

muscles of SLS-1 and SLS-2 spaceflown rats. *Journal of Applied Physiology* 81: 133-144, 1996.

169. Riley DA, Bain JLW, Romatowski JG, and Fitts RH. Skeletal muscle fiber atrophy: altered thin filament density changes slow fiber force and shortening velocity. *American Journal of Physiology - Cell Physiology* 288: C360-C365, 2005.

170. Riley DA, Bain JLW, Thompson JL, Fitts RH, Widrick JJ, Trappe SW, Trappe TA, and Costill DL. Decreased thin filament density and length in human atrophic soleus muscle fibers after spaceflight. *Journal of Applied Physiology* 88: 567-572, 2000.

171. Riley DA, Bain JLW, Thompson JL, Fitts RH, Widrick JJ, Trappe SW, Trappe TA, and Costill DL. Disproportionate loss of thin filaments in human soleus muscle after 17-day bed rest. *Muscle & Nerve* 21: 1280-1289, 1998.

172. Riley DA, Ellis S, Slocom GR, Satyanarayana T, Bain JL, and Sedlak FR. Hypogravity-induced atrophy of rat soleus and extensor digitorum longus muscles. *Muscle & Nerve* 10: 560-568, 1987.

173. Riley DA, Slocum GR, Bain JL, Sedlak FR, Sowa TE, and Mellender JW. Rat hindlimb unloading: soleus histochemistry, ultrastructure, and electromyography. *Journal of Applied Physiology* 69: 58-66, 1990.

174. Rittweger J, Beller G, Ehrig J, Jung C, Koch U, Ramolla J, Schmidt F, Newitt D, Majumdar S, and Schiessl H. Bone-muscle strength indices for the human lower leg. *Bone* 27: 319-326, 2000.

175. Rittweger J and Felsenberg D. Recovery of muscle atrophy and bone loss from 90 days bed rest: Results from a one-year follow-up. *Bone* 44: 214-224, 2009.

176. Rittweger J, Frost HM, Schiessl H, Ohshima H, Alkner B, Tesch P, and Felsenberg D. Muscle atrophy and bone loss after 90 days' bed rest and the effects of flywheel resistive exercise and pamidronate: Results from the LTBR study. *Bone* 36: 1019-1029, 2005.

177. Rolland YM, Perry HM, Patrick P, Banks WA, and Morley JE. Loss of appendicular muscle mass and loss of muscle strength in young postmenopausal women. *The Journals of Gerontology Series A: Biological Sciences and Medical Sciences* 62: 330-335, 2007.

178. Romero-Calvo I, Ocón B, Martínez-Moya P, Suárez MD, Zarzuelo A, Martínez-Augustin O, and de Medina FS. Reversible Ponceau staining as a loading control alternative to actin in Western blots. *Analytical Biochemistry* 401: 318-320, 2010.

179. Sakuma K, Watanabe K, Hotta N, Koike T, Ishida K, Katayama K, and Akima H. The adaptive responses in several mediators linked with hypertrophy and atrophy of skeletal muscle after lower limb unloading in humans. *Acta Physiologica* 197: 151-159, 2009.

180. Salazar JJ, Michele DE, and Brooks SV. Inhibition of calpain prevents muscle weakness and disruption of sarcomere structure during hindlimb suspension. *Journal of Applied Physiology* 108: 120-127, 2010.

181. Saltin B, Blomqvist G, Mitchell JH, Johnson Jr RL, Wildenthal K, and Chapman CB. Response to exercise after bed rest and after training. *Circulation* 38: VII1-78, 1968.

182. Saltin B, Nazar K, Costill DL, Stein E, Jansson E, Essén B, and Gollnick PD. The Nature of the Training Response; Peripheral and Central Adaptations to One-Legged Exercise. *Acta Physiologica Scandinavica* 96: 289-305, 1976.

183. Sandonà D, Desaphy J-F, Camerino GM, Bianchini E, Ciciliot S, Danieli-Betto D, Dobrowolny G, Furlan S, Germinario E, Goto K, Gutsmann M, Kawano F, Nakai N, Ohira T, Ohno Y, Picard A, Salanova M, Schiffl G, Blottner D, Musarò A, Ohira Y, Betto R, Conte D, and Schiaffino S. Adaptation of Mouse Skeletal Muscle to Long-Term Microgravity in the MDS Mission. *PLoS ONE* 7: e33232, 2012.

184. Sandri M, Sandri C, Gilbert A, Skurk C, Calabria E, Picard A, Walsh K, Schiaffino S, Lecker SH, and Goldberg AL. Foxo transcription factors induce the atrophy-related ubiquitin ligase atrogin-1 and cause skeletal muscle atrophy. *Cell* 117: 399-412, 2004.

185. Sashika H, Matsuba Y, and Watanabe Y. Home program of physical therapy: effect on disabilities of patients with total hip arthroplasty. *Archives of Physical Medicine and Rehabilitation* 77: 273-277, 1996.

186. Scheper GC and Proud CG. Does phosphorylation of the cap-binding protein eIF4E play a role in translation initiation? *European Journal of Biochemistry* 269: 5350-5359, 2002.

187. Seene T, Kaasik P, Alev K, Pehme A, and Riso E. Composition and turnover of contractile proteins in volume-overtrained skeletal muscle. *International Journal of Sports Medicine* 25: 438-445, 2004.

188. Seger R and Krebs EG. The MAPK signaling cascade. *The FASEB Journal* 9: 726-735, 1995.

189. Seo Y, Lee K, Park K, Bae K, and Choi I. A proteomic assessment of muscle contractile alterations during unloading and reloading. *Journal of Biochemistry* 139: 71-80, 2006.

190. Shah OJ, Anthony JC, Kimball SR, and Jefferson LS. 4E-BP1 and S6K1: translational integration sites for nutritional and hormonal information in muscle. *American Journal of Physiology-Endocrinology And Metabolism* 279: E715-E729, 2000.

191. Shanely RA, Van Gammeren D, DeRuisseau KC, Zergeroglu AM, McKenzie MJ, Yarasheski KE, and Powers SK. Mechanical ventilation depresses protein synthesis in the rat diaphragm. *American journal of Respiratory and Critical Care Medicine* 170: 994-999, 2004.

192. Shanely RA, Zergeroglu MA, Lennon SL, Sugiura T, Yimlamai T, Enns D, Belcastro A, and Powers SK. Mechanical ventilation–induced diaphragmatic atrophy is associated with oxidative injury and increased proteolytic activity. *American Journal of Respiratory and Critical Care Medicine* 166: 1369-1374, 2002.

193. Sherrington C and Lord SR. Home exercise to improve strength and walking velocity after hip fracture: a randomized controlled trial. *Archives of Physical Medicine and Rehabilitation* 78: 208-212, 1997.

194. Shirazi-Fard Y, Anthony RA, Kwaczala AT, Judex S, Bloomfield SA, and Hogan HA. Previous exposure to simulated microgravity does not exacerbate bone loss during subsequent exposure in the proximal tibia of adult rats. *Bone* 56: 461-473, 2013.

195. Shirazi-Fard Y, Gonzalez E, Morgan D, Davis J, Shimkus K, Boudreaux R, Bloomfield S, and Hogan H. Bone Response to Exercise During Recovery Between Unloading Bouts in Adult Male Rats. *ASME 2012 Summer Bioengineering Conference*. American Society of Mechanical Engineers, 2012, p. 47-48.

196. Shirazi-Fard Y, Kupke JS, Bloomfield SA, and Hogan HA. Discordant recovery of bone mass and mechanical properties during prolonged recovery from disuse. *Bone* 52: 433-443, 2013.

197. Shirazi-Fard Y, Metzger CE, Kwaczala AT, Judex S, Bloomfield SA, and Hogan HA. Moderate intensity resistive exercise improves metaphyseal cancellous bone recovery following an initial disuse period, but does not mitigate decrements during a subsequent disuse period in adult rats. *Bone* 66: 296-305, 2014.

198. Siu PM, Pistilli EE, and Alway SE. Apoptotic responses to hindlimb suspension in gastrocnemius muscles from young adult and aged rats. *American Journal of*

Physiology-Regulatory, Integrative and Comparative Physiology 289: R1015-R1026, 2005.

199. Smith P, Krohn RI, Hermanson G, Mallia A, Gartner F, Provenzano M, Fujimoto E, Goeke N, Olson B, and Klenk D. Measurement of protein using bicinchoninic acid. *Analytical Biochemistry* 150: 76-85, 1985.

200. Srikanthan P and Karlamangla AS. Muscle mass index as a predictor of longevity in older adults. *The American Journal of Medicine* 127: 547-553, 2014.

201. St Pierre B and Tidball JG. Differential response of macrophage subpopulations to soleus muscle reloading after rat hindlimb suspension. *Journal of Applied Physiology* 77: 290-297, 1994.

202. Staron RS, Leonardi MJ, Karapondo DL, Malicky ES, Falkel JE, Hagerman FC, and Hikida RS. Strength and skeletal muscle adaptations in heavy-resistance-trained women after detraining and retraining. *Journal of Applied Physiology* 70(2):631-40, 1991.

203. Stein T, Leskiw M, Schluter M, Donaldson M, and Larina I. Protein kinetics during and after long-duration spaceflight on MIR. *American Journal of Physiology-Endocrinology And Metabolism* 276: E1014-E1021, 1999.

204. Stitt TN, Drujan D, Clarke BA, Panaro F, Timofeyva Y, Kline WO, Gonzalez M, Yancopoulos GD, and Glass DJ. The IGF-1/PI3K/Akt pathway prevents expression of muscle atrophy-induced ubiquitin ligases by inhibiting FOXO transcription factors. *Molecular Cell* 14: 395-403, 2004.

205. Suetta C, Aagaard P, Rosted A, Jakobsen AK, Duus B, Kjaer M, and Magnusson SP. Training-induced changes in muscle CSA, muscle strength, EMG, and rate of force development in elderly subjects after long-term unilateral disuse. *Journal of Applied Physiology* 97: 1954-1961, 2004.

206. Suetta C, Andersen JL, Dalgas U, Berget J, Koskinen S, Aagaard P, Magnusson SP, and Kjaer M. Resistance training induces qualitative changes in muscle morphology, muscle architecture, and muscle function in elderly postoperative patients. *Journal of Applied Physiology* 105: 180-186, 2008.

207. Suetta C, Hvid LG, Justesen L, Christensen U, Neergaard K, Simonsen L, Ortenblad N, Magnusson SP, Kjaer M, and Aagaard P. Effects of aging on human skeletal muscle after immobilization and retraining. *Journal of Applied Physiology* 107: 1172-1180, 2009.

208. Sugiura T, Abe N, Nagano M, Goto K, Sakuma K, Naito H, Yoshioka T, and Powers SK. Changes in PKB/Akt and calcineurin signaling during recovery in atrophied soleus muscle induced by unloading. *American Journal of Physiology-Regulatory, Integrative and Comparative Physiology* 288: R1273-R1278, 2005.

209. Taaffe DR, Henwood TR, Nalls MA, Walker DG, Lang TF, and Harris TB. Alterations in muscle attenuation following detraining and retraining in resistance-trained older adults. *Gerontology* 55: 217-223, 2008.

210. Taillandier D, Aurousseau E, Combaret L, Guezennec C-Y, and Attaix D. Regulation of proteolysis during reloading of the unweighted soleus muscle. *The International Journal of Biochemistry & Cell Biology* 35: 665-675, 2003.

211. Tesch PA, Berg HE, Bring D, Evans HJ, and LeBlanc AD. Effects of 17-day spaceflight on knee extensor muscle function and size. *European Journal of Applied Physiology* 93: 463-468, 2005.

212. Tesch PA and Larsson L. Muscle hypertrophy in bodybuilders. *European Journal of Applied Physiology* 49: 301-306, 1982.

213. Tesch PA, von Walden F, Gustafsson T, Linnehan RM, and Trappe TA. Skeletal muscle proteolysis in response to short-term unloading in humans. *Journal of Applied Physiology* 105(3) 902-6, 2008.

214. Thomason DB, Biggs RB, and Booth FW. Protein metabolism and beta-myosin heavy-chain mRNA in unweighted soleus muscle. *American Journal of Physiology-Regulatory, Integrative and Comparative Physiology* 257: R300-R305, 1989.

215. Thomason DB and Booth FW. Atrophy of the soleus muscle by hindlimb unweighting. *Journal of Applied Physiology* 68: 1-12, 1990.

216. Thomason DB, Herrick RE, Surdyka D, and Baldwin KM. Time course of soleus muscle myosin expression during hindlimb suspension and recovery. *Journal of Applied Physiology* 63: 130-137, 1987.

217. Tischler ME, Henriksen EJ, Munoz KA, Stump CS, Woodman CR, and Kirby CR. Spaceflight on STS-48 and earth-based unweighting produce similar effects on skeletal muscle of young rats. *Journal of Applied Physiology* 74: 2161-2165, 1993.

218. Trappe S, Costill D, Gallagher P, Creer A, Peters JR, Evans H, Riley DA, and Fitts RH. Exercise in space: human skeletal muscle after 6 months aboard the International Space Station. *Journal of Applied Physiology* 106: 1159-1168, 2009.

219. Trappe S, Trappe T, Gallagher P, Harber M, Alkner B, and Tesch P. Human single muscle fibre function with 84 day bed-rest and resistance exercise. *The Journal of Physiology* 557: 501-513, 2004.

220. Trappe TA, Burd NA, Louis ES, Lee GA, and Trappe SW. Influence of concurrent exercise or nutrition countermeasures on thigh and calf muscle size and function during 60 days of bed rest in women. *Acta Physiologica* 191: 147-159, 2007.

221. Tucker K, Seider M, and Booth F. Protein synthesis rates in atrophied gastrocnemius muscles after limb immobilization. *Journal of Applied Physiology* 51: 73-77, 1981.

222. Vazeille E, Slimani L, Claustre A, Magne H, Labas R, Béchet D, Taillandier D, Dardevet D, Astruc T, and Attaix D. Curcumin treatment prevents increased proteasome and apoptosome activities in rat skeletal muscle during reloading and improves subsequent recovery. *The Journal of Nutritional Biochemistry* 23: 245-251, 2012.

223. Wagatsuma A, Kotake N, Kawachi T, Shiozuka M, Yamada S, and Matsuda R. Mitochondrial adaptations in skeletal muscle to hindlimb unloading. *Molecular and Cellular Biochemistry* 350: 1-11, 2011.

224. Wang Z, Zhong J, Gao D, Inuzuka H, Liu P, and Wei W. DEPTOR ubiquitination and destruction by SCFβ-TrCP. *American Journal of Physiology-Endocrinology and Metabolism* 303: E163-E169, 2012.

225. Ward P. The effect of an anabolic steroid on strength and lean body mass. *Medicine and Science in Sports* 5: 277, 1973.

226. Warren G, Stallone J, Allen M, and Bloomfield S. Functional recovery of the plantarflexor muscle group after hindlimb unloading in the rat. *European Journal of Applied Physiology* 93: 130-138, 2004.

227. Wenke JC, Warren GL, Rathbone CR, and Armstrong RB. Mouse plantar flexor muscle size and strength after inactivity and training. *Aviation, Space, and Environmental Medicine* 81: 632-638, 2010.

228. Widrick JJ, Knuth ST, Norenberg KM, Romatowski J, Bain JL, Riley DA, Karhanek M, Trappe S, Trappe TA, and Costill D. Effect of a 17 day spaceflight on contractile properties of human soleus muscle fibres. *The Journal of Physiology* 516: 915-930, 1999.

229. Widrick JJ, Maddalozzo GF, Hu H, Herron JC, Iwaniec UT, and Turner RT. Detrimental effects of reloading recovery on force, shortening velocity, and power of soleus muscles from hindlimb-unloaded rats. *American Journal of Physiology - Regulatory, Integrative and Comparative Physiology* 295: R1585-R1592, 2008.

230. Wilkinson SB, Phillips SM, Atherton PJ, Patel R, Yarasheski KE, Tarnopolsky MA, and Rennie MJ. Differential effects of resistance and endurance exercise in

the fed state on signalling molecule phosphorylation and protein synthesis in human muscle. *The Journal of Physiology* 586: 3701-3717, 2008.

231. Wittwer M, Flück M, Hoppeler H, Müller S, Desplanches D, and Billeter R. Prolonged unloading of rat soleus muscle causes distinct adaptations of the gene profile. *The FASEB Journal* 16: 884-886, 2002.

232. Witzmann F, Kim D, and Fitts R. Recovery time course in contractile function of fast and slow skeletal muscle after hindlimb immobilization. *Journal of Applied Physiology* 52: 677-682, 1982.

233. Yang D, Li L, Liu H, Wu L, Luo Z, Li H, Zheng S, Gao H, Chu Y, and Sun Y. Induction of autophagy and senescence by knockdown of ROC1 E3 ubiquitin ligase to suppress the growth of liver cancer cells. *Cell Death & Differentiation* 20: 235-247, 2013.

234. Zange J, Müller K, Schuber M, Wackerhage H, Hoffmann U, Günther R, Adam G, Neuerburg J, Sinitsyn V, and Bacharev A. Changes in calf muscle performance, energy metabolism, and muscle volume caused by long term stay on space station MIR. *International Journal of Sports Medicine* 18: S308-S309, 1997.

235. Zarzhevsky N, Carmeli E, Fuchs D, Coleman R, Stein H, and Reznick A. Recovery of muscles of old rats after hindlimb immobilisation by external fixation is impaired compared with those of young rats. *Experimental Gerontology* 36: 125-140, 2001.

236. Zhao Y, Xiong X, Jia L, and Sun Y. Targeting Cullin-RING ligases by MLN4924 induces autophagy via modulating the HIF1-REDD1-TSC1-mTORC1-DEPTOR axis. *Cell Death & Disease* 3: e386, 2012.

237. Zhao Y, Xiong X, and Sun Y. DEPTOR, an mTOR Inhibitor, Is a Physiological Substrate of SCFβTrCP E3 Ubiquitin Ligase and Regulates Survival and Autophagy. *Molecular Cell* 44: 304-316, 2011.

238. Zhou M, Klitgaard H, Saltin B, Roy R, Edgerton V, and Gollnick P. Myosin heavy chain isoforms of human muscle after short-term spaceflight. *Journal of Applied Physiology* 78: 1740-1744, 1995.